

SYNTHESIS OF CONDUCTING BLOCK COPOLYMERS AND THEIR  
USE IN THE IMMOBILIZATION OF INVERTASE AND POLYPHENOL  
OXIDASE ENZYME

A THESIS SUBMITTED TO  
THE GRADUATE SCHOOL OF NATURAL AND APPLIED SCIENCES  
OF  
THE MIDDLE EAST TECHNICAL UNIVERSITY

BY

SENEM KIRALP

IN PARTIAL FULFILLMENT OF THE REQUIREMENTS FOR THE  
DEGREE OF

DOCTOR OF PHILOSOPHY

IN

THE DEPARTMENT OF CHEMISTRY

MAY 2004

Approval of the Graduate School of Natural and Applied Sciences

---

Prof. Dr. Canan Özgen  
Director

I certify that this thesis satisfies all the requirements as a thesis for the degree of  
Doctor of Philosophy.

---

Prof. Dr. Hüseyin İşçi  
Head of Department

This is to certify that we have read this thesis and that in our opinion it is fully  
adequate, in scope and quality, as a thesis for the degree of Doctor of  
Philosophy

---

Prof. Dr. Levent Toppare  
Supervisor

Examining Committee Members

Prof. Dr. Levent Toppare

Prof. Dr. Teoman Tinçer

Prof. Dr. Ufuk Bakır

Prof. Dr. Leyla Aras

Prof. Dr. Yusuf Yağcı

## ABSTRACT

### SYNTHESIS OF CONDUCTING BLOCK COPOLYMERS AND THEIR USE IN THE IMMOBILIZATION OF INVERTASE AND POLYPHENOL OXIDASE ENZYMES

Kıralp, Senem

Ph.D., Department of Chemistry

Supervisor: Prof. Dr. Levent Toppare

May 2004, 121 pages

A new thiophene derivative containing menthyl group (MM) was synthesized and polymerized via chemical and electrochemical methods. Polymers obtained and MM itself were used to synthesize copolymers with pyrrole under conditions of constant potential electrolysis. Cyclic Voltammetry, thermal analysis and scanning electron microscopy analyses were performed for the characterization of samples.

Immobilization of invertase and polyphenol oxidase enzymes was performed in the matrices obtained via copolymerization of MM with pyrrole. Immobilization was carried out via entrapment of enzyme in matrices during the polymerization of pyrrole. Temperature optimization, operational stability and shelf-life of the enzyme electrodes were investigated. Maximum reaction rate ( $V_{max}$ ) and Michaelis-Menten constant ( $K_m$ ) were determined.

It is known that wine includes phenolic groups that give astringency in high concentrations. Polyphenol oxidase (PPO) converts mono and diphenols to quinone. By analyzing the product, one can find out the amount of phenolic groups. By using obtained enzyme electrodes via immobilization of PPO, amount of phenolics in different wines were analyzed.

Keywords: Electrochemical polymerization, immobilization, invertase, polyphenol oxidase, wine.

## ÖZ

### İLETKEN KOPOLİMERLERDE İNVERTAZ VE POLİFENOL OKSİDAZ ENZİMLERİNİN TUTUKLANMASI

Kıralp, Senem

Doktora, Kimya Bölümü

Tez Yöneticisi: Levent Toppare

Mayıs 2004, 121 sayfa

Mentil grubu içeren yeni bir tiyofen türevi sentezlendi (MM) ve bu monomer kimyasal ve elektrokimyasal yolla polimerleştirildi. MM kullanılarak pirolle iletken kopolimerler elde edildi. Kopolimerleştirme hem sabit akım hemde sabit gerilim altında gerçekleştirildi. Elde edilen kopolimerlerin karakterizasyonu, dönüşümlü voltametre, taramalı elektron mikroskobu ve termal analizlerle yapıldı.

MM kullanılarak elde edilen kopolimerler invertaz ve polifenol oksidaz tutuklamaları için kullanıldı. Enzim elektrotlarının optimum sıcaklıkları, kararlılıkları ve raf ömürleri tayin edildi. Kinetik parametreleri de ayrıca incelendi.

Polifenol oksidaz enzimi kullanılarak elde edilen enzim elektrotları şaraplarda bulunan ve fazla miktarı şarabın acılaştırmasına sebep olan fenolik

yapıların miktar tayininde kullanıldı. Türkiye’de üretilen iki farklı kırmızı şarabın fenolik miktar analizleri yapıldı.

Anahtar Kelimeler: Elektrokimyasal polimerleşme, enzim tutuklaması, invertaz, polifenol oksidaz, şarap.

**To My Parents**

## **ACKNOWLEDGMENTS**

I would like to express appreciation to my supervisor Prof. Dr. Levent Toppare for his guidance and encouragement throughout this thesis.

I wish to express my sincere thanks to Prof. Dr. Yusuf Yagcı and Prof. Dr. Ufuk Bakır for their valuable discussions and help throughout this study.

I also wish to express my endless thanks to my family especially to my sister Seda Kıralp, for her patience, moral support and encouragement.

I would like to give my special thanks to Semih Seyyidođlu for being my best friend and for his moral support.

I also want to thank to every member in our group for their friendship.

Finally I want to thank with my entire heart to my love Uygur Kayahan for his continuous support, understanding and being near me whenever I want. I could not achieve anything without his love and trust.

Appreciation is extended to colleagues in the Department of Chemistry, Middle East Technical University.



## TABLE OF CONTENTS

ABSTRACT .....	iii
ÖZ.....	v
ACKNOWLEDGMENTS.....	viii
TABLE OF CONTENTS .....	ix
LIST OF TABLES .....	xiii
LIST OF FIGURES.....	xiv

### CHAPTERS

I. INTRODUCTION.....	1
1.1. Conducting Polymers.....	1
1.1.1. Historical Riview of Conducting Polymers.....	1
1.1.2. Principle Structure and Types of Conductive Polymers.....	3
1.1.3. Band theory and Conduction Mechanism in Conducting Polymers .....	5
1.1.3.1. Band Theory of Solids.....	7
1.1.3.2. Conduction Mechanism.....	9
1.1.3.3. Movement of the Charge Carrier Through Polypyrrole.....	10
1.1.4. Synthesis of Conducting Polymers.....	12

1.1.4.1. Chemical Synthesis.....	12
1.1.4.2. Electrochemical Synthesis.....	13
1.1.5. Conducting Copolymers .....	15
1.1.6. Characterization of Conducting polymers.....	16
1.1.6.1. Cyclic Voltammetry.....	17
1.1.7. Applications of Conducting Polymers .....	17
1.2. Enzymes.....	18
1.2.1. Enzyme Nomenclature.....	20
1.2.2. Enzyme Kinetics.....	22
1.2.2.1. Michaelis-Menten Equation .....	23
1.2.2.2. Lineweaver- Burk Plot .....	28
1.2.3. Enzyme Immobilization.....	30
1.2.3.1. Benefits of Enzyme Immobilization.....	30
1.2.3.2. Immobilization Methods.....	31
1.2.4. Invertase.....	36
1.2.5. Polyphenol oxidase (Tyrosinase).....	37
1.2.6. Phenolics in Wines.....	40
1.3. Aim of the Study.....	42
2. EXPERIMENTAL.....	43
2.1. Chemicals.....	43
2.2. Instrumentation.....	44
2.2.1. Electrolysis.....	44
2.2.2. Cyclic Voltammetry (CV) System.....	46
2.2.3. Conductivity Measurements.....	49



2.3.7.1.6. Morphologies of Invertase-Entrapped Films.....	60
2.3.7.2. Immobilization of Polyphenol Oxidase (PPO).....	60
2.3.7.2.1. Preparation of Enzyme Electrodes in Copolymers of MM.....	60
2.3.7.2.2. Preparation of Enzyme Electrodes in Copolymers of MBTA.....	61
2.3.7.2.3. Determination of PPO Activity.....	61
2.3.7.2.4. Kinetic Parameters for Free and Immobilized PPO.....	63
2.3.7.2.5. Determination of Optimum Temperature and pH of Immobilized PPO.....	63
2.3.7.2.6. Determination of Operational and Storage Stability Immobilized PPO.....	63
2.3.7.2.7. Morphologies of PPO Entrapped Films.....	64
2.3.7.2.8. Protein Determination .....	64
2.3.7.2.9. Determination of Amount of Phenolic Compounds in Red Wines.....	65
3. RESULTS AND DISCUSSION.....	66
3.1. Synthesis and Characterization of Menthyl Ester of 3-Thiophene Acetic Acid.....	66
3.2. Chemical Polymerization of MM (CN).....	69
3.3. Galvanostatic Polymerization of MM (GDM).....	71
3.4. Conducting Copolymers.....	72
3.4.1. Copolymers of MM with Thiophene.....	72
3.4.2. Copolymers of MM with Pyrrole .....	73

3.4.3. Block Copolymers of CN and GDM with Pyrrole (CNPP, CNPS, PGDM).....	74
3.4.4. Characterization of Conducting Copolymers of Pyrrole.....	74
3.4.4.1.Cyclic voltammetry.....	74
3.4.4.2.FTIR.....	74
3.4.4.3.Thermal Analysis.....	75
3.4.4.4. Morphologies of the Films.....	80
3.4.4.5.Conductivity Measurements.....	83
3.5. Immobilization of Invertase.....	83
3.5.1. Immobilization of Invertase .....	83
3.5.1.1.Morphologies of Films.....	84
3.5.1.2.Kinetic Parameters.....	84
3.5.1.3.Effect of Temperature.....	87
3.5.1.4.Operation Stability.....	88
3.5.1.5.Shelf-Life.....	88
3.5.2. Immobilization of PPO (Tyrosinase).....	91
3.5.2.1.Tyrosinase Activity.....	91
3.5.2.2.Protein Determination.....	92
3.5.2.3.Kinetic Parameters.....	93
3.5.2.4.Morphologies of Films.....	94
3.5.2.5.Effect of Temperature on Enzyme Activity.....	97
3.5.2.6.Effect of pH on Enzyme Activity.....	99
3.5.2.7.Operational Stability of Enzyme Electrodes.....	102
3.5.2.8.Shelf-Life of Enzyme Electrodes.....	104

3.5.2.9.Determination of Phenolic Compounds in Red Wines.....	106
4. CONCLUSION.....	108
REFERENCES.....	110
VITA.....	117

## LIST OF FIGURES

1.1	Structure of the repeat units of several conjugated polymers.....	4
1.2	Types of conducting polymers.....	5
1.3	Conductivities of various conductors.....	6
1.4	Formation of energy bands and band gap based on the theoretical stacking of ethylene units.....	8
1.5	Physical-chemical “dictionary” for defects in conjugated chains.....	9
1.6	Structural representation of bipolaron formation in polypyrrole and its corresponding energy bands in the mid gap.....	11
1.7	Proposed mechanism for the electrochemical polymerization of aromatic five membered heterocycles; where X=NH, S, or O.....	14
1.8	Typical Protein structure.....	20
1.9	A schematic diagram showing the free energy profile of the course of an enzyme catalyzed reaction involving the formation of enzyme-substrate (ES) and enzyme-product (EP) complexes.....	23
1.10	Computer simulation of the progress curves of $d[ES]/dt$ , $[ES]$ , $[S]$ and $[P]$ for a reaction obeying simple Michaelis-Menten kinetics.....	26

1.11	A normalized plot of the initial rate ( $v_0$ ) against initial substrate concentration ( $[S]_0$ ) for a reaction obeying the Michaelis-Menten kinetics.....	28
1.12	The Lineweaver-Burk Plot.....	29
1.13	Schematic representation of carrier-binding type enzyme immobilization.....	32
1.14	Schematic representation of cross-linking type enzyme immobilization.....	35
1.15	Schematic representation of entrapping enzyme.....	36
1.16	Hydrolysis of sucrose.....	37
1.17	Schematic representation of tyrosinase activity.....	39
2.1	Polymerization cell.....	45
2.2	Triangular wave function.....	46
2.3	A cyclic voltammogram for a reversible reaction.....	48
2.4	Cyclic voltammetry cell.....	49
2.5	Resistance measurement using four-probe technique.....	50
2.6	Synthesis of copolymers of MM with pyrrole.....	53
2.7	Synthesis of copolymers of MM with thiophene.....	58
2.8	Chemical polymerization of MM.....	58
2.9	Galvanostatic polymerization of MM.....	55
2.10	Synthesis of block copolymers of CN and GDM with pyrrole.....	56
2.11	Synthesis of the monomer MBTA.....	57
2.12	Schematic representation of Besthorn's Hydrazone Method.....	62



3.1	NMR spectrum of MM.....	66
3.2	FTIR spectrum of MM.....	67
3.3	Cyclic voltammogram of MM.....	68
3.4	DSC thermogram for MM.....	69
3.5	NMR spectrum of CN.....	70
3.6	FTIR spectrum of CN.....	70
3.7	(a) TGA (b) DSC of CN.....	71
3.8	Schematic representation of synthesis of CN and GDM.....	72
3.9	Cyclic voltammogram of (a) polythiophene (b) polythiophene in the presence of MM.....	73
3.10	Cyclic voltammograms of (a) MM (b) polypyrrole (c) polypyrrole in the presence of MM.....	75
3.11	TGA thermograms for (a) PM-1 (b) PM-2 (c) CNPP (d) CNPS (e) PGDM.....	76
3.12	DSC thermograms for (a) PM-1 (b) PM-2 (c) CNPP (d) CNPS (e) PGDM.....	78
3.13	SEM micrographs of (a) PM-1 (b) PM-2.....	80
3.14	SEM micrographs of CNPP (a) unwashed electrode side (b) washed electrode side.....	81
3.15	SEM micrographs of (a) CNPS solution side (b) CNPS electrode side (c) PGDM solution side.....	82

3.16	Scanning electron micrographs of (a) Ppy (b) CNPS (c) PM-2 matrices in the presence of invertase.....	85
3.17	Effect of temperature on enzyme activity in (a) PM-2 (b) CNPS enzyme electrodes.....	87
3.18	Operational stability of (a) Ppy/PPO (b) PM-2/PPO (c) CNPS/PPO enzyme electrodes.....	89
3.19	Storage stability of (a) Ppy/PPO (b) PM-2/PPO (c) CNPS/PPO enzyme electrodes.....	90
3.20	Calibration curve for Besthorn's Hydrazone Method.....	92
3.21	Calibration curve for protein determination.....	93
3.22	Scanning electron micrographs of (a) Ppy (b) PM-2 (c) CNPS (d) MBTA enzyme electrodes.....	96
3.23	Temperature stability (a)Free PPO (b)Ppy/PPO (c)PM-2/PPO (d)CNPS/PPO (e)MBTA/PPO.....	97
3.24	pH stability of (a) Free PPO (b) Ppy/PPO (c) PM-2/PPO (d) CNPS/PPO (e) MBTA/PPO.....	100
3.25	Operational stability for (a) Ppy/PPO (b) PM-2/PPO (c) CNPS/PPO (d)MBTA/PPO.....	103
3.26	Shelf life for (a) Ppy/PPO (b) PM-2/PPO (c) CNPS/PPO (d) MBTA/PPO.....	105

## LIST OF TABLES

3.1	Conductivities of polymers of MM.....	83
3.2	Kinetic parameters for free and immobilized invertase.....	86
3.3	Protein amounts for enzyme electrodes.....	93
3.4	Kinetic parameters for free and immobilized PPO.....	95
3.5	Total phenolics in two different red wines, determined by enzyme electrodes.....	107

## LIST OF ABBREVIATION

AN	Acetonitrile
CCE	Constant current electrolysis
CN	Homopolymer of MM via chemical polymerization
CNPP	Block copolymer of CN with pyrrole in the presence of PTSA
CNPS	Block copolymer of CN with pyrrole in the presence of SDS
CPE	Constant potential electrolysis
CV	Cyclic Voltammetry
DCCI	N,N'-dicyclohexylcarbodiimide
DCM	Dichloromethane
DSC	Differential scanning calorimetry
FTIR	Fourier Transform Infrared Spectrophotometer
GDM	Homopolymer of MM via galvanostatic polymerization
MBTA	Methylbutyl 2-(3-thienyl)acetate
MBTH	3-methyl-2-benzothiazolinone
MM	Menthyl Ester of 3-Thiophene Acetic Acid
NM	Nitromethane
NMR	Nuclear Magnetic Resonance Spectrometer
PGDM	Block copolymer of GDM with pyrrole in the presence of PTSA

PM-1	Copolymer of MMwith pyrrole in the presence of PTSA
PM-2	Copolymer of MM with pyrrole in the presence of SDS
PMBTA	Homopolymer ofmethylbutyl 2-(3-thienyl)acetate
PPO	Polyphenol oxidase
Ppy	Polypyrrole
PTSA	<i>p</i> -toluene sulfonic acid
SDS	Sodium dodecylsulfate
SEM	Scanning electron Microscope
TBAFB	Tetrabutylammonium tetrafluoroborate
TGA	Thermal gravimetry analysis
THF	Tetrahydro furan

## **CHAPTER 1**

### **INTRODUCTION**

#### **1.1 Conducting Polymers**

Since the discovery of an increase by nearly 10 orders of magnitude of the electrical conductivity of polyacetylene when it was doped (oxidized or reduced) with iodine or other acceptors (dopants), in 1977 [1] conjugated polymers have been studied intensively. Polyacetylene was the first conjugated polymer to show this special electrical property. A number of researchers in physics, chemistry, and materials science study conjugated polymers from several different perspectives. Studies of the electronic structure of the neutral and doped conjugated polymers have opened potential application areas.

##### **1.1.1 Historical Review of Conducting Polymers**

Conventional polymers, which are saturated polymers or plastics, have been used for many applications traditionally because of their attractive chemical, mechanical, and electrically insulating properties. Although the idea of using polymers for their electrically conducting properties dates back at least

to the 1960s [2], the use of organic “ $\pi$  conjugated” polymers as electronic materials [1, 3] in molecular based electronics is relatively new.

Pristine (neutral or undoped) conjugated polymers are insulators or semiconductors. However, when the conjugated polymers are “doped” (oxidized or reduced) they can have metallic electrical conductivity [4, 5]. In addition to the study of the high electrical conductivities, which can be applied to the manufacture of conducting transparent plastic [6] and conducting fabrics [7], the fast and high nonlinear optical application of conjugated organic compounds is also a topic of major interest [8].

In the 1980s the concepts of solitons, polarons, and bipolarons were developed, in the context of both transport properties [9-13] and optical properties [1, 14].

More recently, conjugated polymers are receiving attention as promising materials for electronic applications. In particular, conjugated polymers as well as  $\pi$ -conjugated oligomers [15] play a central role in organic-based transistors and integrated circuits [16, 17], photovoltaic devices [18] and especially organic-based light emitting devices [19].

Even solid state lasers are under development [20]. In fact, in the case of polymer-based light emitting devices (LEDs), the development of device structures has led to the establishment of high-tech companies and academic institutes [21,22].

### 1.1.2 Principle Structure and Types of Conducting Polymers

Following their discovery and first characterization, the interest in conducting polymer started to increase with the preparation of  $(CH)_x$ , also with the discovery that polyacetylene could be doped by charge-transfer reactions with oxidizing and reducing reagents and the discovery that the doped polymer exhibits a dramatic increase in conductivity [23].

Although the discovery of metallic conducting polyacetylene has made a great progress, much more should be done for understanding structure-property relationship.

Polymers containing highly loosely held electrons in their backbones, often referred to as conjugated polymer or conductive polymer. The concepts of conductivity and electroactivity of conjugated polymers were quickly broadened from polyacetylene to include a number of conjugated hydrocarbon and/or aromatic heterocyclic polymers such as poly (p-phenylene) [24, 25], poly(p-phenylene vinylene) [26], polypyrrole [27, 28] and polythiophene [29-31]. Structures of repeat units of several conjugated polymers are shown in Figure 1.1 [32, 33].

Conducting polymers can be classified into four categories from the stand point of molecular structure.

- a) Totally  $\Pi$  conjugated polymers, can be transformed into conductive polymers by using effective dopants. Polypyrrole and polyacetylene are examples for this category. (Figure 1.2 a)
- b) Non-conjugated polymers containing  $\Pi$ -electron system as poly(N-vinyl imidazole) in Figure 1.2 b.



- c) Metallomacrocylic polymers, which contain covalently linked  $\Pi$ -systems in a face to face orientation. These kind of polymers loaded with electroactive counter ions, conduct current by electron self exchange reactions between neighboring redox sites. (Figure.1.2 c)
- d) Composite polymers which are prepared by dispersing highly conductive polymer into inert polymers such as poly (vinylchloride).

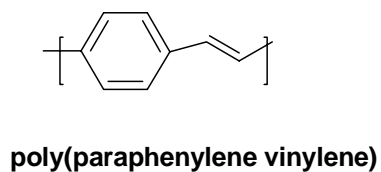
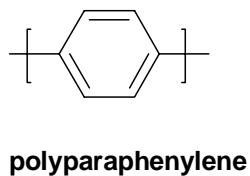
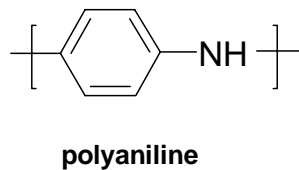
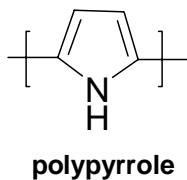
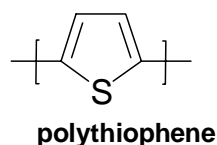
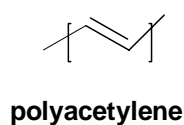
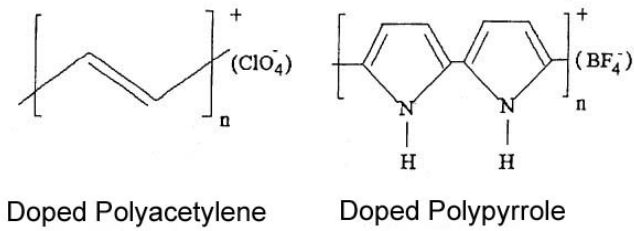


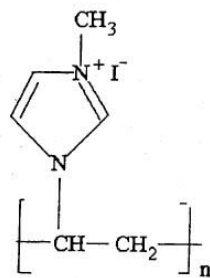
Figure 1.1 Structure of the repeat units of several conjugated polymers



Doped Polyacetylene

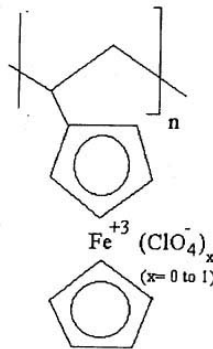
Doped Polypyrrole

(a)



Poly(1-methyl-3-vinylimidazolium iodide)

(b)



Poly(vinylferrocene)

(c)

Figure 1.2 Types of conducting polymers

### 1.1.3 Band theory and Conduction mechanism in Conducting Polymers

Electronic conduction in metals had been understood for many decades. Figure 1.3 shows conductivities of various conductors and their relation in one another.

A good understanding of electronic conduction in polymers is the result of extensive research in the field. Electronic conduction in general is the

transport of charge carriers (electrons, holes, polarons, solitons, etc.) through a medium (metal, polymer, etc.) under the influence of electric field. Thus, the conductivity displayed by any medium is characterized by the number of charge carriers available and their ability to move through the medium.

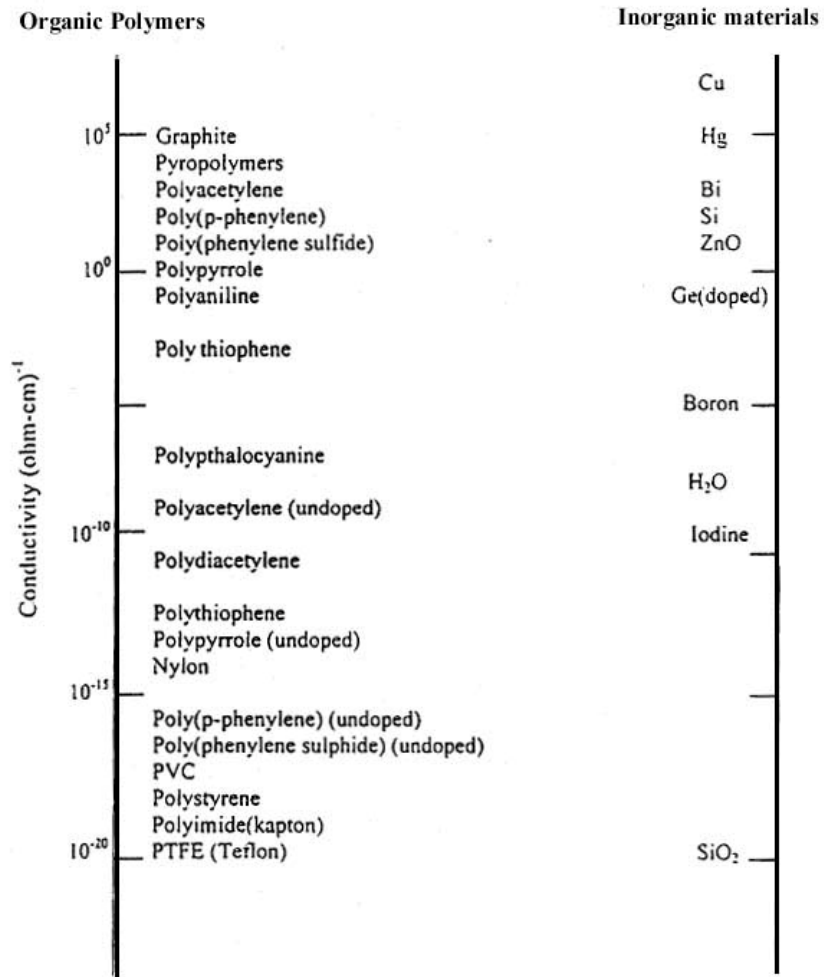


Figure 1.3 Conductivities of various conductors

In order to discuss charge carriers and their mobility, it is first necessary to establish exactly what a charge carrier is and how they are formed. The basic ideas or concepts of band theory are useful frameworks for establishing the origins of electronic conduction and charge carriers.

### **1.1.3.1 Band Theory of Solids**

According to Huckel theory,  $\pi$  and  $\pi^*$  orbitals are separated by an energy (Figure 1.4). For example if two ethylene molecules are stacked directly on top of one another and are allowed to interact, two sets of two molecular orbitals are formed that are separated by an energy. As more and more ethylene units accumulate, the corresponding number of  $\pi$  and  $\pi^*$  states are formed with two electrons per state. As the number of units becomes larger, the states begin to form a continuous band. In the case of ethylene, the preferred energy state is the bonding state and the band formed by the  $\pi$  states will be entirely full as shown. This band is the highest occupied molecular orbital (HOMO) or valence band. Also, the highest occupied state is called the Fermi Level. The  $\pi^*$  state will be empty and is called the lowest unoccupied molecular orbital (LUMO) or conduction band.

According to band theory, for a polymer to be conductive an electron must be moved from the highest occupied state to the next lowest unoccupied state, which will be from the valence band to the conduction band. The energy that it takes to create this electron jump can come from various energy sources

(heat, photon, etc.). Looking at Figure 1.4, the most obvious problem with the electron moving into the conduction band is the gap between the bands that the electron must traverse. The region between the bands represents forbidden energy levels. This forbidden region is called a band gap and the energy represented by the gap,  $E_g$ , defines what type of conductor the material is, namely insulator or semiconductor. Typically, a semiconductor has a band gap in the range of 0.5 to 3.0 eV, while insulators have gaps greater than 3.0 eV. Diamond, for example, is an excellent insulator and has a band gap of 6.0 eV.

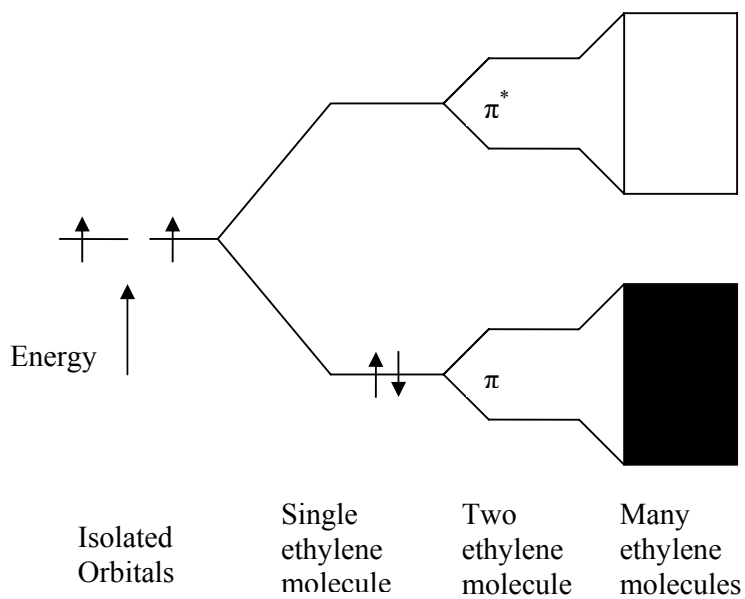


Figure 1.4 Formation of energy bands and band gap based on the theoretical stacking of ethylene units. [34]

### 1.1.3.2 Conduction Mechanism

In 1977 it was discovered that by doping the polymer one could improve conductivity by several orders of magnitude [3]. Doping a polymer means more than just oxidizing or reducing the polymer to give electrons or create holes in the bands. Doping is the creation of defects in the polymer's structural chain without destroying the chain. These defects in the polymer, which can be radicals, anions, cations or combinations of these, are the charge carriers. They are called solitons and polarons. Figure 1.5 shows the structure of solitons and polarons as well as bi-solitons and bi-polarons.

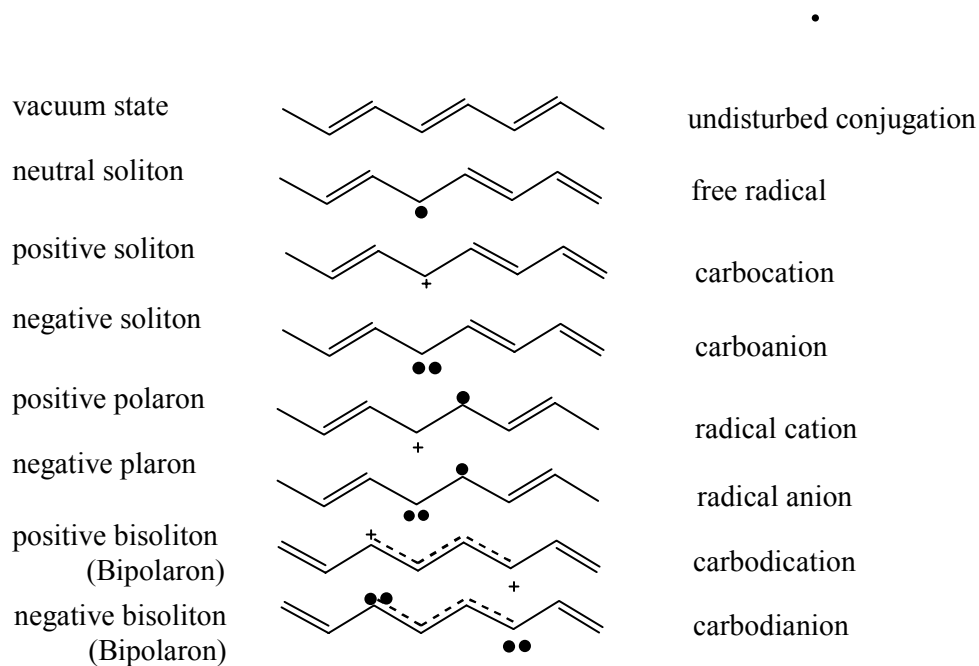


Figure. 1.5 Physical-chemical “dictionary” for defects in conjugated chains [35].

Polypyrrole as an example, (see Figure 1.6) when an electron is removed from the chain, a radical cation or polaron is formed. A polaron has both a bonding and an antibonding state. These states show up in the mid gap with the bonding state holding the unpaired electron. Removal of another electron creates another polaron and the mid gap states are now both empty because the electrons, having formed a new  $\pi$  bond, will reenter the HOMO band. Rearrangement of the polarons gives rise to a carbocation species or bipolaron. Each of the cations by themselves represents a positive soliton. As the number of bipolarons formed increases, so does the density of the bipolaron states in the mid gap. When the number of states becomes large enough, bipolaron bands are formed just as the valence and conduction bands are formed. A very important event has just occurred; a new band has been created much closer to the valence band that provides a much lower energy gap for an electron to move into facilitate conduction. This is what gives conducting polymers their semiconductor properties. Therefore the conductivity of the conducting polymer being investigated will be affected by the number of bipolarons or charge carriers formed.

### **1.1.3.3 Movement of the Charge Carrier Through Polypyrrole**

Once charge carriers are formed in polypyrrole the charge transport is characterized by inter- and intra-chain hopping [34]. Intra-chain hopping has been thoroughly investigated [37-40]. The most widely used model for

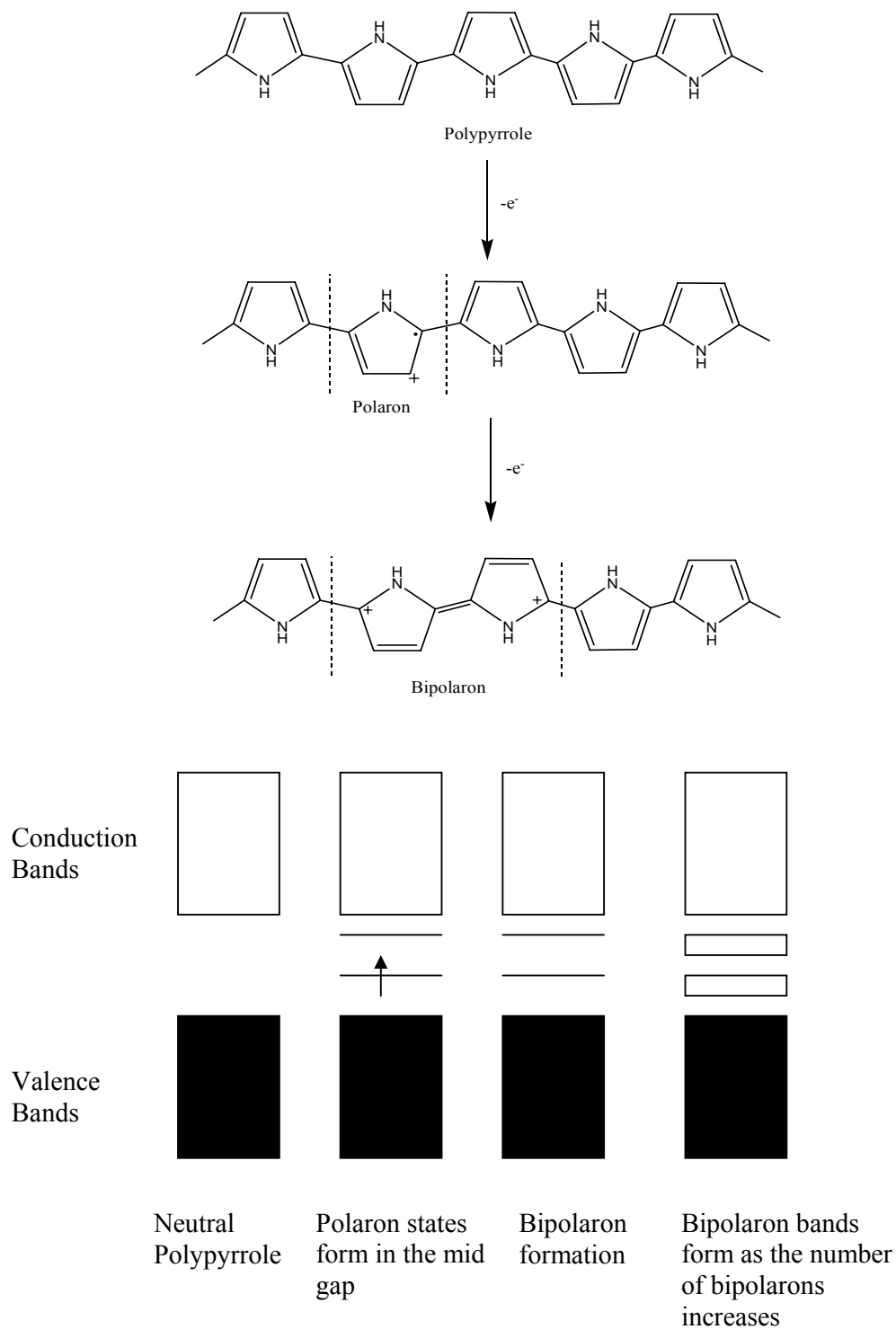


Figure 1.6 Structural representation of bipolaron formation in polypyrrole and its corresponding energy bands in the mid gap [36]



movement of a charge is given by Mott [36] which most accurately predicts the behavior of a charge carrier “hopping” along the chain. Mott’s model works for polypyrrole at low doping levels, however, it is not valid as the doping level increases. This would seem to suggest that the conductivity is limited by the inter-chain hopping or, in other words, the transport of charge from one chain to another.

Intra-chain mechanisms remain something of a mystery. This is largely due to the fact that it is difficult to show exactly what is hopping. Several possibilities are plausible. (1) the transport of an entire bipolaron as if it were a particle hopping from one chain to another; (2) the transport of the bipolaron as its component solitons, coming together on the receiving chain to reform the bipolaron; (3) as each component soliton hops it meets a soliton on the receiving chain to form new bipolarons

#### **1.1.4 Synthesis of Conducting Polymers**

Conducting polymers can be synthesized via chemical or electrochemical routes, although the former has been largely superseded by electrochemical methods. However, many polymers, most notably polyacetylene, are still only accessible via chemical synthesis.

##### **1.1.4.1 Chemical Synthesis**

A large number of conducting polymers can be synthesized via catalytic oxidation [41, 24]. However, control over polymer morphology is extremely limited, purification can be problematic and processing is virtually impossible.

However, a number of alternative synthetic routes have been developed which involve soluble precursor polymers.

Polyheterocycles are usually polymerized with  $\text{FeCl}_3$  as the chemical oxidant, although other oxidants can also be used. Reduction to the neutral state is accomplished by addition of a strong base such as ammonium hydroxide or hydrazine. Benzene can also undergo oxidative polymerization with  $\text{AlCl}_3/\text{CuCl}_2$  to yield poly (*p*-phenylene).

#### **1.1.4.2 Electrochemical Synthesis**

Electrochemical synthesis of conducting polymers offers many advantages over chemical synthesis, including the *in-situ* deposition of the polymer at the electrode surface, and, hence, eliminating processibility problems and the control of the thickness, morphology and degree of polymer doping by the quantity of charge passed. In addition, the polymers are simultaneously oxidized to their doped conducting forms during polymer growth.

Electropolymerization is achieved by the electro-oxidation of the heterocycle in an inert organic solvent containing a supporting electrolyte [42]. A schematic of the generally accepted mechanism for electropolymerization of five membered heterocycles [27] is shown in Figure 1.7. The initial electrochemical step (E) is a one electron oxidation of the monomer to form its radical cation. A high concentration of these species is maintained at the anode surface because the rate of electron transfer greatly exceeds the monomer diffusion rate to the electrode surface. The second step, a chemical reaction (C), involves the spin-pairing of two radical cations to form a dihydro dimer

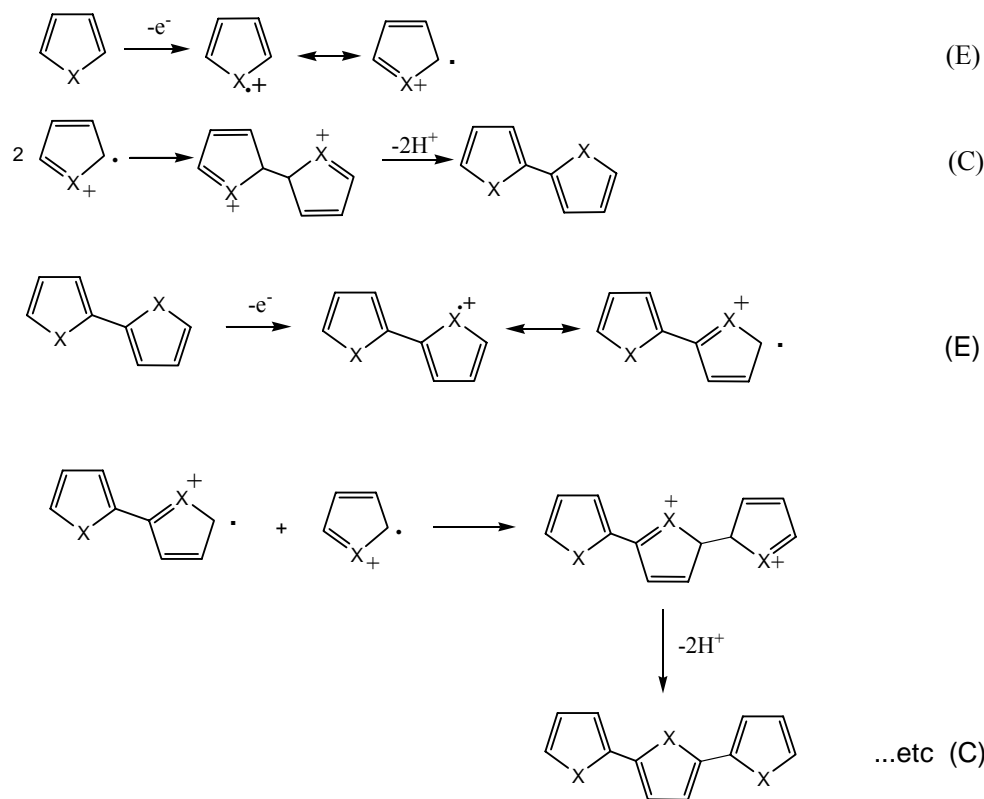


Figure 1.7 Proposed mechanism for the electrochemical polymerization of aromatic five membered heterocycles; where X=NH, S, or O.

dication, which subsequently undergoes the loss of two protons and re-aromatization to form the dimer. Aromatization is the driving force of the chemical step (C). Coupling occurs primarily through the  $\alpha$ -carbon atom of the heterocyclic ring since these are the positions of highest unpaired electron  $\pi$ -spin density and hence reactivity. At the applied potential, the dimer, which is more easily oxidized than the monomer, exists in a radical cation form and undergoes further coupling reactions with other radical cations. This electropolymerization mechanism, according to the general scheme E(CE)<sub>n</sub> continues until the

oligomer becomes insoluble in the electrolytic medium and precipitates on the anode surface [43]. Non- $\alpha,\alpha'$ -linkages (e.g.  $\alpha,\beta'$  and  $\beta,\beta'$  coupling) can occur to variable extents, causing breaks in conjugation and hence, reduction in film conductivity.

Since conjugated oligomers are oxidized at less positive potentials than their corresponding monomer, polymer oxidation occurs concurrently with electro-deposition. Typically, one electron is removed from the polymeric backbone for every three-four monomer units to form polar structures, responsible for inherent conductivity. Anions, termed 'dopants', are thus incorporated into the film to maintain electro-neutrality. The doping terminology of conductive polymers should be distinguished from its conventional use in semi-conductor physics, since considerably higher concentration of dopants are employed in the former, typically up to 33% [44].

The type of counterion used can greatly affect the conductivity of the film [45]. For example, for equal degrees of doping, polypyrrole typically has conductivities in the range of 30-100  $\text{Scm}^{-1}$  with tetrafluoroborate ion, whereas with perchlorate anions, enhanced conductivities of 60-200  $\text{Scm}^{-1}$  can be achieved [46].

### **1.1.5 Conducting Copolymers**

Synthesis of conducting copolymer composites, graft and block copolymers is a method used to overcome the drawbacks of conducting polymers which are insoluble, hard and brittle. Properties of conducting polymers can be controlled by the incorporation of two or more structurally

different units into the same polymer chain. Copolymers from pyrrole, pyrrole derivatives, thiophene, bithiophene and other combination of aromatic compounds have been reported [47-51].

Electropolymerization of the conducting component on electrode previously coated with the insulating polymer is common approach for the preparation of conducting composites and copolymers. Electrochemical polymerization of pyrrole and thiophene may occur on an ordinary insulating polymer film [52-54].

Polycarbonate and polystyrene [55], poly (methyl methacrylate) [56-58], polyimide[59], polyamide[60], polysiloxanes[61], poly(tetrahydrofuran) [62, 63] were previously used as the host matrices.

#### **1.1.6 Characterization of Conducting Polymers**

Conducting polymers can be characterized by a variety of analytical techniques. Many examples exist in the literature, some of which include; cyclic voltammetry for understanding redox processes in the conducting polymers, optical characterization of conducting polymers for non-linear optical materials, nuclear magnetic resonance for structure confirmation, chain orientation and molecular motion, gel permeation chromatography for molecular weight, differential scanning calorimetry and thermogravimetry analysis for evidence of glass and melting transitions and decomposition temperatures.

### **1.1.6.1 Cyclic Voltammetry**

Cyclic voltammetry is one of the most useful methods, which allows one to scan the potential of the working electrode in the anodic and cathodic directions. It allows one to observe the peaks due to the redox behavior of a substrate. Cyclic voltammetry gives the exact reaction potentials of the monomer as well as the information about the chemical reactions present during the process. Also, it can easily be understood from the cyclic voltammograms whether the chemical reaction is reversible or not.

In cyclic voltammograms, current response is plotted as a function of applied potential. The current depends on the voltage scan rate, rate of electron transfer and diffusion layer of the electroactive substrate to the surface of the electrode.

### **1.1.7 Applications of Conducting Polymers**

The application of conducting polymers can be divided into three main classes. The first use is in their neutral form, which provides the advantages of their semi-conducting and luminescent properties. Examples of applications are semi-conducting materials for field effect transistors [64], and active material in an electroluminescent device [65, 66]. The second category of applications involves using the polymer in its doped or conducting form, and some representative applications in this category are electrostatic charge dissipation and EMI shielding [67, 68], electrode materials for capacitors [69, 70], and enzyme immobilization [71-73]. The third category uses the ability of the polymer to reversibly switch between its conducting and reduced forms. Upon

switching between two states, the polymer undergoes color, conductivity and volume changes. Applications that use these properties include battery electrodes [74], actuators [75], sensors [76], drug delivery [77], electrochromics [78-80].

## **1.2 Enzymes**

Enzymes have a number of distinct advantages over conventional chemical catalysts. Foremost amongst these are their specificity and selectivity not only for particular reactions but also in their discrimination between similar parts of molecules (regiospecificity) or optical isomers (stereospecificity). They catalyze only the reactions of very narrow ranges of reactants (substrates), which may consist of a small number of closely related classes of compounds (e.g. trypsin catalyzes the hydrolysis of some peptides and esters in addition to most proteins), a single class of compounds (e.g. hexokinase catalyses the transfer of a phosphate group from ATP to several hexoses), or a single compound (e.g. glucose oxidase oxidizes only glucose amongst the naturally occurring sugars). This means that the chosen reaction can be catalysed to the exclusion of side-reactions, eliminating undesirable by-products. Thus, higher productivities may be achieved, reducing material costs. As a bonus, the product is generated in an uncontaminated state so reducing purification costs and the downstream environmental burden. Often a smaller number of steps may be required to produce the desired end-product. In addition, certain stereospecific reactions (e.g. the conversion of glucose into fructose) cannot be achieved by classical chemical methods without a large expenditure of time and effort.

Enzymes work under generally mild processing conditions of temperature, pressure and pH. This decreases the energy requirements, reduces the capital costs due to corrosion-resistant process equipment and further reduces unwanted side-reactions. The high reaction velocities and straightforward catalytic regulation achieved in enzyme-catalyzed reactions allow an increase in productivity with reduced manufacturing costs due to wages and overheads[81, 82].

There are some disadvantages in the use of enzymes which cannot be ignored but which are currently being addressed and overcome. In particular, the high cost of enzyme isolation and purification still discourages their use, especially in areas which currently have an established alternative procedure. The generally unstable nature of enzymes, when removed from their natural environment, is also a major drawback to their more extensive use[83]. These drawbacks can be eliminated by enzyme immobilization

The existence of enzymes has been known for well over a century. Some of the earliest studies were performed in 1835 by the Swedish chemist Jon Jakob Berzelius who termed the chemical action “catalytic”. It was not until 1926, however, that the first enzyme was obtained in pure form, a feat accomplished by James B. Sumner of Cornell University. Sumner was able to isolate and crystallize the enzyme urease from the jack bean. His work was to earn him the 1947 Nobel Prize.

John H. Northrop and Wendell M. Stanley of the Rockefeller Institute for Medical Research shared the 1947 Nobel Prize with Sumner. They discovered a complex procedure for isolating pepsin. This precipitation



technique devised by Northrop and Stanley has been used to crystallize several enzymes [84-86]

All known enzymes are proteins. They are high molecular weight compounds made up principally of chains of amino acids linked together by peptide bonds. (Figure 1.8)

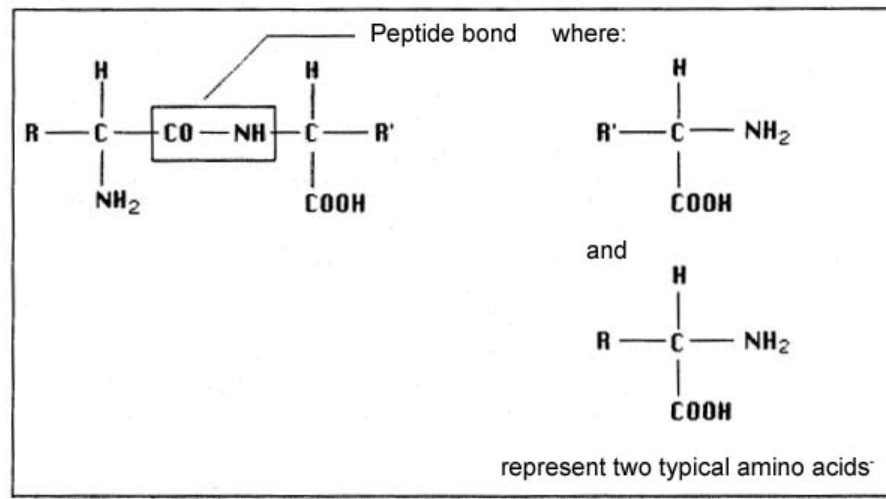


Figure 1.8 Typical Protein structure

### 1.2.1 Enzyme Nomenclature

All enzymes contain a protein backbone. In some enzymes this is the only component in the structure. However, there are additional non-protein moieties usually present which may or may not participate in the catalytic activity of the enzyme. Covalently attached carbohydrate groups are commonly encountered structural features which often have no direct bearing on the catalytic activity, although they may well affect an enzyme's stability and

solubility. Other factors often found are metal ions (cofactors) and low molecular weight organic molecules (coenzymes). These may be loosely or tightly bound by noncovalent or covalent forces. They are often important constituents contributing to both the activity and stability of the enzymes. This requirement for cofactors and coenzymes must be recognized if the enzymes are to be used efficiently and is particularly relevant in continuous processes where there may be a tendency for them to become separated from an enzyme's protein moiety.

Enzymes are classified according to the report of a Nomenclature Committee appointed by the International Union of Biochemistry (1984). This enzyme commission assigned each enzyme a recommended name and a 4-part distinguishing number. It should be appreciated that some alternative names remain in such common usage that they will be used, where appropriate, in this text. The enzyme commission (EC) numbers divide enzymes into six main groups according to the type of reaction catalyzed.

(1) Oxidoreductases which involve redox reactions in which hydrogen or oxygen atoms or electrons are transferred between molecules. This extensive class includes the dehydrogenases (hydride transfer), oxidases (electron transfer to molecular oxygen), oxygenases (oxygen transfer from molecular oxygen) and peroxidases (electron transfer to peroxide).

(2) Transferases which catalyse the transfer of an atom or group of atoms (e.g. acyl-, alkyl- and glycosyl-), between two molecules, but excluding such transfers as are classified in the other groups (e.g. oxidoreductases and hydrolases).

(3) Hydrolases which involve hydrolytic reactions and their reversal. This is presently the most commonly encountered class of enzymes within the field of enzyme technology and includes the esterases, glycosidases, lipases and proteases.

(4) Lyases which involve elimination reactions in which a group of atoms is removed from the substrate. This includes the aldolases, decarboxylases, dehydratases and some pectinases but does not include hydrolases

(5) Isomerases which catalyse molecular isomerizations and includes the epimerases, racemases and intramolecular transferases.

(6) Ligases, also known as synthetases, form a relatively small group of enzymes which involve the formation of a covalent bond joining two molecules together, coupled with the hydrolysis of a nucleoside triphosphate.

### **1.2.2 Enzyme Kinetics**

In order for a reaction to occur, reactant molecules must contain sufficient energy to cross a potential energy barrier, the activation energy. All molecules possess varying amounts of energy depending, for example, on their recent collision history but, generally, only a few have sufficient energy for reaction. The lower the potential energy barrier to reaction, the more reactants have sufficient energy and, hence, the faster the reaction will occur. All catalysts, including enzymes, function by forming a transition state, with the reactants, of lower free energy than would be found in the uncatalyzed reaction (Figure 1.9). Even quite modest reductions in this potential energy barrier may produce large increases in the rate of reaction (e.g. the activation energy for the

uncatalyzed breakdown of hydrogen peroxide to oxygen and water is  $76 \text{ kJ M}^{-1}$  whereas, in the presence of the enzyme catalase, this is reduced to  $30 \text{ kJ M}^{-1}$  and the rate of reaction is increased by a factor of  $10^8$ , sufficient to convert a reaction time measured in years into one measured in seconds).

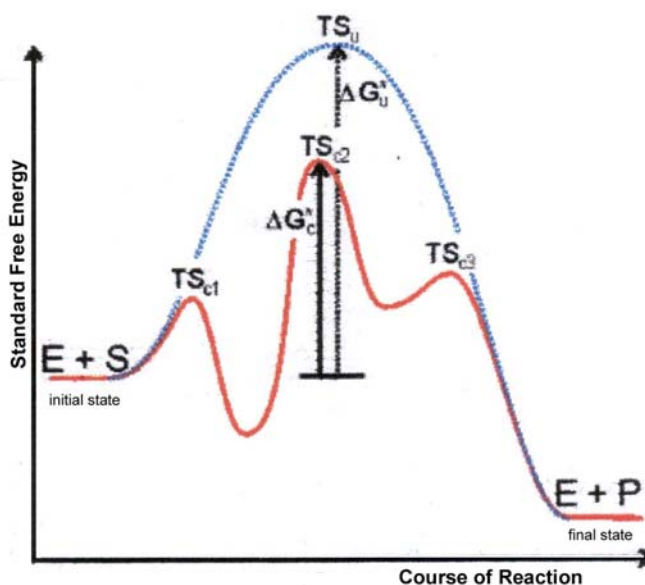


Figure 1.9. A schematic diagram showing the free energy profile of the course of an enzyme catalysed reaction involving the formation of enzyme-substrate (ES) and enzyme-product (EP) complexes, i.e.  $E + S \rightleftharpoons ES \rightleftharpoons EP \rightleftharpoons E + P$

### 1.2.2.1 Michaelis-Menten Equation

It is established that enzymes form a bound complex to their reactants (i.e. substrates) during the course of their catalysis and prior to the release of products. This can be simply illustrated, using the mechanism based on that of Michaelis and Menten [87, 81] for a one-substrate reaction, by the reaction sequence:

Enzyme+Substrate  $\rightleftharpoons$  (Enzyme-substrate complex)  $\rightarrow$  Enzyme +Product



where  $k_{+1}$ ,  $k_{-1}$  and  $k_{+2}$  are the respective rate constants, typically having values of  $10^5 - 10^8 \text{ M}^{-1} \text{ s}^{-1}$ ,  $1 - 10^4 \text{ s}^{-1}$  and  $1 - 10^5 \text{ s}^{-1}$  respectively; the sign of the subscripts indicating the direction in which the rate constant is acting. For the sake of simplicity the reverse reaction concerning the conversion of product to substrate is not included in this scheme. This is allowable (1) at the beginning of the reaction when there is no, or little, product present, or (2) when the reaction is effectively irreversible. Reversible reactions are dealt with in more detail later in this chapter. The rate of reaction ( $v$ ) is the rate at which the product is formed.

$$v = \frac{d[P]}{dt} = k_{+2}[ES] \quad (1.1)$$

where  $[ ]$  indicates the molar concentration of the material enclosed (i.e.  $[ES]$  is the concentration of the enzyme-substrate complex). The rate of change of the concentration of the enzyme-substrate complex equals the rate of its formation minus the rate of its breakdown, forwards to give product or backwards to regenerate substrate. Therefore:

$$\frac{d[ES]}{dt} = k_{+1}[E][S] - (k_{-1} + k_{+2})[ES] \quad (1.2)$$

During the course of the reaction, the total enzyme at the beginning of the reaction ( $[E]_0$ , at zero time) is present either as the free enzyme ( $[E]$ ) or the ES complex ( $[ES]$ ).

$$\text{i.e. } [E]_0 = [E] + [ES] \quad (1.3)$$

therefore:

$$\frac{d[ES]}{dt} = k_{+1}([E]_0 - [ES])[S] - (k_{-1} + k_{+2})[ES] \quad (1.4)$$

Gathering terms together,

$$\frac{d[ES]}{dt} = k_{+1}[E]_0[S] - k_{+1}[ES][S] - (k_{-1} + k_{+2})[ES]$$

$$\frac{d[ES]}{dt} = k_{+1}[E]_0[S] - (k_{+1}[S] + k_{-1} + k_{+2})[ES]$$

this gives:

$$\frac{\frac{d[ES]}{dt}}{k_{+1}[S] + k_{-1} + k_{+2}} + [ES] = \frac{k_{+1}[E]_0[S]}{k_{+1}[S] + k_{-1} + k_{+2}} \quad (1.5)$$

The differential equation 1.5 is difficult to handle, but may be greatly simplified if it can be assumed that the left hand side is equal to [ES] alone. This assumption is valid under the sufficient but unnecessarily restrictive steady state approximation that the rate of formation of ES equals its rate of disappearance by product formation and reversion to substrate (i.e.  $d[ES]/dt$  is zero). It is additionally valid when the condition:

$$\frac{\frac{d[ES]}{dt}}{k_{+1}[S] + k_{-1} + k_{+2}} \ll [ES] \quad (1.6)$$

is valid. This occurs during a substantial part of the reaction time-course over a wide range of kinetic rate constants and substrate concentrations and at low to moderate enzyme concentrations. The variation in [ES],  $d[ES]/dt$ , [S] and [P]

with the time-course of the reaction is shown in Figure 1.10, where it may be seen that the simplified equation is valid throughout most of the reaction.

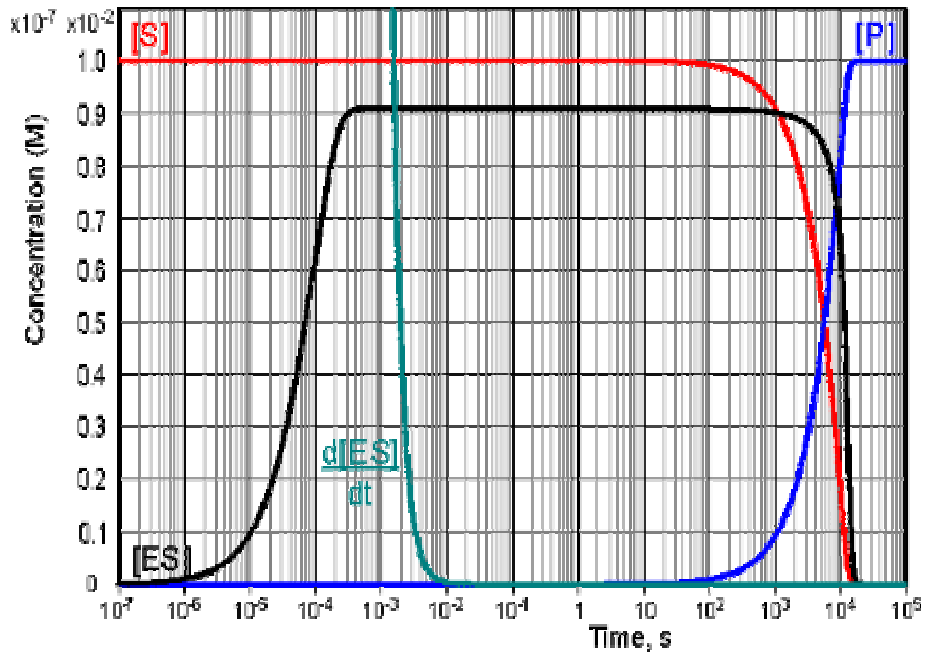


Figure 1.10. Computer simulation of the progress curves of  $d[ES]/dt$ ,  $[ES]$ ,  $[S]$  and  $[P]$  for a reaction obeying simple Michaelis-Menten kinetics

$\frac{d[ES]}{dt}$  is much less than  $[ES]$  during both of the latter two phases.

The Michaelis-Menten equation (below) is simply derived from equations 1.1 and 1.5, by substituting  $K_m$  for  $\frac{k_{-1} + k_{+2}}{k_{+1}}$ .  $K_m$  is known as the Michaelis constant with a value typically in the range  $10^{-1}$  -  $10^{-5}$  M. When  $k_{+2} \ll k_{-1}$ ,  $K_m$  equals the dissociation constant ( $k_{-1}/k_{+1}$ ) of the enzyme substrate complex.

$$v = k_{+2}[ES] = \frac{k_{+2}[E]_0[S]}{[S] + K_m} \quad (1.7)$$

or, more simply

$$v = \frac{V_{\max}[S]}{[S] + K_m} \quad (1.8)$$

where  $V_{\max}$  is the maximum rate of reaction, which occurs when the enzyme is completely saturated with substrate (i.e. when  $[S]$  is very much greater than  $K_m$ ,  $V_{\max}$  equals  $k_{+2}[E]_0$ , as the maximum value  $[ES]$  can have is  $[E]_0$  when  $[E]_0$  is less than  $[S]_0$ ). Equation 1.8 may be rearranged to show the dependence of the rate of reaction on the ratio of  $[S]$  to  $K_m$ ,

$$v = \frac{V_{\max}}{1 + \frac{K_m}{[S]}} \quad (1.9)$$

and the rectangular hyperbolic nature of the relationship, having asymptotes at  $v = V_{\max}$  and  $[S] = -K_m$ ,

$$(V_{\max} - v)(K_m + [S]) = V_{\max}K_m \quad (1.10)$$

The substrate concentration in these equations is the actual concentration at the time and, in a closed system, will only be approximately equal to the initial substrate concentration ( $[S]_0$ ) during the early phase of the reaction. Hence, it is usual to use these equations to relate the initial rate of reaction to the initial, and easily predetermined, substrate concentration (Figure 1.11).





Figure 1.11 A normalized plot of the initial rate ( $v_0$ ) against initial substrate concentration ( $[S]_0$ ) for a reaction obeying the Michaelis-Menten kinetics (equation 1.8).

### 1.2.2.2 Lineweaver- Burk Plot

The graph of the Michaelis-Menten equation,  $v_0$  against  $[S_0]$  (Figure 1.11), is not entirely satisfactory for the determination of  $V_{\max}$  and  $K_m$ . Unless after a series of experiments, there are at least three consistent points on the plateau of the curve at different  $[S_0]$  values, then an accurate value of  $V_{\max}$ , and hence of  $K_m$ , cannot be obtained: the graph, being a curve, cannot be accurately extrapolated upwards from values of  $[S_0]$  which are far from saturating.

Lineweaver and Burk [81] overcame this problem without making any fresh assumptions. They simply took the Michaelis-Menten equation

$$v = \frac{V_{\max}[S]}{[S] + K_m}$$

and inverted it:

$$\frac{1}{v_0} = \frac{[S_0] + K_m}{V_{\max}[S_0]} = \frac{[S_0]}{V_{\max}[S_0]} + \frac{K_m}{V_{\max}[S_0]} \quad (1.11)$$

$$\frac{1}{v_0} = \frac{K_m}{V_{\max}} \cdot \frac{1}{[S_0]} + \frac{1}{V_{\max}} \quad (1.12)$$

This is of the form of  $y=mx + c$ , which is the equation of a straight line graph; a plot of  $y$  against  $x$  has a slope  $m$  and intercept  $c$  on the  $y$ -axis.

A plot of  $1/v_0$  against  $1/[S_0]$  (the Lineweaver-Burk plot) for systems obeying the Michaelis-Menten equation is shown in Figure 1.12. the graph being linear, can be extrapolated even if no experiment has been performed at anything approximating to a saturating substrate concentration, and from the extrapolated graph the values of  $K_m$  and  $V_{\max}$  can be determined as shown in Figure 1.12.

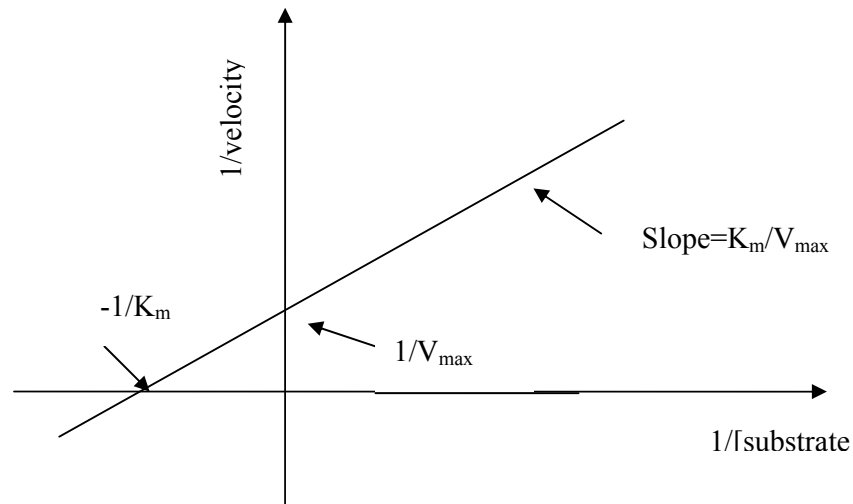


Figure 1.12 The Lineweaver-Burk Plot

### **1.2.3 Enzyme Immobilization**

The term 'immobilized enzyme' was adopted at the first Enzyme Engineering Conference, held at Hennicker, New Hampshire, in 1971. It describes 'enzyme physically confined at or localized in a certain region of space with retention of their catalytic activity, and which can be used repeatedly and continuously'. [88]

#### **1.2.3.1 Benefits of Enzyme Immobilization**

Immobilization is the conversion of enzymes from a water-soluble, mobile state to a water-insoluble, immobile state. It prevents enzyme diffusion in the reaction mixtures and facilitates their recovery from the product stream by solid liquid separation techniques. The advantages of immobilization are (1) multiple and repetitive use of a single batch of enzymes; (2) creation of buffer by the support against changes in pH, temperature and ionic strength in the bulk solvent, as well as protection from shear forces; (3) no contamination of processed solution with enzyme; and (4) analytical considerations, especially with respect to long-life for activity and predictable decay rates. Generally, an enzyme is attached to a solid support material so that substrate can be continually converted to product. Thus enzymes can be recycled and used many times. The goals are to increase the enzyme's stability, to increase the ability to recycle the enzyme, and to separate the enzyme easily from the product. [89]

### **1.2.3.2 Immobilization Methods**

When immobilizing an enzyme to a surface, it is most important to choose a method of attachment that will prevent loss of enzyme activity by not changing the chemical nature or reactive groups in the binding site of the enzyme. In other words, attach the enzyme but do as little damage as possible. Considerable knowledge of the active site of the enzyme will prove helpful in achieving this task. It is desired to avoid reaction with the essential binding site group of the enzyme. Alternatively, an active site can be protected during attachment as long as the protective groups can be removed later on without loss of enzyme activity. In some cases, this protective function can be fulfilled by a substrate or a competitive inhibitor of the enzyme.

The surface on which the enzyme is immobilized is responsible for retaining the structure in the enzyme through hydrogen bonding or the formation of electron transition complexes. These links will prevent vibration of the enzyme and thus increase thermal stability. The micro environment of surface and enzyme has a charged nature that can cause a shift in the optimum pH of the enzyme. This may be accompanied by a general broadening of the pH region in which the enzyme can work effectively, allowing enzymes that normally do not have similar pH regions to work together.

#### ***1. Carrier-Binding***

The carrier-binding method is the oldest immobilization technique for enzymes. In this method, the amount of enzyme bound to the carrier and the

activity after immobilization depend on the nature of the carrier. The following picture shows how the enzyme is bound to the carrier:

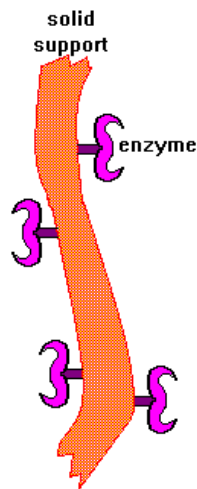


Figure 1.13 Schematic representaion of Carrier-binding type enzyme immobilization.

The selection of the carrier depends on the nature of the enzyme itself, as well as the particle size, surface area, molar ratio of hydrophilic to hydrophobic groups and chemical composition.

In general, an increase in the ratio of hydrophilic groups and in the concentration of bound enzymes, results in a higher activity of the immobilized enzymes. Some of the most commonly used carriers for enzyme immobilization are polysaccharide derivatives such as cellulose, dextran, agarose, and polyacrylamide gel.

According to the binding mode of the enzyme, the carrier-binding method can be further sub-classified into:

### Physical Adsorption

This method for the immobilization of an enzyme is based on the physical adsorption of enzyme protein on the surface of water-insoluble carriers. Hence, the method causes little or no conformational change of the enzyme or destruction of its active center. If a suitable carrier is found, this method can be both simple and cheap. However, it has the disadvantage that the adsorbed enzyme may leak from the carrier during use due to a weak binding force between the enzyme and the carrier [90].

### Ionic Binding

The ionic binding method relies on the ionic binding of the enzyme protein to water-insoluble carriers containing ion-exchange residues.

Polysaccharides and synthetic polymers having ion-exchange centers are usually used as carriers. The binding of an enzyme to the carrier is easily carried out, and the conditions are much milder than those needed for the covalent binding method. Hence, the ionic binding method causes little changes in the conformation and the active site of the enzyme. Therefore, this method yields immobilized enzymes with high activity in most cases.

Leakage of enzymes from the carrier may occur in substrate solutions of high ionic strength or upon variation of pH. This is because the binding forces between enzyme proteins and carriers are weaker than those in covalent binding.

The main difference between ionic binding and physical adsorption is that the enzyme to carrier linkages are much stronger for ionic binding although weaker than in covalent.

## Covalent Binding

The most intensely studied of the immobilization techniques is the formation of covalent bonds between the enzyme and the support matrix. When trying to select the type of reaction by which a given protein should be immobilized, the choice is limited by two characteristics: (1) the binding reaction must be performed under conditions that do not cause loss of enzymatic activity, and (2) the active site of the enzyme must be unaffected by the reagents used.

The conditions for immobilization by covalent binding are much more complicated and less mild than in the cases of physical adsorption and ionic binding. Therefore, covalent binding may alter the conformational structure and active center of the enzyme, resulting in major loss of activity and/or changes of the substrate. However, the binding force between enzyme and carrier is so strong that no leakage of the enzymes occurs, even in the presence of substrate or solution of high ionic strength.

## ***2. Cross-linking***

Immobilization of enzymes has been achieved by intermolecular cross-linking of the protein, either to other protein molecules or to functional groups on an insoluble support matrix. Cross-linking an enzyme to itself is both expensive and insufficient, as some of the protein material will inevitably be acting mainly as the support. This will result in relatively low enzymatic activity. Generally, cross-linking is best used in conjunction with one of the

other methods. It is used mostly as a means of stabilizing adsorbed enzymes and also for preventing leakage. [91].

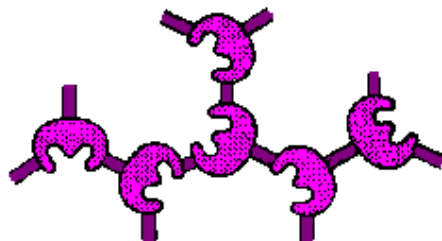


Figure 1.14 Schematic representation of Cross-Linking type enzyme immobilization.

The most common reagent used for cross-linking is glutaraldehyde. Cross-linking reactions are carried out under relatively severe conditions. These harsh conditions can change the conformation of active center of the enzyme; and so may lead to significant loss of activity.

### ***3. Entrapping Enzymes***

The entrapment method of immobilization is based on the localization of an enzyme within the lattice of a polymer matrix or membrane. It is done in such a way as to retain protein while allowing penetration of substrate. It can be classified into **lattice** and **micro capsule** types [92].

This method differs from the covalent binding and cross linking in that the enzyme itself does not bind to the gel matrix or membrane. This results in a wide applicability. The conditions used in the chemical polymerization reaction



are relatively severe and result in the loss of enzyme activity. Therefore, careful selection of the most suitable conditions for the immobilization of various enzymes is required.

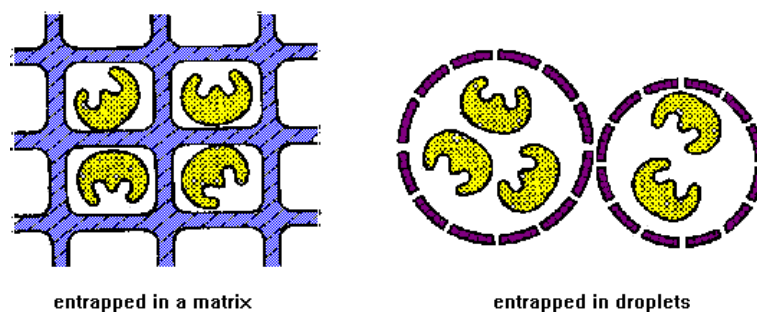


Figure 1.15 Schematic representation of entrapping enzyme

**Lattice-Type** entrapment involves entrapping enzymes within the interstitial spaces of a cross-linked water-insoluble polymer. Some synthetic polymers such as *polyarylamide*, *polyvinylalcohol*, etc... and natural polymer (starch) have been used to immobilize enzymes using this technique.

**Microcapsule-Type** entrapping involves enclosing the enzymes within semi permeable polymer membranes.

#### 1.2.4 Invertase

$\beta$ -fructofuranosidase (E.C No.3.2.1.26) catalysis the hydrolysis of sucrose to glucose and fructose which is known as the invert sugar. Sucrose crystallizes more readily than invert sugar, so the latter is widely used in the production of noncrystallizing creams, in making jam and artificial honey.

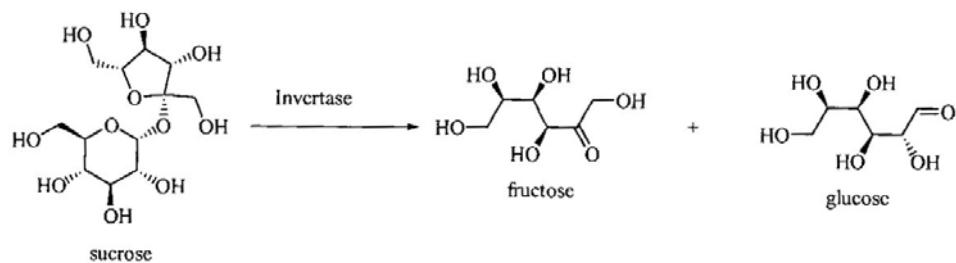


Figure 1.16 Hydrolysis of sucrose

Invertase occurs in the small intestine of mammals and in the tissues of certain animals and plants. It may be obtained in a relatively pure state from yeast, which is a very good source.

Although, invertase has rather lower probability of achieving commercial use in immobilized form, it is one of the most studied of all enzymes because of being a model enzyme for experimental purposes.

Invertase has been immobilized to a wide range of carriers by a large number of techniques [93-97]. Entrapment of invertase in various conducting polymer matrices by electropolymerization was described in detail by our group [98-100].

### 1.2.5 Polyphenol Oxidase (Tyrosinase)

One of the most “versatile” enzymes in nature is tyrosinase (EC. No. 1.14.18.1). Tyrosinase was discovered by Bertnard and Bourquelot about 100 years ago. In analyzing certain varieties of mushrooms, they observed that as

oxidation progressed, the mushrooms changed color and finally become dark brown or black. Subsequently studies showed that this new oxidase catalyzed the aerobic oxidation of mono-phenols, and the final product of tyrosine oxidation was melanin [101].

Tyrosinase is a tetramer which weights about 130,000 Daltons. Its active site contains two copper atoms which exist in three states; met, oxy, and deoxy. It occurs extensively in the pylogenetic scale. The enzyme is commonly found in yeast, mushrooms, grapes, bananas, apples, potatoes, frogs and mammals.

Tyrosinase catalyzes two reactions via separate active sites:

- (1) the orthohydroxylation of monophenols, commonly referred to as the cresolase activity and
- (2) the oxidoreduction of orthodiphenols to orthoquinones, commonly referred to as the catecholase activity.

Tyrosinase catalyzes the synthesis of melanin through the hydroxylation of tyrosine to dihydroxyphenylalanine (DOPA) and the subsequent oxidation of DOPA to dopaquinone. The unstable dopaquinone will polymerize and precipitate into melanin. However, in the presence of a reductor, the reaction will stop at the diphenol level [102]. The cresolase activity of tyrosinase is of particular importance because it synthesizes DOPA. DOPA is a precursor of dopamine, an important neural message transmitter. Patients who suffer from

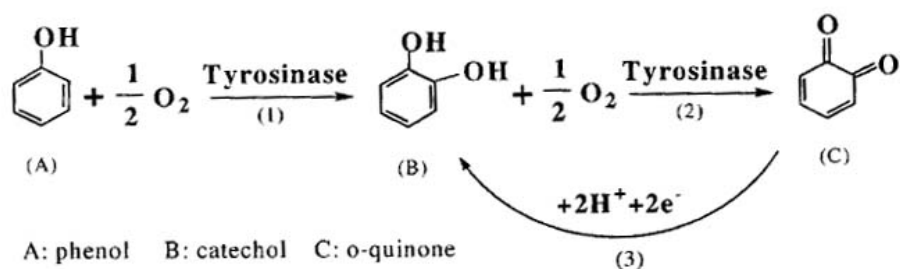


Figure 1.17 Schematic representation of tyrosinase activity.

Parkinson's disease shows a significant decrease in the concentration of dopamine found in the substantia nigra of the brain. [103].

The catecholase activity also has important applications, since this activity can be used in the analysis of phenols and its derivatives. Phenolic pollutants are frequently found in surface waters and in the effluent of industrial discharge sources. Some of the industrial sources of phenol discharge include oil refineries, coke and coal conversion plants, plastics and petrochemical companies, dyes, textiles, timber, mining, and the pulp and paper industries. Virtually all phenols are toxic. Moreover, they have a high oxygen demand and can deplete the oxygen in the body of water [104]. As a consequence, this may affect the ecosystem of water sources where phenols are discharged.

Atlow et al. [105] have reported a successful application of soluble tyrosinase in the "cleansing" of polluted waters. Tyrosinase causes the precipitation of phenols, which can then be filtered out from surface waters and

industrial discharge sources. The enzyme has also been used as a sensor to detect the concentration of phenols in waste water [106-107].

The detection of phenols is not only of importance in industry but also in the medical field. Tyrosinase has been used as part of an enzyme-electrode system to detect catechols and assess catecholamines in the urine of patients with neural crest tumors [108].

Tyrosinase also has applications in the food industry, as it is responsible for the browning of fruits and vegetables. Interest in the enzyme has been demonstrated by tannin oil companies due to the role that it plays in melanogenesis. Also, it has been considered for use in melanin-related disorders, such as albinism, vitiligo, and melanoma [109].

Although tyrosinase has widespread applications, its use is limited by its inherent instability and rapid inactivation. By using enzyme immobilization technology, good operational stability and long-term stability can be achieved for tyrosinase.

### **1.2.6 Phenolics in Wines**

Wine contains many phenolic substances. The phenolics have a number of important functions in wine affect the tastes of bitterness and astringency, especially in red wines. Second, the color of red wine is caused by phenolics. They are also bactericidal agents and impart antioxidant properties, being especially found in the skin and seeds of the grapes.

There are two types of phenols in wines. “flavonoids” and “non-flavonoids”. The flavonoids are composed of three benzene rings and react

readily, binding to other molecules and there are between 6,000 and 8,000 species of flavonoids. A group of flavonoids, called the flavon-3-ols, have been well characterized in wine. Flavon-3-ols are usually concentrated in grape seeds, stems and skin. When these parts of the grape are left in for as long as possible during the wine-making process, more flavon-3-ols end up in the resulting wine than if the seeds, stems and skin are removed earlier.

The non-flavonoids in wine comprise many classes of chemicals including hydroxycinnamates, benzoates, and stilbenes. Much ado has been made in the media about the health benefits of a particular kind of stilbene, called "resveratrol," which is unique to grapes and is not found in other fruits or vegetables.

The chemical composition of a wine is influenced by the climatic and atmospheric conditions, soil type, vine cultivation and the treatment to which it is subjected. Due to this reason amount of phenolics vary from one brand and type of wine to another. Process difference cause red wines to contain almost ten times higher amount of phenolics.

The typical methods for the determination of phenolic compounds are gas and liquid chromatography. These methods involve complex sample pre-treatment procedures and are unsuitable for on site or field based analyses.

A biosensing approach with advantages of high specificity, high sensitivity and rapid detection mechanism may provide a solution [110, 111]. In this study immobilization of polyphenol oxidase enzyme in a conducting polymer electrode was studied as an alternative method for the determination of phenolic compounds.

### **1.3 Aim of the Study**

- (a) To achieve the synthesis of menthyl ester of 3-thiophene acetic acid and characterization.
- (b) To synthesize the conducting copolymers of menthyl ester of 3-thiophene acetic acid with thiophene or pyrrole and to investigate the electrochemical, thermal, morphological and conducting properties of resultant copolymers.
- (c) To check the possibility of enzyme immobilization, invertase and tyrosinase, in copolymers obtained via electrochemical polymerization and to characterize the enzyme electrodes.
- (d) To determine the phenolic compound concentration in red wines by using the tyrosinase electrodes.

## CHAPTER 2

### EXPERIMENTAL

#### 2.1 Chemicals

Acetonitrile (AN) (Merck), methanol (Merck), nitromethane (NM) (Sigma), tetrabutylammonium tetrafluoroborate (TBAFB), *p*-toluene sulfonic acid (PTSA) (Sigma) and sodium dodecylsulfate (SDS) (Aldrich) were used without further purification. Pyrrole and thiophene (Aldrich) were distilled just before use. Dichloromethane was purified by usual methods and dried over CaH<sub>2</sub> or Na wire. Thiophene-3-acetic acid (Fluka) and menthol (Fluka) were used as received.

Invertase ( $\beta$ -fructofuranoxidase), type V (E.C no 3.2.1.26) and Tyrosinase (PPO) [E.C 1.14.18.1] was purchased from Sigma. Substrate for invertase, sucrose, was obtained from Merck. For the preparation of Nelson Reagent that is used in the assay of invertase activity, sodium carbonate (Riedel de Haen), sodium potassium tartarate (Riedel de Haen), sodium bicarbonate (Merck), sodium sulfate (Merck), copper sulfate (Merck) were used as received. For the preparation of



arsenomolibdate reagent, ammonium heptamolibdate (Merck) sodium hydrogen arsenate (Merck) were used as received

3-methyl-2-benzothiazolinone (MBTH), acetone and sulfuric acid used in spectrophotometric activity determination of PPO were also obtained from Sigma. For the preparation of citrate buffer, tri-sodium citrate-2 hydrate and citric acid were used as received. Catechol was purchased from Sigma. All catechol solutions were prepared in citrate buffer.

Bovine serum albumin and Folin & Ciocalteu's Phenol Reagent (Sigma) were used as purchased

## **2.2 Instrumentation**

### **2.2.1 Electolysis**

The electrochemical techniques generally used in the electrochemical synthesis of conducting polymers are constant potential (potentiometric) or constant current (galvanostatic) electrolysis.

Constant current electrolysis (CCE) is carried out in a two electrode system which are working and counter electrodes. The current is controlled during the electrolysis and the potential is allowed to alter. The film thickness can be easily controlled by inspection of the polymerization time. The increase in the film resistance may cause variation of potential which may lead to side reactions.

Constant potential electrolysis (CPE) is carried out in a three electrode system namely working, counter and reference electrodes. The cell for controlled potential electrolysis system is shown in Figure 2.1. The working and the counter electrodes were platinum foils with an area of  $2\text{ cm}^2$ . The total volume was 50 ml and the counter and the working electrode compartments were separated by porosity No 1 sintered glass disc. The reference electrode was  $\text{Ag}^0/\text{Ag}^+$ . The electrolysis cell was made capable of passing  $\text{N}_2$  gas through and /or above the solution by providing suitable gas inlets.

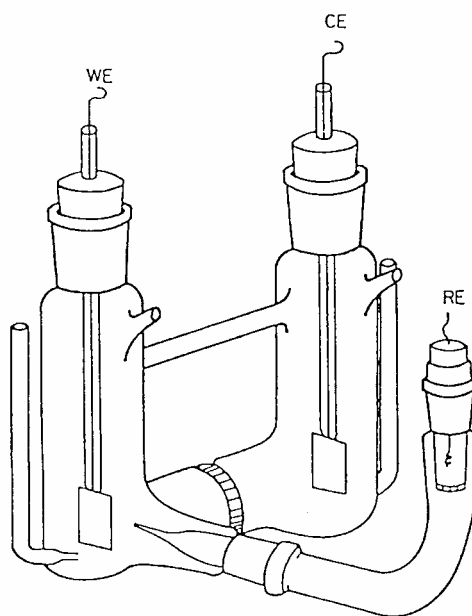


Figure 2.1 Polymerization Cell

The voltage between the working and the reference electrodes is called as the polymerization potential ( $E_{pot}$ ). The applied potential is determined by cyclic voltammetry.

### 2.2.2 Cyclic Voltammetry (CV) System

The CV system was composed of a potentiostat, a function generator, an XY recorder, and a cyclic voltammetry cell. Function generator or wave generator applies a triangular wave potential to the cell so that the working electrode potential is swept linearly through the voltammetric wave and then backs again (Figure 2.2). During these scans, potential-time response and I-V curves are obtained.

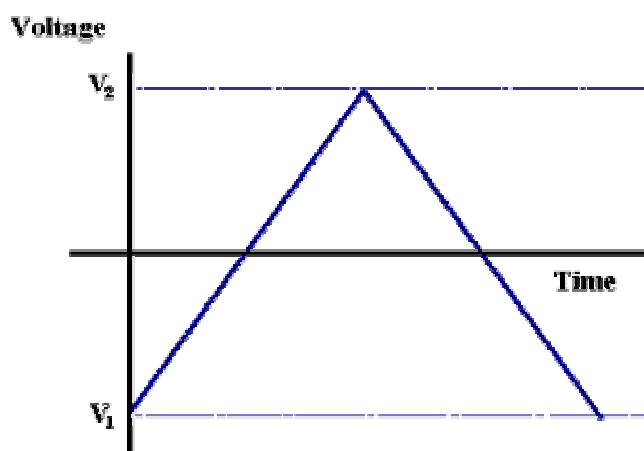


Figure 2.2 Triangular wave function

A typical cyclic voltammogram recorded for a reversible single electrode transfer reaction is shown in Figure 2.3. Solution contains only a single electrochemical reactant. The forward scan produces a current peak for any analyte that can be reduced through the range of the potential scan. The current will increase as the potential reaches the reduction potential of the analyte, but then falls off as the concentration of the analyte is depleted close to the electrode surface. As the applied potential is reversed, it will reach a potential that will reoxidize the product formed in the first reduction reaction, and produce a current of reverse polarity from the forward scan. This oxidation peak will usually have a similar shape to the reduction peak. The peak current,  $i_p$ , is described by the Randles-Sevcik equation:

$$i_p = (2.69 \times 10^5) n^{3/2} A C D^{1/2} v^{1/2} \quad (2.1)$$

where  $n$  is the number of moles of electrons transferred in the reaction,  $A$  is the area of the electrode,  $C$  is the analyte concentration (in moles/cm<sup>3</sup>),  $D$  is the diffusion coefficient, and  $v$  is the scan rate of the applied potential.

For a reversible electrochemical reaction the CV recorded has certain well defined characteristics.

I) The voltage separation between the current peaks is

$$\Delta E = E_p^a - E_p^c = \frac{59}{n} mV \quad (2.2)$$

II) The positions of peak voltage do not alter as a function of voltage scan rate

III) The ratio of the peak currents is equal to one

$$\left| \frac{i_p^a}{i_p^c} \right| = 1. \quad (2.3)$$

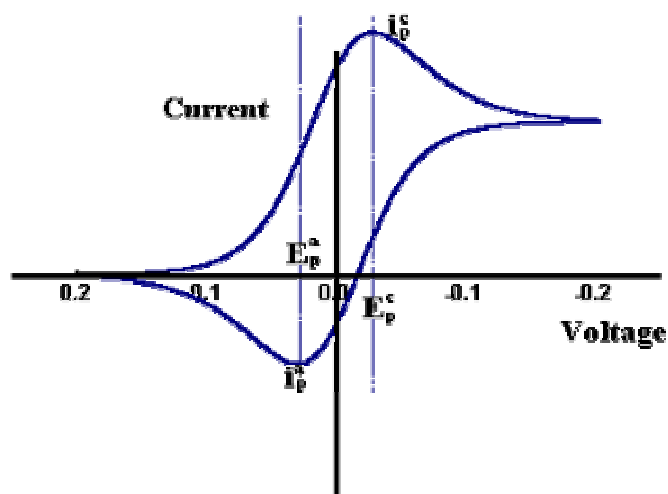


Figure 2.3 A cyclic voltammogram for a reversible reaction

IV) The peak currents are proportional to the square root of the scan rate

$$i_p^a \quad \text{and} \quad i_p^c \propto \sqrt{V} \quad (2.4)$$

The cyclic voltammetry cell was consisted of three electrodes; a platinum wire as working electrode, a spiral platinum as counter electrode and Ag wire as reference electrode (Figure 2.4). TBAFB was used as a supporting electrolyte which has a concentration of 0.1 M. It was necessary to pass dry nitrogen gas through the solution before every scan. In order to eliminate the signals which may come from any impurity present in the system, the background cyclic voltammogram was taken each time. After obtaining

background signal, a monomer was added ( $10^{-3}\text{M}$ ) and the potential was swept to determine the peak potentials where the monomer is reduced or oxidized.

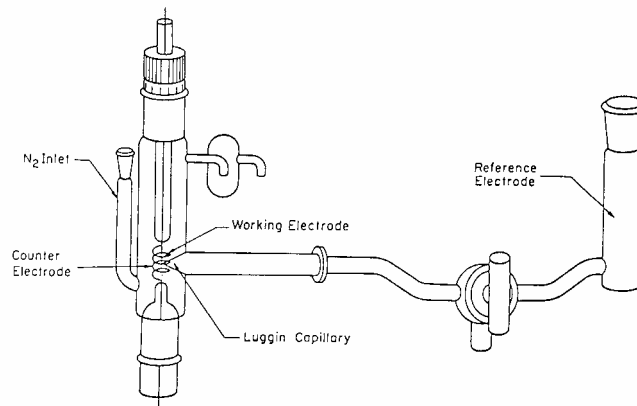


Figure 2.4 Cyclic Voltammetry Cell

### 2.2.3 Conductivity Measurements

In order to measure the conductivity of pressed pellets or films of doped polymers, “the four probe technique” is used. Schematic representation of this technique is shown in Figure 2.5.

In this technique, current is applied to the outer contact of a sample of known geometry, while the voltage drop is measured between the inner contacts. The system involves a special probe head, which is composed of four equally spaced spring-loaded electrodes. The head is lowered onto the sample until the four probes make good contact with the sample. A constant current is passed through the two outermost probes and the voltage drop across the two inner ones is measured. In order to measure the resistance of the sample itself without that of

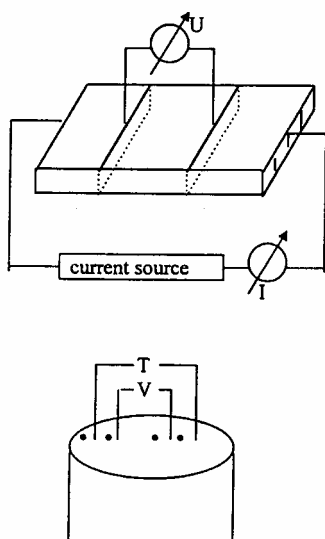


Figure 2.5 Resistance Measurement using Four-Probe Technique

the contacts and that of the wires leading to the voltmeter, it is necessary to keep the current passing through these contacts and wires sufficiently low. By this way, the current to the sample is supplied by two separate contacts. The conductivity of the sample is calculated by the formula, given below;

$$\sigma = \frac{1}{2\pi s} \cdot \frac{i}{V} \quad (2.5)$$

s = Spacing between probes (usually 0.1 cm)

i = Current passed through outer probes

v = Voltage drop across inner probes

The formula is used only when the sample thickness is much greater than the spacing between the probes. Moreover, it is assumed that the conductive material is completely space filled. If the conductivity of a pellet is to be measured, it usually represents lower limits, since the pellets are made of

compact powders, which contain various amount of void space. Conductivities of compact powder pellets of materials can be as small as a factor of  $10^2$  than that of a completely space filled materials.

#### **2.2.4 Thermal Analysis**

Thermal characterization of polymers was carried out using a Dupont modular thermal analyzer system in conjunction with 951 Thermal Gravimetric Analyzer and 910 Differential Scanning Calorimeter. Thermal gravimetry analysis (TGA) experiments were performed under a dry nitrogen purge. A constant heating rate of  $10^\circ\text{C}/\text{min}$  was used during differential scanning calorimetry (DSC) experiments.

#### **2.2.5 Nuclear Magnetic Resonance Spectrometer**

NMR spectra were registered on a Bruker-NMR Spectrometer (DPX-400) instrument.

#### **2.2.6 Fourier Transform Infrared Spectrophotometer (FTIR)**

The FTIR spectra of conducting polymer blends were measured as dispersed in KBr pellets, using a Nicolet-510 FTIR and Mattson 1000 FTIR Spectrometer.

#### **2.2.7 Scanning Electron Microscope (SEM)**

The morphological studies on composite films were done by a JEOL Scanning Microscope Model JSM-6400.



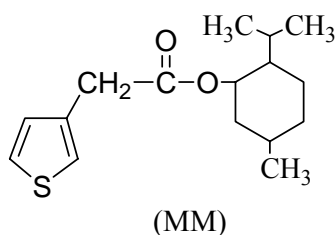
## 2.2.8 UV- Visible Spectrophotometry

A Shimadzu UV-1601 model spectrophotometer was employed in the determination of activities of both free and immobilized enzyme.

## 2.3 Experimental Procedures

### 2.3.1. Synthesis of Menthyl Containing Thiophene Monomer (MM)

To a solution of thiophene-3-acetic acid (3.55g) and (-)-menthol (3.9g) in 40 mL dry THF, N,N'-dicyclohexylcarbodiimide (DCCI) (3.09g) dissolved in 15 mL of THF was added at ice bath temperature. The solution was stirred for 1h and then the reaction mixture was allowed to come to room temperature. The stirring was continued for 24h; the precipitated dicyclohexyl urea was filtered off (55% of the theoretical quantity). THF was removed by rotaevaporatory. The crude product was purified by passing through a silica gel column using a mixture of hexane/ethyl acetate 3/2 (v/v) as the eluent, followed by recrystallization from the same mixture. The process was repeated for two more times to obtain the ester as white crystals (yield, 35%) [112].



## 2.3.2 Synthesis of Copolymers of MM

### 2.3.2.1 Synthesis of Copolymers of MM with Pyrrole (PM-1, PM-2)

Working electrode (Pt,  $2\text{cm}^2$ ) was coated with 1% w/v MM – dichloromethane solution. Electrolyses were performed in the presence of 0.02 M pyrrole (Py), 0.05M *p*-toluene sulfonic acid (PTSA), or 0.05M sodium dodecyl sulphate (SDS) in water. 1.0V was applied for 90 min. Same procedure was repeated for Acetonitrile (AN)/tetrabutylammonium tetrafluoroborate (TBAFB) system, where 50 mg MM was dissolved in the solution (Figure 2.6) [112].

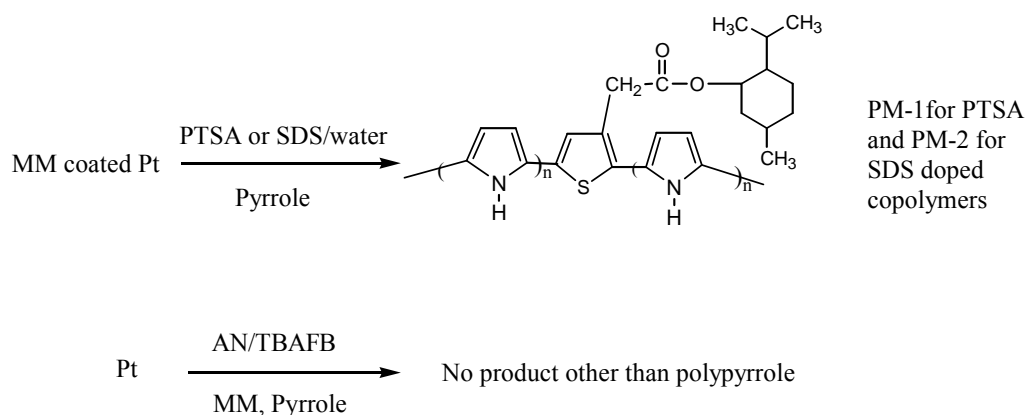


Figure 2.6. Synthesis of copolymers of MM with pyrrole.

### 2.3.2.2 Synthesis of Copolymers of MM with Thiophene

Copolymerization of thiophene must take place in acetonitrile since thiophene is completely insoluble in water. 0.05M TBAFB in acetonitrile was

used as the supporting electrolyte and a constant potential of 2.0 V was applied for 2 h to a solution containing 50 mg MM (Figure 2.7)

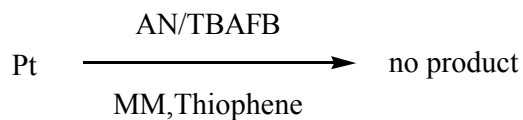


Figure 2.7. Synthesis of copolymers of MM with thiophene

### 2.3.3 Chemical Polymerization of MM (CN)

100 mg MM was dissolved in 5mL  $\text{CCl}_4$  and put in three-necked flask. Nitromethane solution of  $\text{FeCl}_3$  (2 M) was added dropwise to the solution of MM at 0 °C (Figure 2.8). The reaction was carried out for 24 h under constant flow of nitrogen and continuous stirring. After 24 h, this mixture was poured onto methanol, and then water was added until precipitate was observed. The precipitate was washed several times with water and methanol and dried under vacuum. The product was named as CN. The yield was 40% (CN) [112].

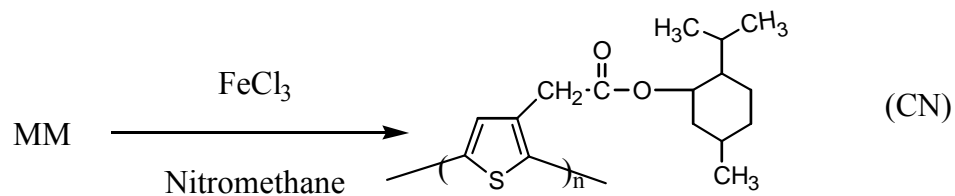


Figure 2.8. Chemical polymerization of MM

### 2.3.4 Galvanostatic Polymerization of MM (GDM)

Constant current electrolyses were performed in one component cell with two Pt electrodes as the working ( $2\text{cm}^2$ ) and counter electrodes ( $2\text{cm}^2$ ). Acetonitrile/TBAFB and dichloromethane (DCM)/TBAFB were used as the electrolysis media. For each medium, 100 mg monomer was introduced and electrolyses were carried at 20 mA for 90 min (Figure 2.9). Throughout this time, the cell was in ice bath. A black precipitate was obtained at the end of both electrolyses. After filtering and washing with water to remove TBAFB, the precipitate (GDM) was dried under vacuum.

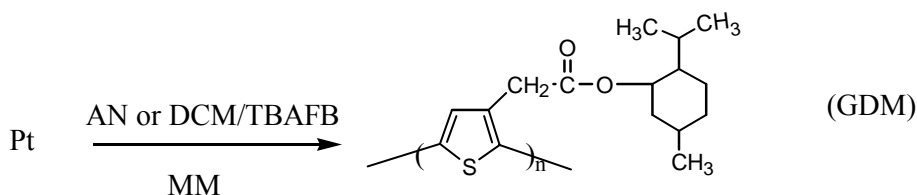


Figure 2.9 Galvanostatic polymerization of MM

### 2.3.5 Synthesis of Block Copolymers of CN and GDM with Pyrrole (CNPP, CNPS, PGDM)

A Pt working electrode ( $2\text{cm}^2$ ) was coated either with chemically synthesized polymer, CN, or galvanostatically synthesized polymer GDM from their DCM solution. CNPP and CNPS were synthesized in water using PTSA or SDS electrolytes respectively. Since GDM is insoluble in water, copolymerization with pyrrole was carried out in water/PTSA solvent/electrolyte couple (Figure 2.10) [112].

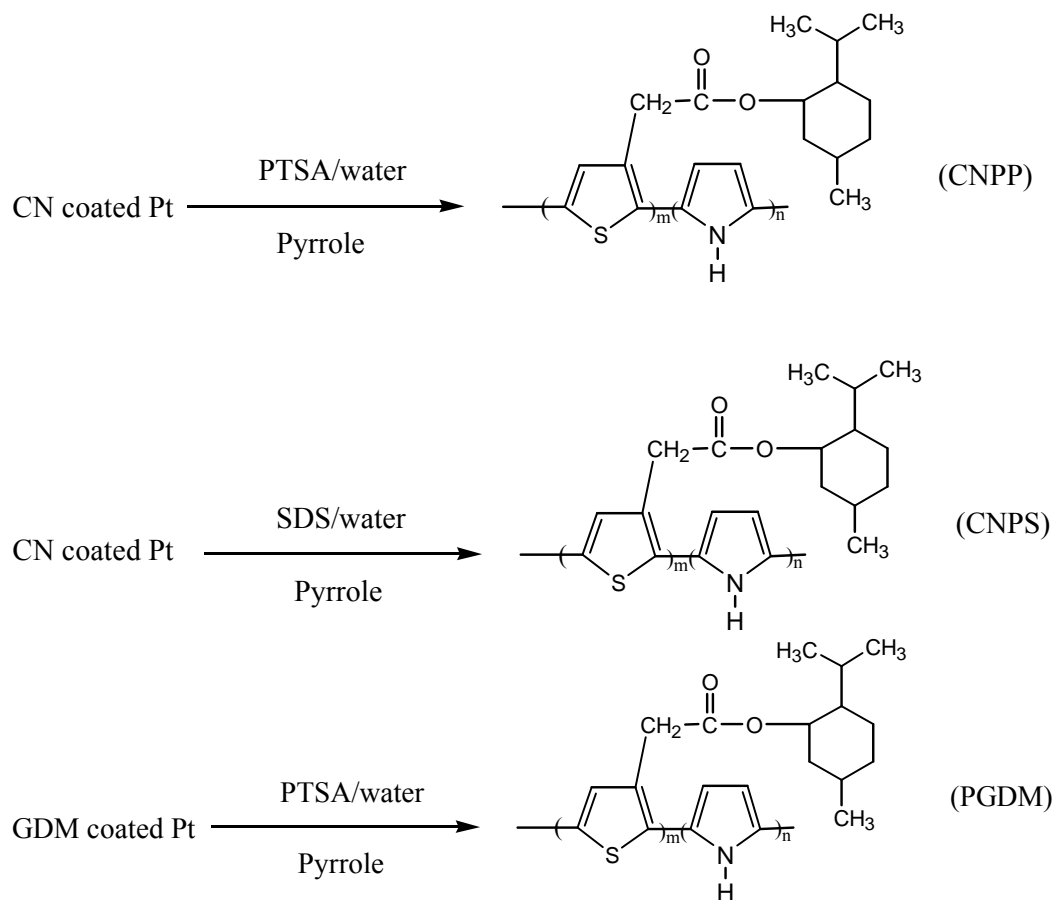


Figure 2.10. Synthesis of block copolymers of CN and GDM with pyrrole

### 2.3.6. Synthesis of Monomer MBTA

In order to synthesize the monomer the following procedure was described. In an 250 mL round bottom flask equipped with magnetic stirrer, a Dean-Stark trap and condenser 11.95 mL (0.167 mol) (S)-(-)-2-methylbutanol, 12.815 g (0.09 mol) of thiophene-3-acetic acid, 0.489 g (2.57 mmol) p-toluene

sulfonic acid were introduced in 100 mL benzene. The reaction was maintained 8h at reflux. After that time the solution was washed with a diluted solution of  $\text{NaHCO}_3$ , several times with water, dried over  $\text{MgSO}_4$  and the solvent removed at rotaevaporatory. The crude product (liquid) was purified by passing through a silicagel column using hexane as the eluent. The solvent was removed rotaevaporatory and a yellow liquid (MBTA) was obtained. The schematic representation of synthesis process is given below (Figure 2.11). [113]

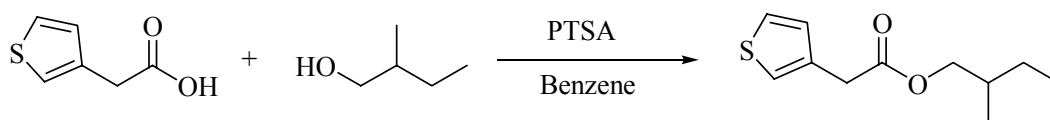


Figure 2.11 Synthesis of the monomer MBTA

### 2.3.7 Immobilization of Enzymes

#### 2.3.7.1 Immobilization of Invertase

##### 2.3.7.1.1 Preparation of Enzyme Electrodes in Copolymers of MM

Immobilization of invertase was achieved by electropolymerization of pyrrole either on bare or previously MM or CN coated platinum (Pt) electrode. Electropolymerization was performed in a typical three electrode cell, consisting of the Pt ( $1.5 \text{ cm}^2$  each) as the working and the counter electrodes and an  $\text{Ag}^0/\text{Ag}^+$  reference electrode. Enzyme electrodes were prepared in a 10 ml

acetate buffer containing 0.4 mg/ml invertase, 0.4 mg/ml SDS and 0.01M pyrrole. Immobilization was carried out at a constant potential of +1.0V for 30 min at room temperature. The reaction between pyrrole and thiophene moiety on MM and CN yields conducting copolymers which entrap invertase. Enzyme electrodes were kept at 4°C in acetate buffer solution when not in use.

#### **2.3.7.1.2 Determination of Invertase Activity**

The activities of free and immobilized enzyme were determined using Nelson's method. Nelson's Reagent was composed of two solutions, which are reagent A and reagent B. Sodium carbonate (25g), sodium potassium tartarate (25g), sodium bicarbonate (20g), sodium sulfate (200g) were dissolved in distilled water and diluted to 1L for the preparation of Reagent A. Reagent B was obtained by dissolving copper sulfate (15g) in 100 mL distilled water. Finally Nelson Reagent was prepared by mixing Reagent A and B in 25:1 (v/v).

Arsenomolibdate reagent was obtained by dissolving ammonium heptamolibdate (25g), in 450 mL distilled water and 21 mL concentrated sulfuric acid. Sodium hydrogen arsenate (3g) was dissolved in distilled water and added to the above solution. The resultant solution was incubated for 24-48 hours at 37 °C and stored in dark.

For the determination of free invertase activity different concentration of invertase solutions (0,001- 0,01 mg/mL) were vortexed and then 0.1 ml 0.3M sucrose solution added to start the reaction (pH = 4.6). After 2 min, 1ml Nelson reagent was added to stop the reaction. After 20 minutes of incubation in boiling

water bath, 1ml of arsenomolibdate solution and 7 ml distilled water were added to each test tube. After mixing, absorbance was measured at 540nm.

For immobilized invertase, sucrose solution in buffer were placed in test tubes and put in a water bath at 25°C. Enzyme electrode was immersed in a test tube and shaken for 2 min. The rest of procedure was the same as for free enzyme activity measurements.

#### **2.3.7.1.3 Kinetic Parameters for Immobilized Invertase**

Kinetic studies of the enzymatic reaction for both free and immobilized enzyme were performed at varying concentrations of sucrose. Activity assay performed according to Section 1.3.6.1.2.

#### **2.3.7.1.4 Determination of Optimum Temperature for Immobilized Invertase**

Optimum temperature determinations were carried out by changing incubation temperature between 10°C and 80°C, in a constant sucrose concentration (10 Km) for each temperature. The rest of the procedure was the same as the invertase activity measurements described in section 1.3.6.1.2.

#### **2.3.7.1.5 Determination of Operational and Storage Stability for Immobilized Invertase**

Stability of electrodes in terms of repetitive uses was performed in more than 25 successive measurements. In order to determine the storage stability of



enzyme electrodes were preserved in buffer solution at 4°C, their activities were measured daily for more than 60 days.

#### **2.3.7.1.6 Morphologies of Invertase-Entrapped Films**

Enzyme immobilization procedure was carried out until obtaining free standing films. After washing with buffer solution to remove unbound enzyme and supporting electrolyte, SEM analysis was performed.

#### **2.3.7.2 Immobilization of Polyphenol Oxidase (PPO)**

##### **2.3.7.2.1 Preparation of Enzyme Electrodes in Copolymers of MM**

Thiophene functionalized menthyl monomer (MM) was used to synthesize copolymers with pyrrole which at the end, form a matrix for immobilization of PPO. Immobilization of PPO was achieved by electropolymerization of pyrrole either on bare or previously MM or CN coated platinum (Pt) electrode.

Electropolymerization was performed in a typical three electrode cell, consisting of the Pt (1.5 cm<sup>2</sup> each) as the working and counter electrodes and a Ag<sup>0</sup>/Ag<sup>+</sup> reference electrode.

Enzyme electrodes were prepared in 10 ml citrate buffer (pH=6.5) containing 1 mg/ml SDS as the supporting electrolyte, 0.01M pyrrole and 0.3 mg/ml PPO. Immobilization was carried out at a constant potential of +1.0V.

The reaction between pyrrole and thiophene moiety of MM yields conducting copolymers which entrap PPO within. Enzyme electrodes were kept at 4°C in citrate buffer solution when not in use.

#### **2.3.7.2.2 Preparation of Enzyme Electrodes in Copolymers of MBTA**

The homo-polymerization of MBTA was achieved by constant current electrolysis in one compartment cell consisting of platinum working and counter electrodes. Experiments were carried out in dichloromethane (10mL)–tetrabutylammonium tetrafluoroborate (TBAFB) (0.2 M) solvent-electrolyte system with 50 mg monomer at 0°C using 30 mA for 10 min. [112]

Immobilization of polyphenol oxidase (PPO) was achieved by electropolymerization of pyrrole on previously PMBTA coated platinum electrode. The solution consists 0.3 mg ml<sup>-1</sup> polyphenol oxidase, 0.6 mg ml<sup>-1</sup> supporting electrolyte (sodium dodecyl sulfate) and 0.01M pyrrole and 10 ml citrate buffer (pH=6.5). Immobilization was performed in a typical three electrode cell, consisting of the Pt working and counter electrodes and a Ag/Ag<sup>+</sup> reference electrode. Immobilization was carried out at a constant potential of +1.0 V for min at room temperature. Enzyme electrodes were kept at 4°C in citrate buffer solution when not in use.

#### **2.3.7.2.3 Determination of PPO Activity**

The activities of free and immobilized PPO was determined by using Besthorn's Hydrazone Method.

Besthorn's Hydrazone Method [114] includes spectrophotometric measurements. In this method 3-methyl-2-benzothiozolinone (MBTH) interacts with the quinones produced by the enzyme to yield red products instead of brown colored pigments in the absence of the color reagent [115]. The pathway proposed by Rodriguez et al is shown in Figure 2.12 [116].

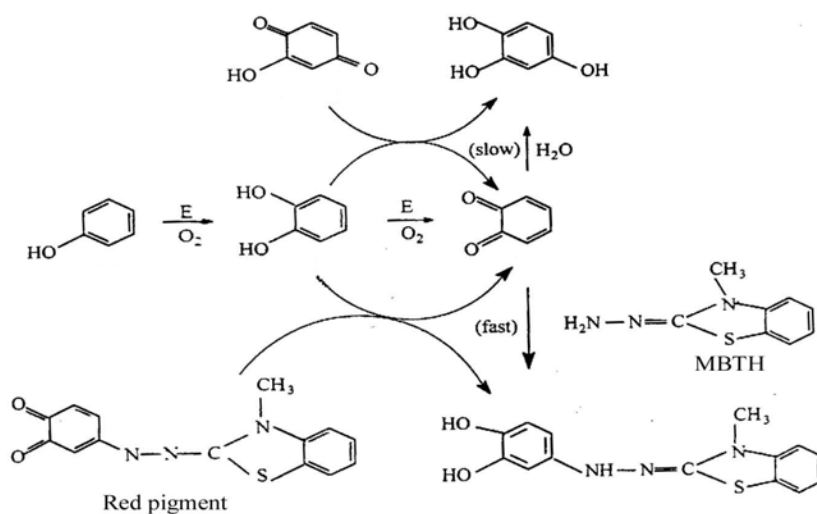


Figure 2.12 Schematic representation of Besthorn's Hydrazone Method

For the determination of free PPO activity different concentrations of catechol were prepared. Solutions contain 1.0 ml citrate buffer, 0.5 ml MBTH (0.3% in ethanol) and 0.5 ml catechol. 1 minute of reaction time was given after the addition of 0.5 ml enzyme solution (0.1mg/ml). 0.5 ml sulfuric acid (5% v/v) was added to stop the enzymatic reaction. Quinone produced reacts with MBTH to form a red color complex and this complex was dissolved by adding 3.0 ml

acetone in the test tube. After mixing, absorbance was measured at 495 nm by using a Shimadzu UV-Visible spectrophotometer.

For immobilized PPO, different concentrations of catechol were prepared (3.0 ml) and put in water bath at 25°C. 1 ml MBTH solution was added. Enzyme electrode immersed in the solution and shaken for 5 minutes. 1 ml sulfuric acid and 1 ml acetone were added for a total volume of 6 ml. After mixing, absorbances were measured at 495 nm.

#### **2.3.7.2.4 Kinetic Parameters for Free and Immobilized PPO**

Kinetic studies of the enzymatic reaction for both free and immobilized PPO were performed at varying concentrations of catechol. Activity assay performed according to Section 1.3.6.2.2.

#### **2.3.7.2.5 Determination of Optimum Temperature and pH of Immobilized PPO**

Optimum temperature and pH determinations were carried out by changing incubation temperature and pH between 10°C-90°C and 2-12 respectively. The rest of the procedure was the same as the determination of PPO activity.

#### **2.3.7.2.6 Determination of Operational and Storage Stability Immobilized PPO**

Enzymes can easily lose their catalytic activity and denatured, so careful storage and handling are essential. To determine the stability against repetitive

use and shelf-life of enzyme electrodes, the activity of electrode was checked. 40 measurements in the same day were done to perform the operational stability. For storage stability activity measurements were performed for 40 days.

#### **2.3.7.2.7 Morphologies of PPO Entrapped Films**

Enzyme immobilization procedure was carried out until obtaining free standing films. After washing with buffer solution to remove unbound enzyme and supporting electrolyte, SEM analysis was performed.

#### **2.3.7.2.8 Protein Determination**

Protein determination measurements were performed by Bradford's Method. Bradford reagent was prepared by mixing 25 ml phosphoric acid, 12.5 ml ethanol and 25 mg Coomassie Brilliant Blue (G-dye). The mixture was diluted to 50 ml with distilled water. During measurements, a solution of Bradford reagent was prepared by mixing 1 volume stock solution with 4 volumes of distilled water.

For the preparation of protein calibration curve, bovine serum albumin (BSA) was used. Different concentrations of BSA were prepared as 1 ml, and 2 ml of diluted Bradford reagent was added. The absorbance of these solutions was measured at 595 nm.

#### **2.3.7.2.9 Determination of Amount of Phenolic Compounds in Red Wines**

This study was designated to determine total phenolic compounds by using the fabricated enzyme electrodes. Total phenolic compounds in wines produced in Turkey were reported as 2000-3000 mg/L [117-119].

Polyphenol oxidase enzyme act on –OH groups on phenolic compounds. Via activity determination of enzyme electrodes in red wines we obtain the total –OH groups

Two Turkish red wines (Brand K and Brand D) were analyzed for their concentration of phenolic compounds by using free and immobilized enzymes

Red wines are diluted with citrate buffer (pH 6.5) to a 1:3 volume and activity assay was achieved as in section 1.3.6.2.2.

## CHAPTER 3

### RESULTS AND DISCUSSION

#### 3.1 Synthesis and Characterization of Menthyl Ester of 3-Thiophene Acetic Acid

Menthyl Ester of 3-Thiophene acetic acid was synthesized by esterification reaction of thiophene acetic acid with menthol. NMR spectrum of obtained product was shown in Figure 3.1.

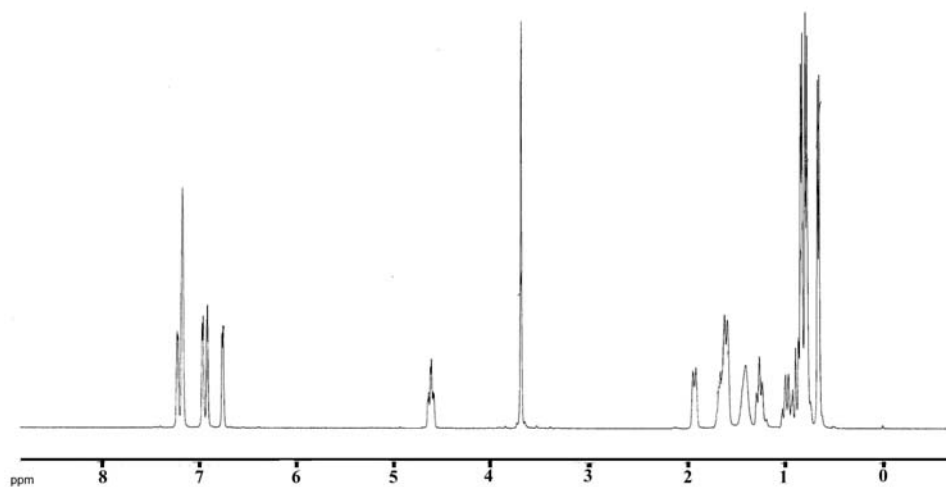


Figure 3.1 NMR spectrum of MM

$^1\text{H-NMR}$  spectrum of the monomer was taken by using a Bruker 250 MHz spectrometer with  $\text{CDCl}_3$  as the solvent and tetramethylsilane as the internal standard.  $^1\text{H-NMR}$  data for the monomer:  $^1\text{H-NMR}$  ( $\delta$ , ppm): 7.29-7.02 (m, 3H), from 3-thienyl ring, 4.65 (s, 1H),  $\text{COO-CH-}$  in menthyl), 3.77 (s, 2H),  $\text{Th-CH}_2\text{-COO-}$ , 1.08-1.89 (m, 18H), menthyl.

For MM,  $\text{C-H}_\alpha$  stretching modes which arise from thienylene are observed at  $3108\text{ cm}^{-1}$  and  $757\text{ cm}^{-1}$ . Carbonyl group and  $\text{C-O-C}$  are present at around  $1733\text{ cm}^{-1}$  and  $1063\text{ cm}^{-1}$ , respectively. Other peaks which belong to MM are  $2944$ ,  $2863$ ,  $1456$ ,  $1390$ ,  $833\text{ cm}^{-1}$ .

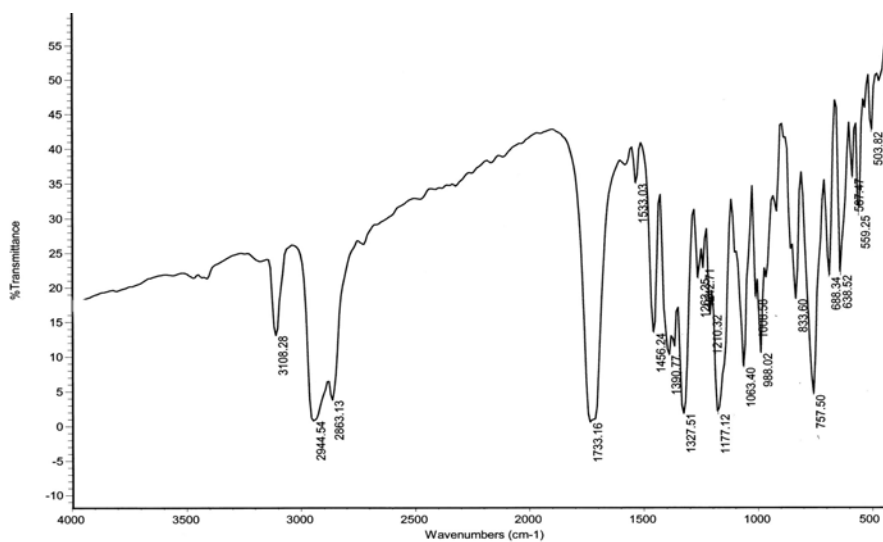


Figure 3.2 FTIR spectrum of MM



Acetonitrile and TBAFB were used as the solvent and electrolyte respectively for cyclic voltammetry studies. As seen from Figure 3.3, MM has no redox peak, which implies that MM is not an electroactive material.

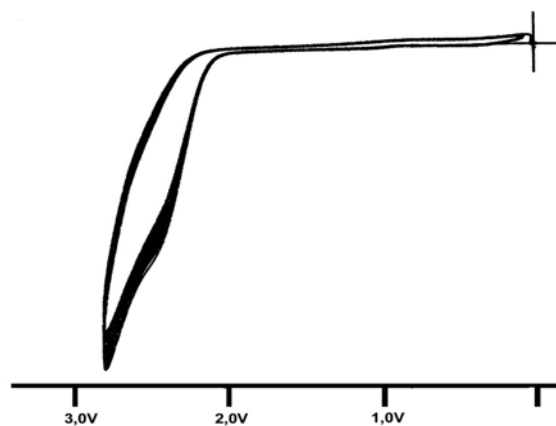


Figure 3.3 Cyclic Voltammogram of MM

Thermal Gravimetry Analysis and Differential Scanning Calorimetry were used to examine thermal behavior of monomer and polymers.

TGA showed weight losses for MM at 265°. No residue was observed for MM. DSC thermogram for monomer shows a sharp melting point at 118°C (Figure3.4).

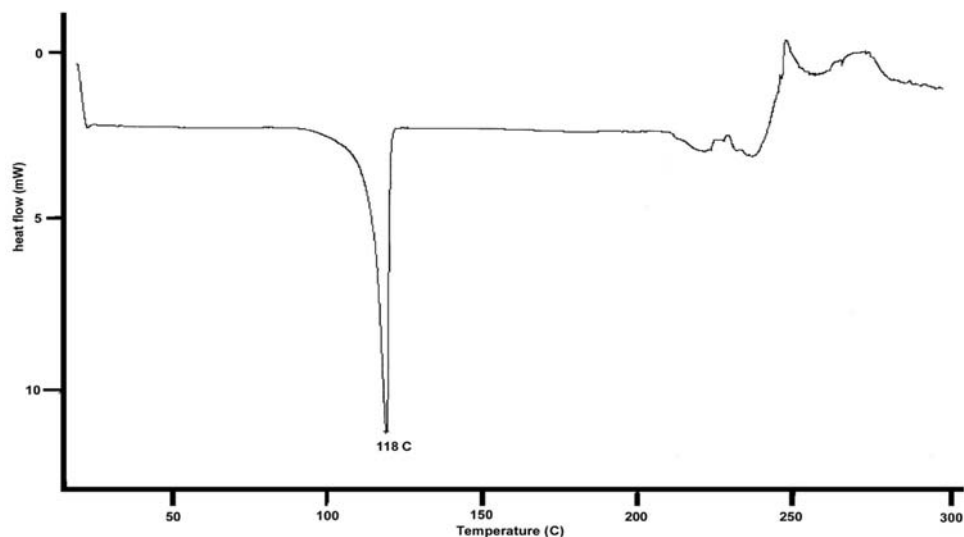


Figure 3.4 DSC Thermogram for MM

### 3.2. Chemical Polymerization of MM (CN)

Synthesis of homopolymer of MM was performed in the presence of nitromethane solution of  $\text{FeCl}_3$  via chemical polymerization. The product, CN, was obtained with a yield of 40 %. Broadening peaks in the NMR spectrum implies the polymerization (Figure 3.5)

Product of chemical polymerization, CN, shows carbonyl group and C-O-C revealing successful polymerization. The peak at  $757\text{ cm}^{-1}$  indicating C-H $_{\alpha}$  stretching disappears completely, whereas absorption peak at  $840\text{ cm}^{-1}$  (C-H $_{\beta}$  vibration mode) was observed.

Another difference between CN and MM spectra arises from the absorption peak at  $1646\text{ cm}^{-1}$  which is observed for CN spectrum indicating the conjugation.

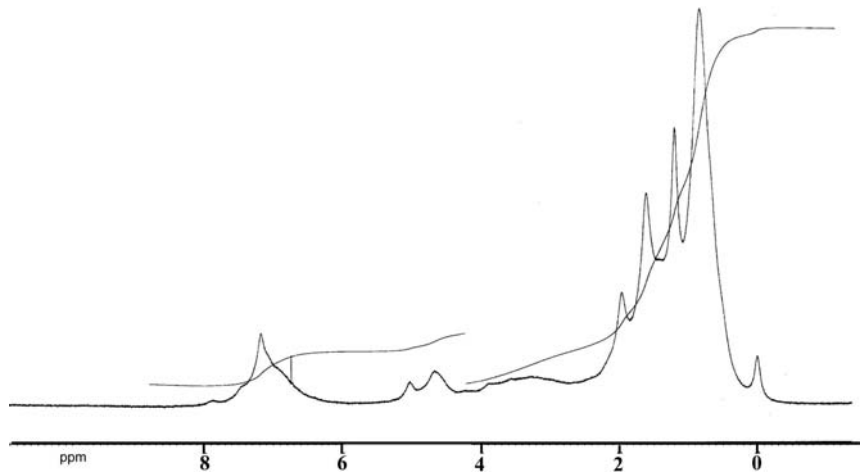


Figure 3.5 NMR spectrum of CN

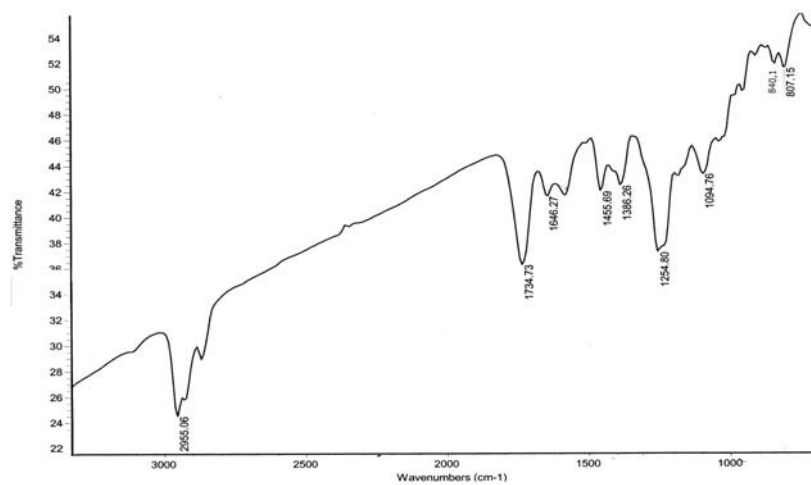
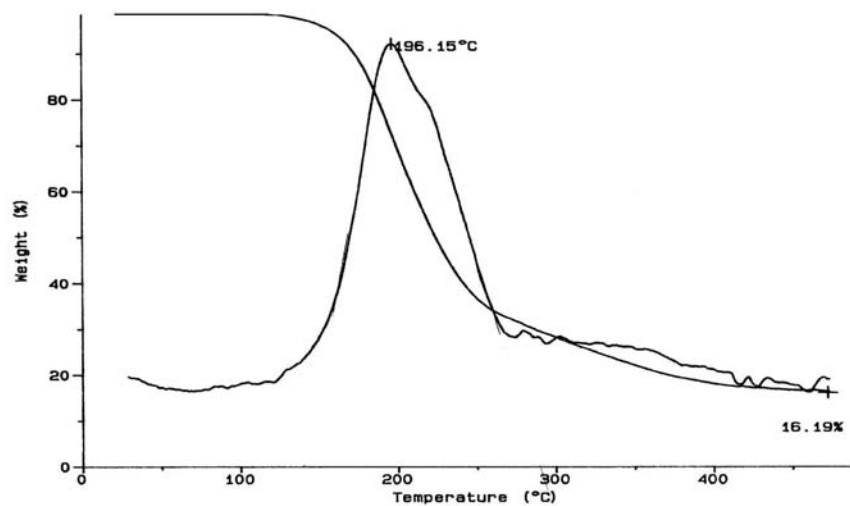
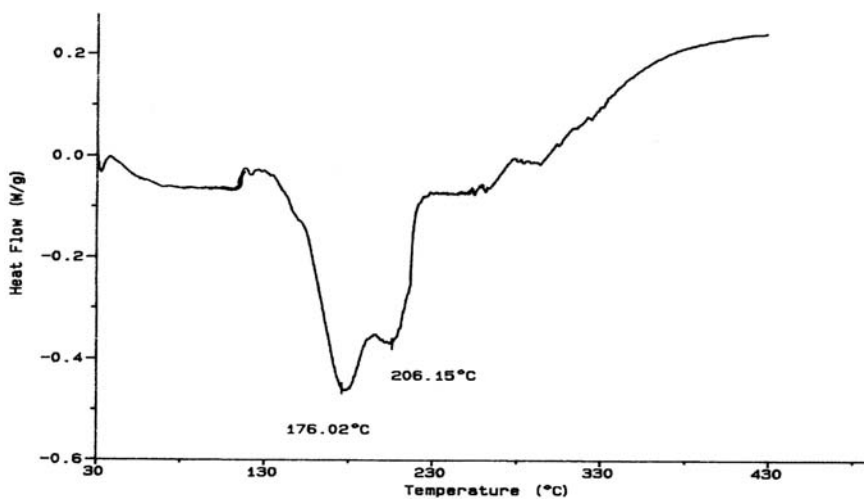


Figure 3.6 FTIR spectrum of CN

TGA showed weight losses for CN at around 196°C (Figure 3.7a). No residue was observed for MM whereas it was 16.2% for CN. As to the DSC, two transitions are observed at 176°C and 206°C (Figure 3.7b), which are due to the decomposition of the sample.



(a)



(b)

Figure 3.7 (a) TGA (b) DSC of CN

### 3.3. Galvanostatic Polymerization of MM (GDM)

NMR, FTIR and Thermal analysis for GDM exhibit similar behavior with CN. This is an expected result because the product obtained with galvanostatic polymerization is same with that of chemical polymerization.

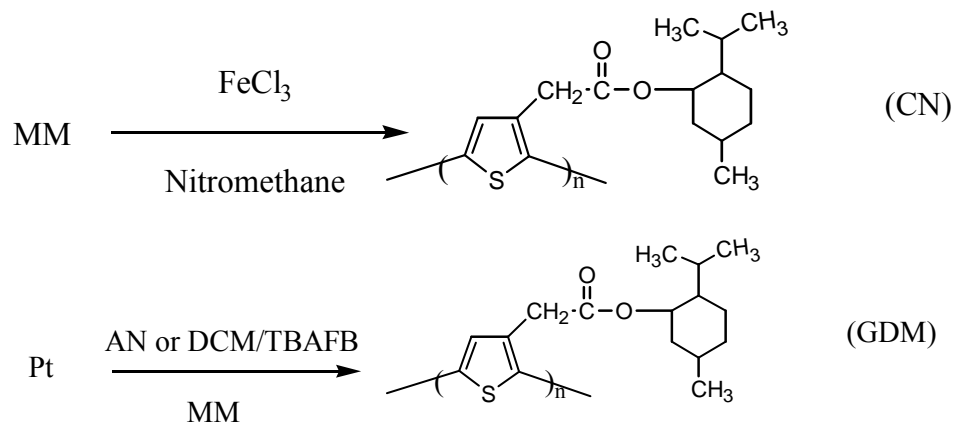


Figure 3.8 Schematic representation of synthesis of CN and GDM

### 3.4 Conducting Copolymers

#### 3.4.1 Copolymers of MM with Thiophene

Our initial effort was to synthesize the copolymers of MM with thiophene, where no satisfactory results were obtained. The cyclic voltammograms of pure thiophene, and thiophene in the presence of MM, conclude that not only the copolymerization with MM, but also the formation of pure polythiophene was prevented. Voltammogram of thiophene in the presence of MM reveals no redox peak, not even the standard peak due to the growth of pure polythiophene. At the beginning, for few runs the peak increases after which stops growing and the peak height reduces thereon. This may indicate the formation of soluble oligomers, which leave the electrode surface after a certain

chain length. Presence of MM in the electrolysis medium prevents the growth of polythiophene chains (Figure 3.9)

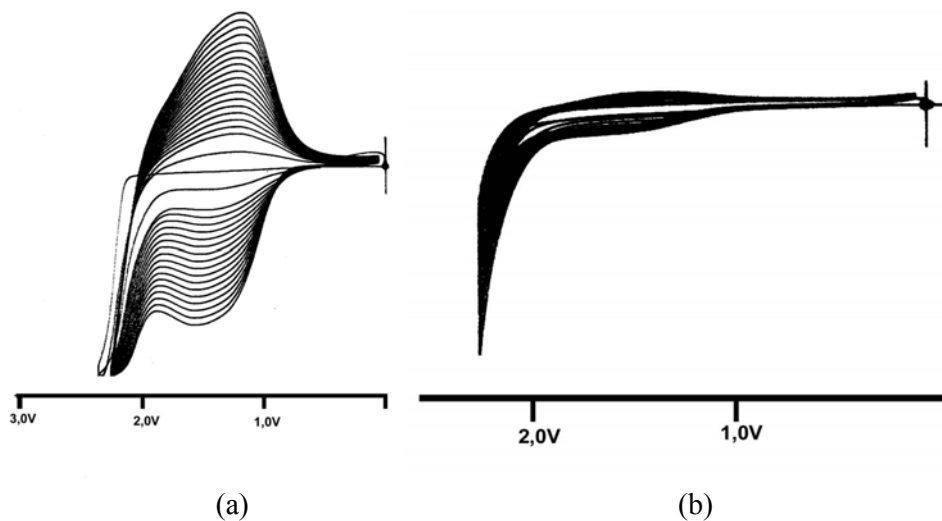


Figure 3.9 Cyclic voltammogram of (a) polythiophene (b) polythiophene in the presence of MM.

### 3.4.2 Copolymers of MM with Pyrrole

Since no product was obtained with thiophene, all copolymerizations involving MM were performed in the presence of pyrrole. Different supporting electrolytes such as *p*-toluene sulfonic acid (PTSA), sodium dodecyl sulphate (SDS) and tetrabutylammonium tetrafluoroborate (TBAFB) and different solvents such as water and acetonitrile were used. Products were coded as PM-1 and PM-2 according to the electrolysis medium utilized (Figure 2.6).

### **3.4.3 Block Copolymers of CN and GDM with Pyrrole (CNPP, CNPS, PGDM)**

Homopolymers obtained via chemical and galvanostatic polymerization which are coded as CN and GDM respectively, were used as the precursor of copolymerization with pyrrole (Figure 2.10)

### **3.4.4 Characterization of Conducting Copolymers of Pyrrole**

#### **3.4.4.1 Cyclic voltammetry**

Acetonitrile and TBAFB were used as the solvent and electrolyte respectively for cyclic voltammetry studies. Figure 3.10 shows the voltammogram of pure pyrrole and the voltammogram of pyrrole in the presence of MM. For this solvent – electrolyte couple, addition of pyrrole to the medium makes no significant difference.

#### **3.4.4.2 FTIR**

FTIR analysis is an important characterization method which is used to prove that copolymerizations were succeeded. Significant features of pristine MM are carbonyl group and C-O-C which are around  $1733\text{ cm}^{-1}$  and  $1063\text{ cm}^{-1}$ , respectively. PM-1 and PM-2 contain an absorption band at  $1730\text{ cm}^{-1}$ . This carbonyl band reveals that copolymerization takes place between the two components since FTIR analyses were performed after a rigorous washing of films with the solvent of MM.

Also for CNPP, CNPS and PGDM, FTIR spectra contain peaks indicating the presence of carbonyl functional group, which is labeled as a proof of copolymerization.

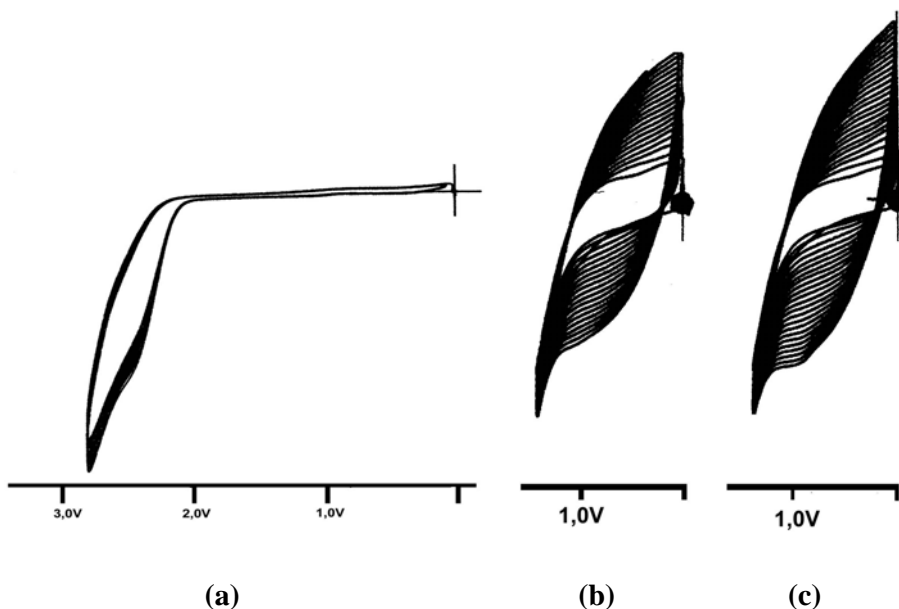


Figure 3.10 Cyclic voltammograms of (a) MM (b) polypyrrole (c) polypyrrole in the presence of MM.

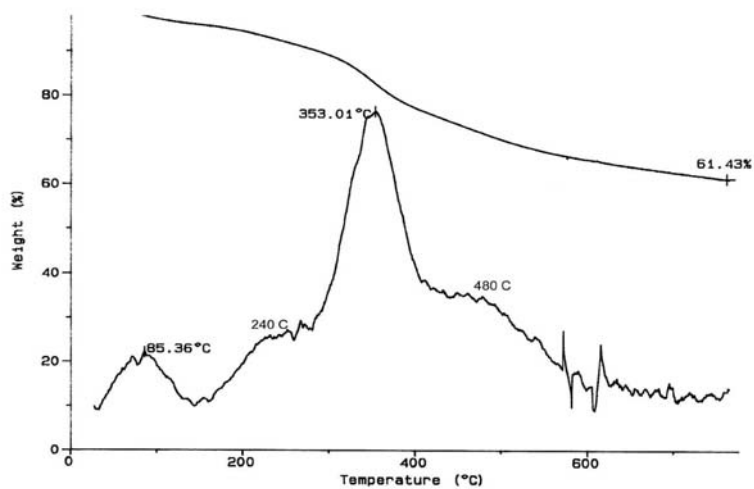
#### 3.4.4.3 Thermal Analysis

Copolymers synthesized with MM in the presence of pyrrole (PM-1 and PM-2) show four transitions. For PM-1, obtained by using PTSA as the supporting electrolyte, these transitions are at 85°C, 240°C, 353°C and 480°C. 85°C and 353°C are the temperatures for the removal of water and the dopant ion respectively. For PM-2, transitions at 80°C, 129°C, 254°C and 512°C were observed (Figures 3.11a and 3.11b). Similarly removal of water and dopant ion is observed at 80°C and 254°C. There is a difference in the decomposition

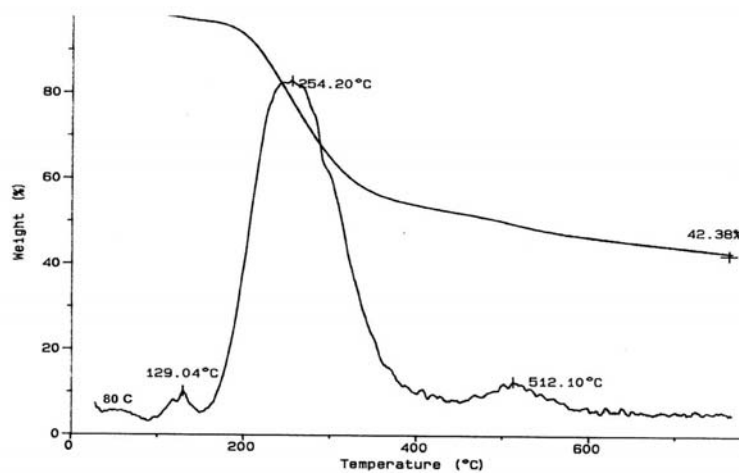


temperature, which is 480°C for PM-1 and 512°C for PM-2, indicating that thermal stability of the latter is a better.

High pyrrole content in the CNPP, CNPS and PGDM give rise to weight loss behaviors similar to that of pristine polypyrrole (Figures 3.11c and 3.11d)



(a)



(b)

Figure 3.11 TGA thermograms for (a) PM-1 (b) PM-2 (c) CNPP (d) CNPS (e) PGDM

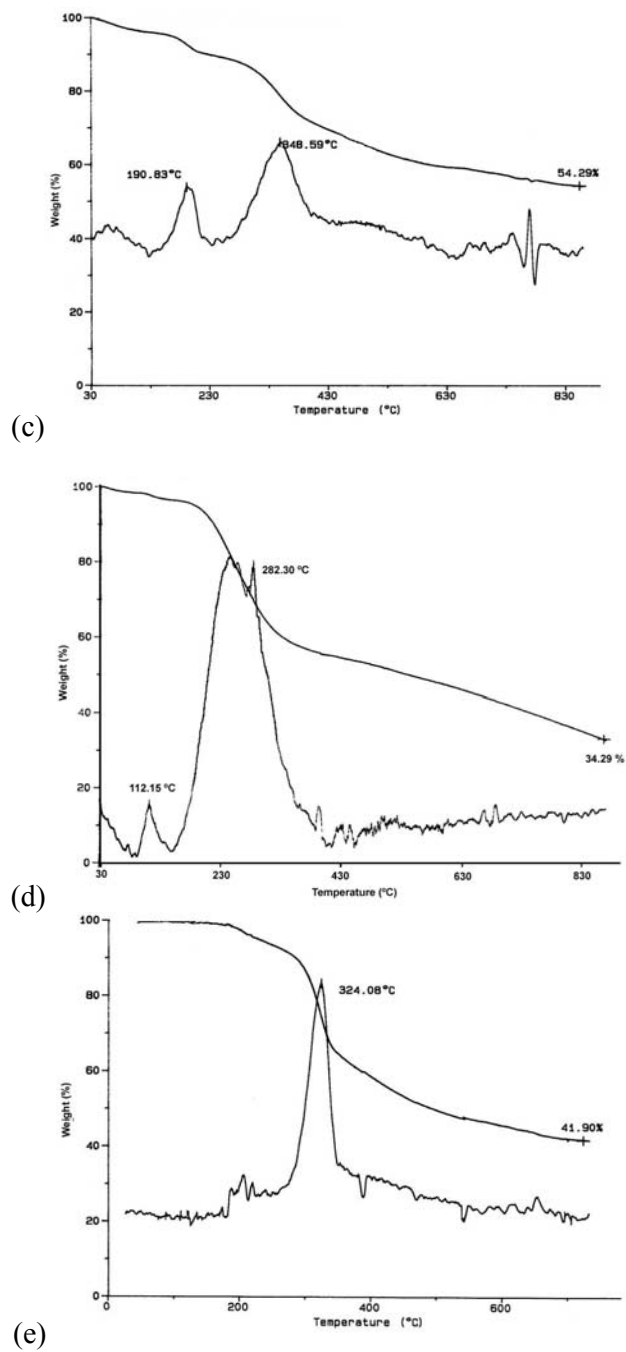
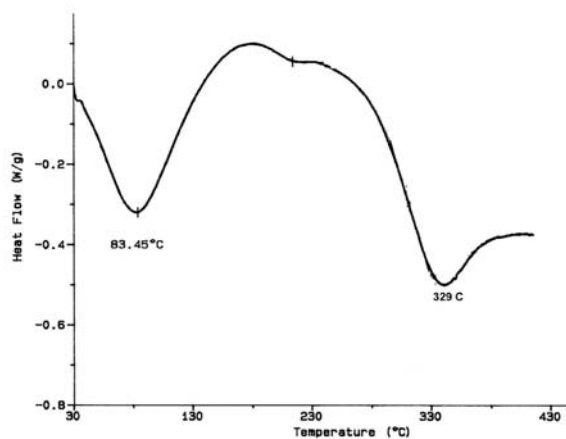


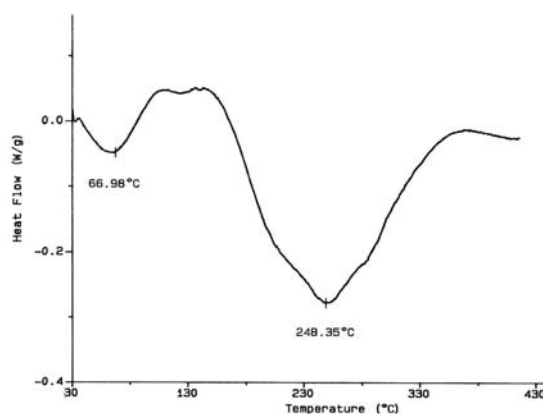
Figure 3.11 (Cont.)

DSC thermograms for copolymers of PM-1 and PM-2 show two transitions at 83°C, 329°C and 66°C, 248°C respectively (Figure 3.12). Same behavior was also observed for CNPP and CNPS.

Transitions about 330°C and 250°C are due to the removal of dopant ions, PTSA and SDS.



(a)



(b)

Figure 3.12 DSC thermograms for (a) PM-1 (b) PM-2 (c) CNPP (d) CNPS (e) PGDM

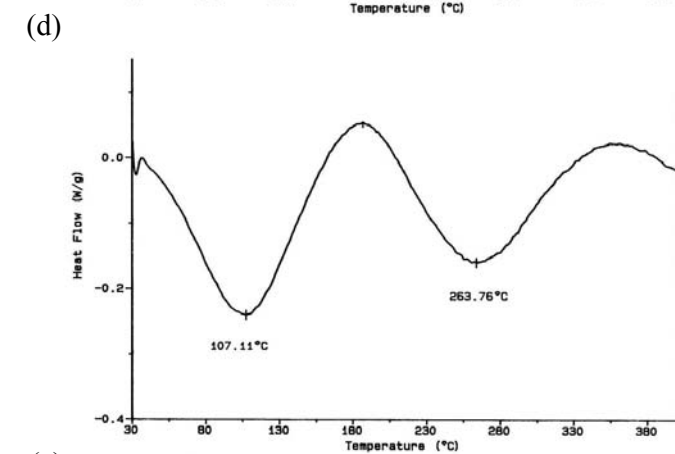
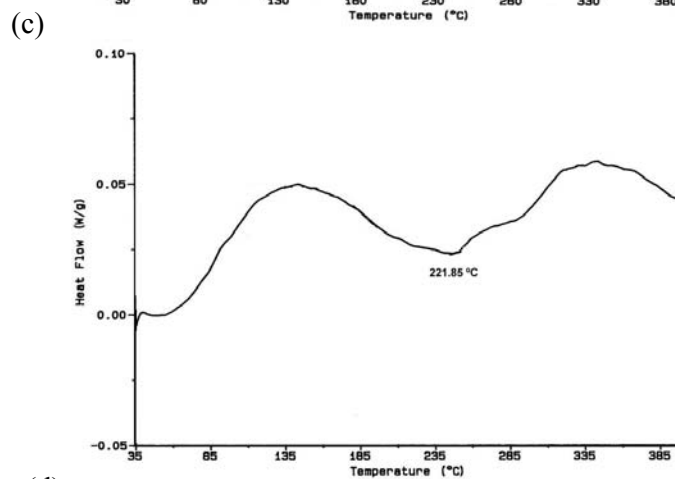
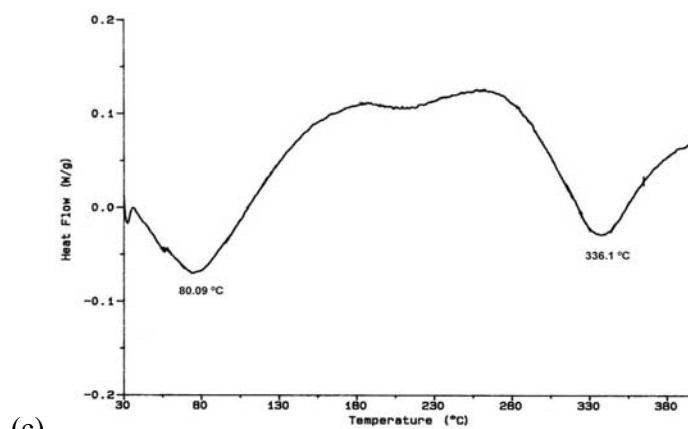


Figure 3.12 (Cont.)

#### 3.4.4.4 Morphologies of the Films

In order to examine the morphology of copolymer films, SEM studies were carried out.

Copolymers of MM with pyrrole, i.e. PM-1 and PM-2, exhibit different morphologies than that of pure polypyrrole, which has a smooth surface on the electrode side and standard cauliflower structure on the solution side. For both copolymers, solution side has standard cauliflower structure, but electrode sides are interesting. For PM-1, electrode side contains regular islands, whereas PM-2 has rather a smoother surface (Figure 3.13).

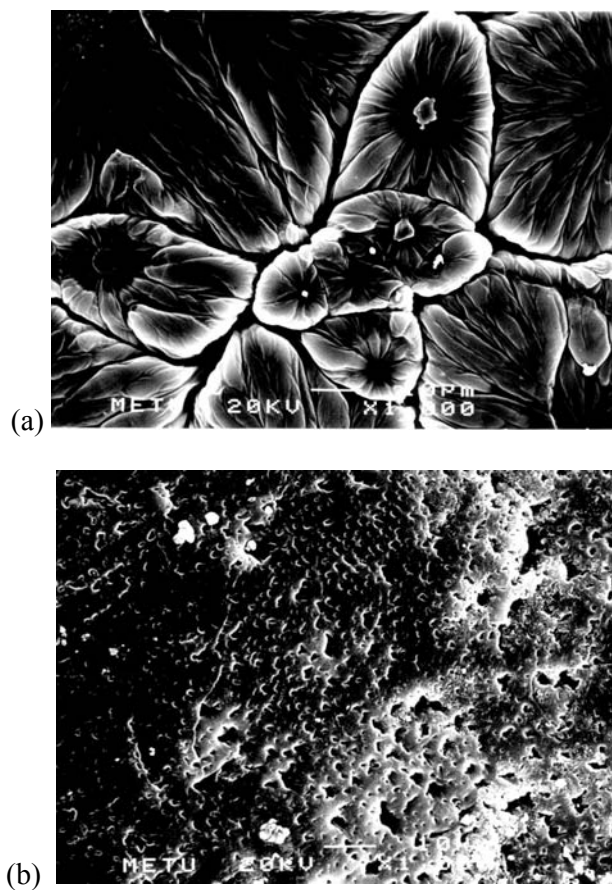


Figure 3.13 SEM micrographs of (a) PM-1 (b) PM-2

In the case of CNPP, solution side has standard cauliflower structure. For unwashed films electrode sides are smooth due to CN layer that did not react with pyrrole, but when films are washed (with the solvent of MM) regular islands are observed indicating the removal of unreacted CN (Figure 3.14). Solution sides of CNPS and PGDM are totally different from the others and contains granules. Also the electrode side of CNPS presents a different picture where there exist separated irregular islands (Figure 3.15).

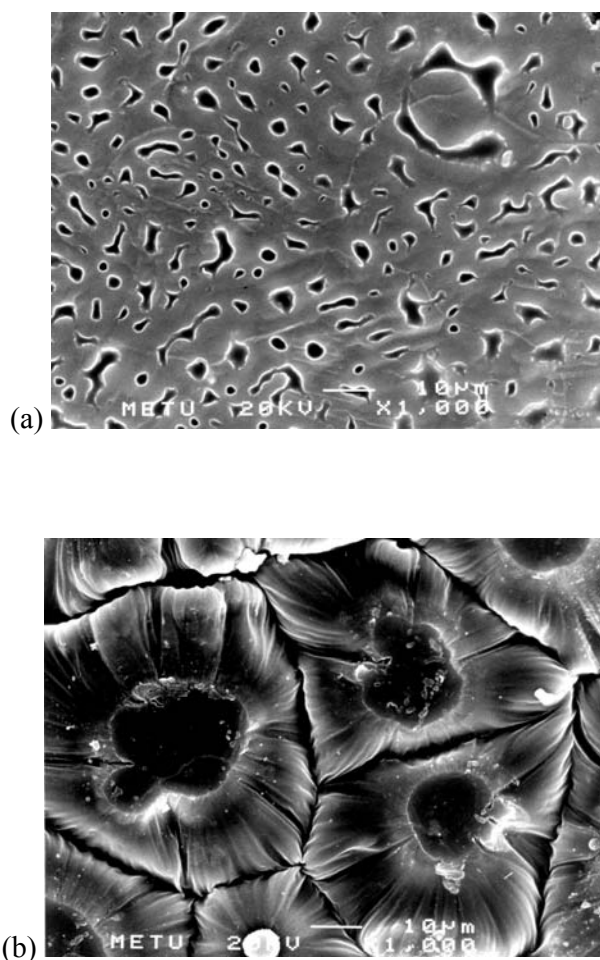


Figure 3.14 SEM micrographs of CNPP (a) unwashed electrode side (b) washed electrode side

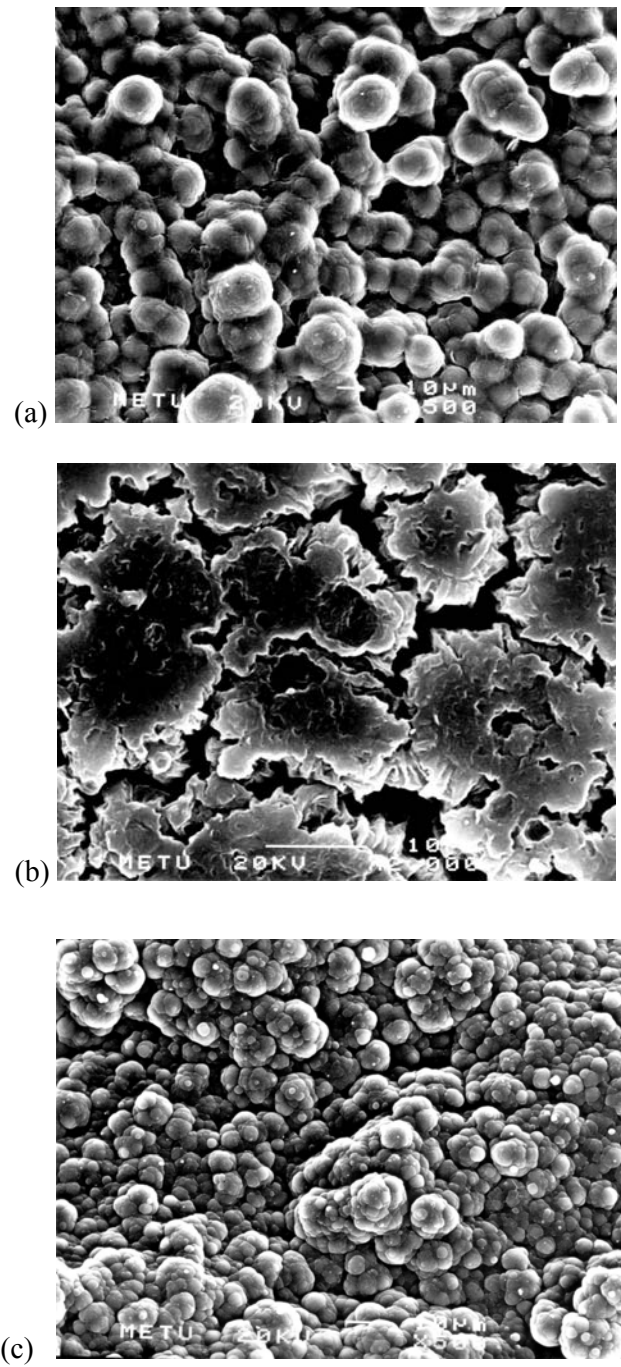


Figure 3.15 SEM micrographs of (a) CNPS solution side (b) CNPS electrode side (c) PGDM solution side.

### 3.4.4.5 Conductivity Measurements

Standard four-probe technique was used for conductivity measurements. Conductivities were in the range of 0-4 S/cm and no significant difference was observed between the electrode and solution sides of the films. In Table 1 although PM-2, which is doped with SDS, exhibits the best conductivity, whilst there is no order of magnitude difference between the polymer films.

Table 3.1 Conductivities of polymers of MM (a: pellet)

	Electrode Side (S/cm)	Solution Side (S/cm)
CN <sup>a</sup>	$3.7 \times 10^{-3}$	$3.7 \times 10^{-3}$
PM-1	3.4	3.2
PM-2	4.1	4.0
CNPP	0.7	0.2
CNPS	0.8	0.6

## 3.5 Immobilization of Enzymes

### 3.5.1 Immobilization of Invertase

Immobilization of invertase was achieved in PM-2 and CNPS copolymers via constant potential electrolysis. For comparing the obtained data, pure polypyrrole was also used as a matrix for the immobilization of invertase. Optimum reaction conditions during immobilization and activity assay were determined in the previous studies [98-100]. Although the enzyme is available at



a small cost, there is a little economic advantage to its repeated and continuous utilization in immobilized form; thus it serves a model enzyme for the immobilization of expensive and more applicable enzymes, such as tyrosinase.

### **3.5.1.1 Morphologies of Films**

Scanning electron microscopy (SEM) was performed to study surface morphology of polymer films (polypyrrole (Ppy), copolymers of MM and CN with pyrrole (PM-2 and CNPS)).

When the invertase was immobilized, morphology was dramatically changed, structure was damaged and enzyme clusters were observed (Figure 3.16). When micrographs of these three matrices in the presence of invertase were analyzed, it is seen that invertase was entrapped homogeneously in all matrices. However, PM-2 matrix is different than the other two in terms of the concentration of enzyme clusters entrapped in the matrix. This difference affects the Michaelis-Menten constant significantly [120].

### **3.5.1.2 Kinetic Parameters**

The kinetic studies of the reaction catalyzed by both free and immobilized invertase were performed at various concentrations of the substrate. The Michaelis-Menten constant,  $K_m$ , and maximum velocity,  $V_{max}$ , were obtained from the Lineweaver-Burk plots. The calculated values of the kinetic parameters are listed in Table 3.2

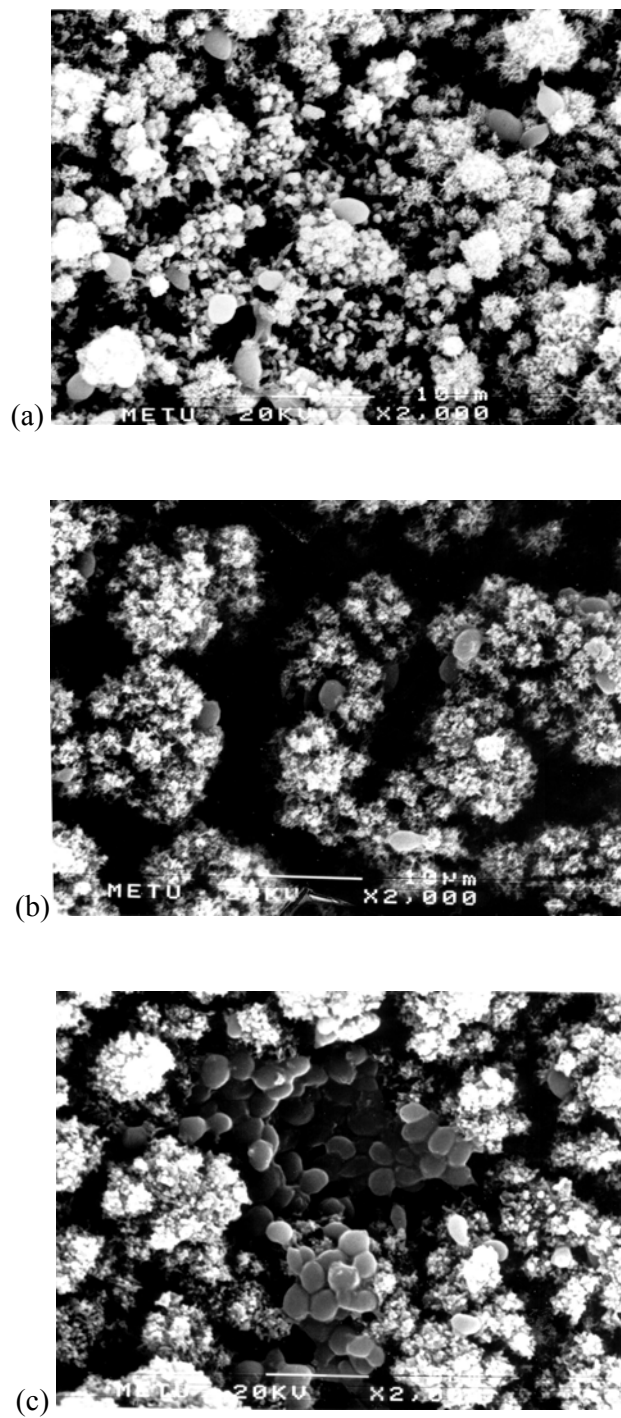


Figure 3.16 Scanning electron micrographs of (a) Ppy (b) CNPS (c) PM-2 matrices in the presence of invertase

The kinetic behavior of invertase was altered via immobilization. For free invertase  $V_{\max}$  and  $K_m$  values are 82.3  $\mu\text{mol}/\text{min.mL}$  and 24.3 mM respectively.  $V_{\max}$  values for Ppy and CNPS matrices are consistent within themselves but they are significantly different from that of the free invertase. Ppy and CN/Ppy matrices show similar  $K_m$  values with free invertase, which indicates that these matrices provide a microenvironment which does not prevent enzyme and substrate to come together.

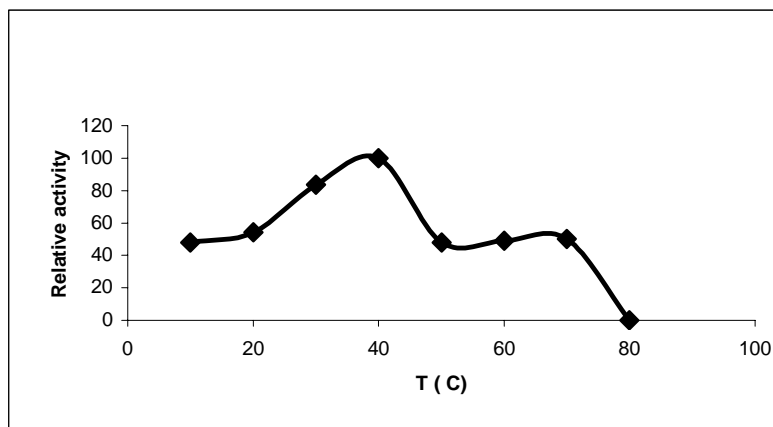
MM/Ppy matrix exhibits a smaller  $K_m$  value than free invertase. A smaller  $K_m$  value than free enzyme, indicates that this matrix provide a microenvironment which is more suitable than that of in bulk solution.

Table 3.2 Kinetic parameters for free and immobilized invertase

	$K_m$ (mM)	$V_{\max}$ ( $\mu\text{mol}/\text{min.electrode}$ )
Ppy/invertase	24.4	2.9
CNPS/invertase	22.3	2.2
PM-2/invertase	4.9	0.9

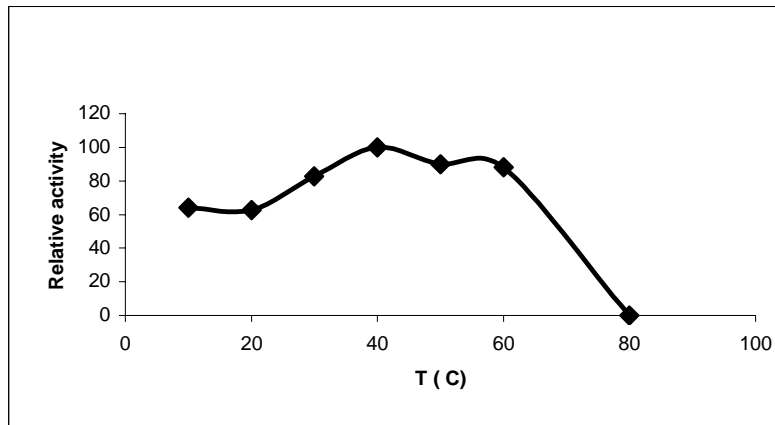
### 3.5.1.3 Effect of Temperature

The effect of incubation temperature on the relative enzyme activities was investigated and illustrated in Figure 3.17. The maximum activity for free enzyme was found to be 50°C. Ppy electrode reveals a temperature of 50°C where invertase shows maximum activity, whereas CNPS and PM-2 electrodes yield a maximum activity at 40°C. Hence, a lower temperature is attained in the measurement of activity in these matrices. In the case of CNPS, immobilized enzyme exhibit stability against temperature change between temperatures 30°C and 60°C.



(a)

Figure 3.17 Effect of temperature on PPO enzyme activity in (a) PM-2 (b) CNPS enzyme electrodes



(b)

Figure 3.17 (Cont.)

#### 3.5.1.4 Operational Stability

Stability of electrodes in terms of repetitive uses was studied in more than 25 successive measurements and Figure 3.18 shows the relative activities of the electrodes versus time. A slight decrease in activity was observed, however, after first few measurements only small fluctuations were observed. PM-2 electrode is the enzyme electrode which shows the highest initial loss in activity with lowest fluctuation in the stability.

#### 3.5.1.5 Shelf-Life

Shelf-lives for three enzyme electrodes were also studied (Figure 3.19). Ppy and CNPS matrices lost their activity at the 60<sup>th</sup> day completely. Ppy matrix show 40% decrease in activity in the first 10 days and stays almost constant up to 30 days, whereas CNPS matrix shows a continuous decrease until the 25<sup>th</sup> day. PM-2 matrix is the most stable electrode in terms of shelf-life.

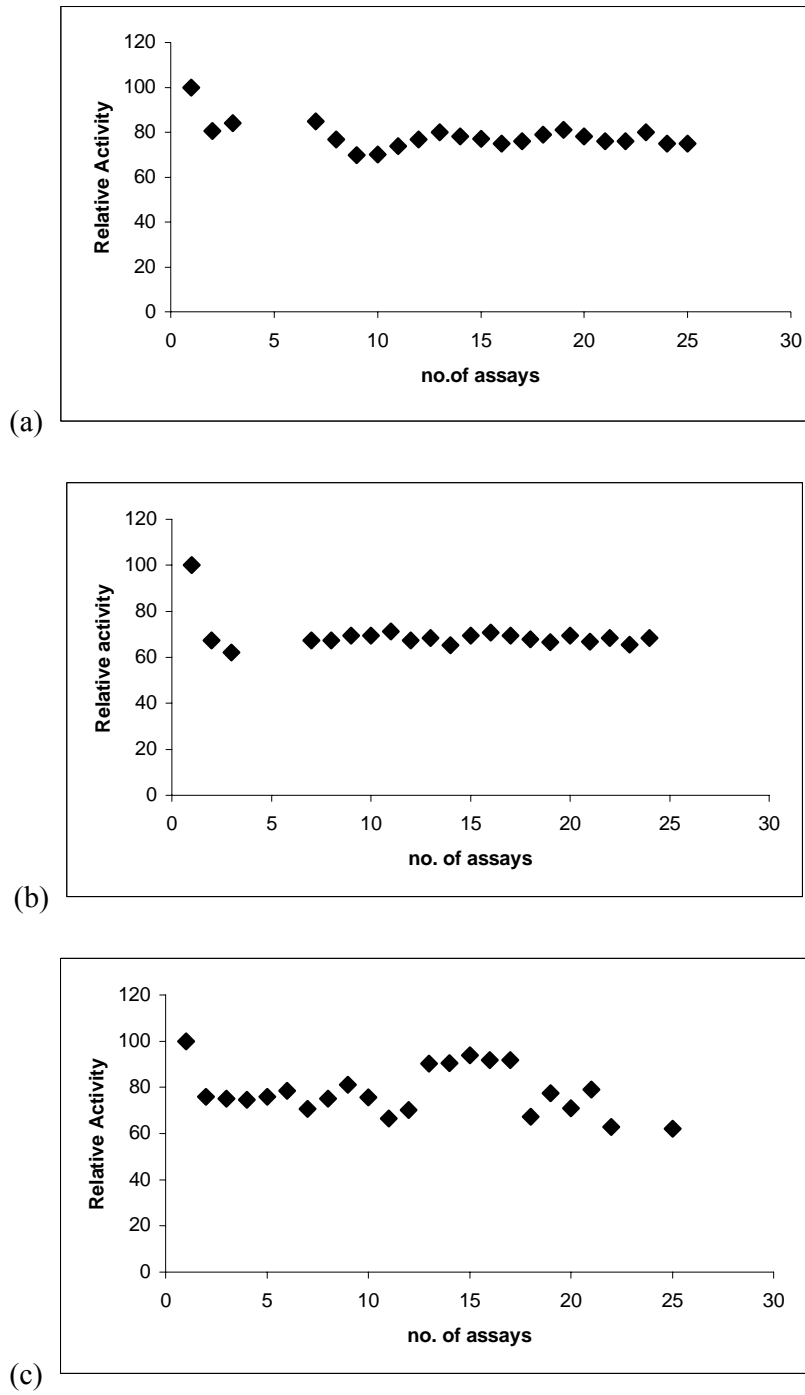


Figure 3.18 Operational stability of (a) Ppy/PPO (b) PM-2/PPO (c) CNPS/PPO enzyme electrodes

Its activity was measured up to 90 days and it was observed that only 25% of initial activity was lost. The initial loss of enzyme activity might be due to desorption, leakage through the membrane, erosion of the support material or structural changes in the enzyme during immobilization process.

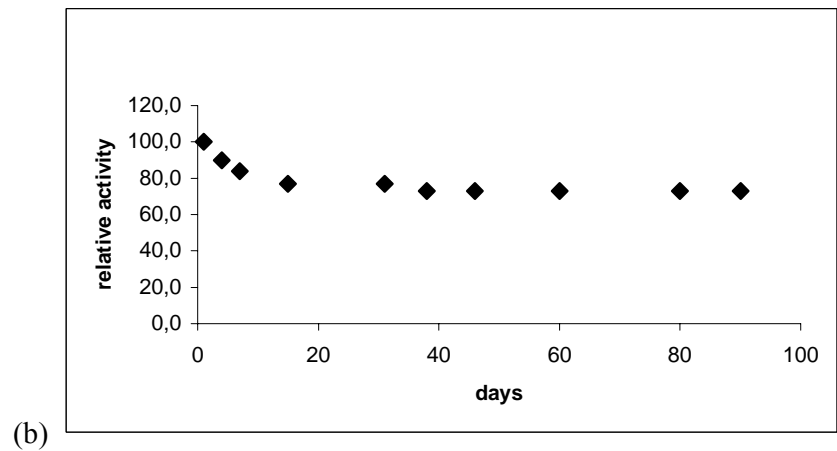
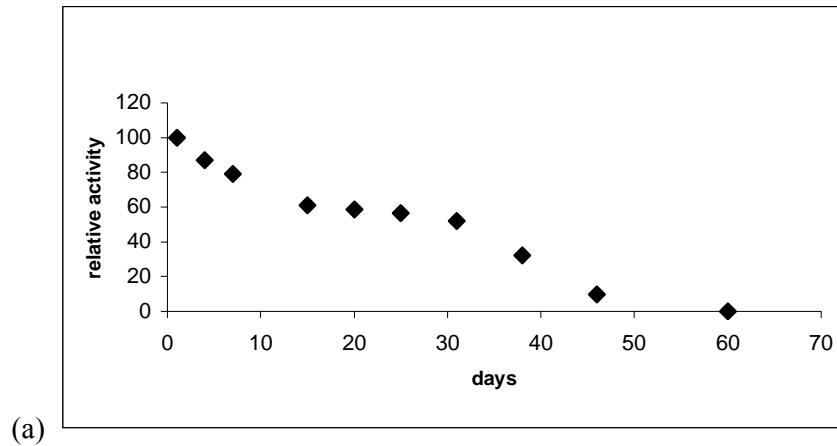


Figure 3.19 Storage stability of (a) Ppy/PPO (b) PM-2/PPO (c) CNPS/PPO enzyme electrodes

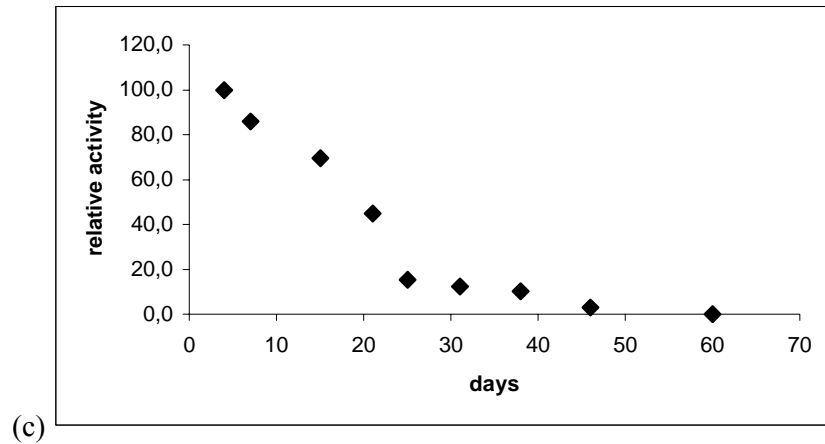


Figure 3.19 (Cont.)

### 3.5.2 Immobilization of PPO (Tyrosinase)

#### 3.5.2.1 Tyrosinase Activity

The enzyme assay is based on the measurement of *o*-quinone generated in enzymatic reaction.

The method described in section 2.3.7.2.3 is based on the spectrophotometric measurements of absorbance of the compound produced when the 3-methyl-2-benzothiozolinone (MBTH) interacts with the quinones produced by the enzyme to yield red products.

Figure 2.12 shows the coloration reaction of *o*-quinone by Besthorn's Hydrazone Method.



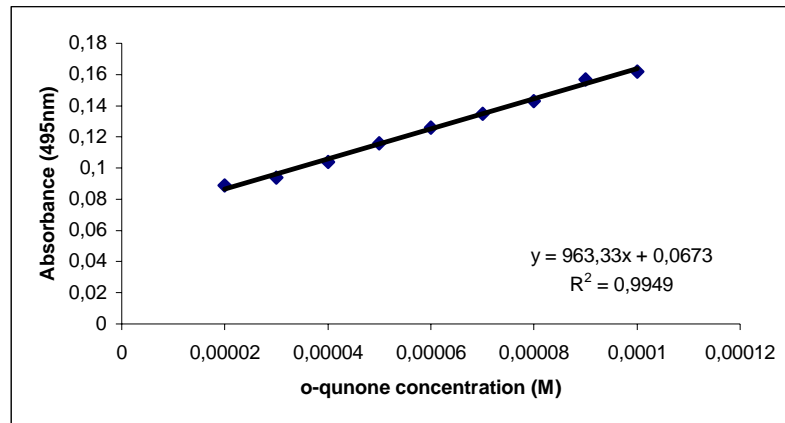


Figure 3.20 Calibration Curve for Besthorn's Hydrazone Method

### 3.5.2.2 Protein Determination

Determination of amount of immobilized protein was performed as it was described in section 2.3.7.2.8. Figure 3.21 shows the calibration curve which is prepared by using bovine serum albumin.

Results of protein determination experiments showed that Ppy/PPO and PM-2/PPO electrodes entrapped  $9.6 \times 10^{-3}$  and  $8.9 \times 10^{-3}$  mg protein in each electrode respectively. Other two enzyme electrodes that were obtained by homopolymers contain less amount of protein compared to the Ppy and PM-2 electrodes (Table 3.3) [121].

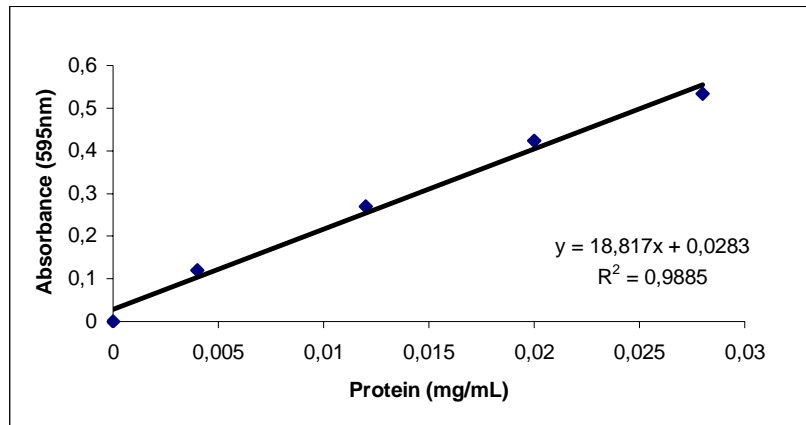


Figure 3.21 Calibration curve for protein determination.

Table 3.3 Protein amounts for enzyme electrodes

Free PPO	0.46 mg protein /mg enzyme powder
Ppy/PPO	0.0096 mg protein/electrode
PM-2/PPO	0.0089 mg protein/electrode
CNPS/PPO	0.0030 mg protein/electrode
MBTA/PPO	0.0043 mg protein/electrode

### 3.5.2.3 Kinetic Parameters

The maximum reaction rate,  $V_{max}$ , and Michaelis-Menten constant,  $K_m$ , were obtained from Lineweaver-Burk plots. Free PPO has a maximum reaction rate of 11.2  $\mu\text{mol}/\text{min. mg protein}$  and  $K_m$  of 4 mM (Table 3.4).

Rate of reaction was expected to decrease due to immobilization, but when the reaction rates compared from the point of protein amount, it is seen

that there is no difference between free PPO and enzyme electrodes. Enzyme electrodes have reaction rates as 11.3  $\mu\text{mol}/\text{min}\cdot\text{mg}$  protein. This means that immobilization does not affect the rate of product formation.

$K_m$  is a parameter that is inversely proportional to the affinity of enzyme to substrate. Large  $K_m$  indicates lower affinity. Ppy and PM-2 enzyme electrodes exhibit very large  $K_m$  values compared to free PPO. These values explain the higher reaction rates than expected values, since enzyme and substrate form the product and immediately leave each other to give way for the next substrate.

$V_{\text{max}}$  values for CNPS and MBTA can be accounted by the protein amounts which were low. Enzyme electrodes formed by homopolymers of MM and MBTA exhibit lower  $K_m$  values which are 45mM and 18mM respectively. At this point, presence of homopolymers reminds a discussion related with the low values of  $K_m$ . Enzyme may prefer the homopolymer (i.e. CN and MBTA) part of the copolymer to be more efficient. In the case of MBTA chain length of homopolymer is longer compared to CN, thus the lower value of  $K_m$  for MBTA may be due to this phenomenon.

#### **3.5.2.4 Morphologies of Films**

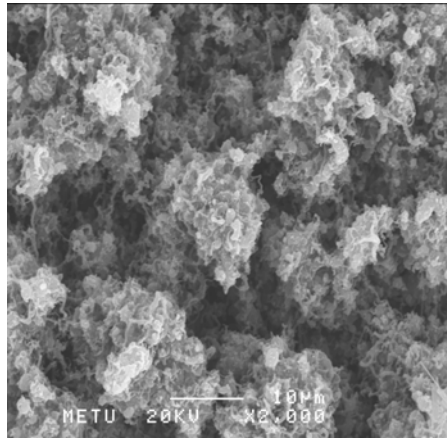
SEM micrographs of the enzyme entrapped films help us to explain the kinetic parameters from the view of morphology.

When we examine the scanning electron micrographs of four electrodes in Figure 3.22, one can see that both Ppy/PPO and PM-2/PPO electrodes have very compact morphology that make it difficult for substrate to diffuse into the

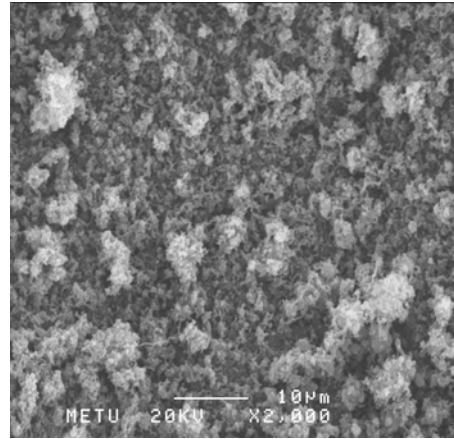
matrix. This may account for the high  $K_m$  values. However, PMBTA/PPO electrode gives rise to easy diffusion for substrate by making enzymes more available. Due to that reason this electrode gives a small  $K_m$  value as 18 mM.

Table 3.4 Kinetic parameters for free and immobilized PPO

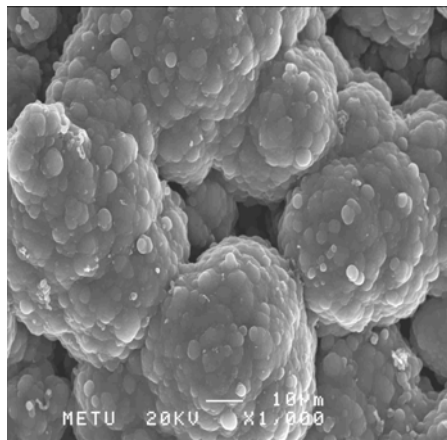
	$V_{max}$ ( $\mu\text{mol}/\text{min ml}$ )	$K_m$ (mM)
Ppy/PPO	0.027 (0.110 $\mu\text{mol}/\text{min}$ electrode)	100
PM-2/PPO	0.025 (0.100 $\mu\text{mol}/\text{min}$ electrode)	200
CNPS/PPO	0.0085 (0.034 $\mu\text{mol}/\text{min}$ electrode)	45
MBTA/PPO	0.012 (0.048 $\mu\text{mol}/\text{min}$ electrode)	18



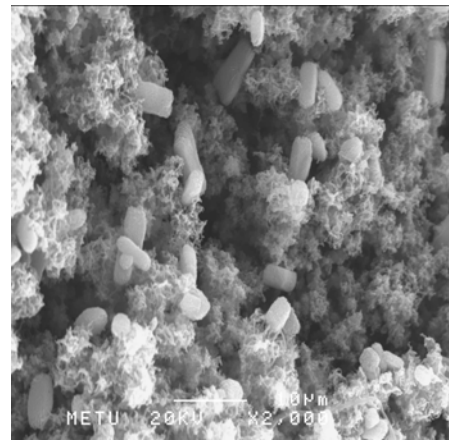
(a)



(b)



(c)



(d)

Figure 3.22 Scanning electron micrographs of (a) Ppy (b) PM-2 (c) CNPS (d) MBTA enzyme electrodes

### 3.5.2.5 Effect of Temperature on Enzyme Activity

The influence of the reaction temperature on the activity of the free and immobilized PPO is given in Figure 3.23. Both free and immobilized polyphenol oxidase in Ppy/PPO electrode showed an optimal temperature of 40°C. Free PPO lost its activity completely at 50°C but PPO immobilized in Ppy electrode lost only its 40% of its original activity at 50°C. PM-2/PPO electrode showed a maximum at 60°C and exhibit stability up to 80°C. Immobilized PPO in this electrode retained 50% of its optimum activity up to 80°C.

In the case of CNPS/PPO electrode, maximum activity was observed at 60°C, with a little amount of activity loss after this temperature. At temperatures between 50°C and 70°C, MBTA/PPO enzyme electrode exhibit high resistance to temperature change. Almost no activity loss was observed between these temperatures.

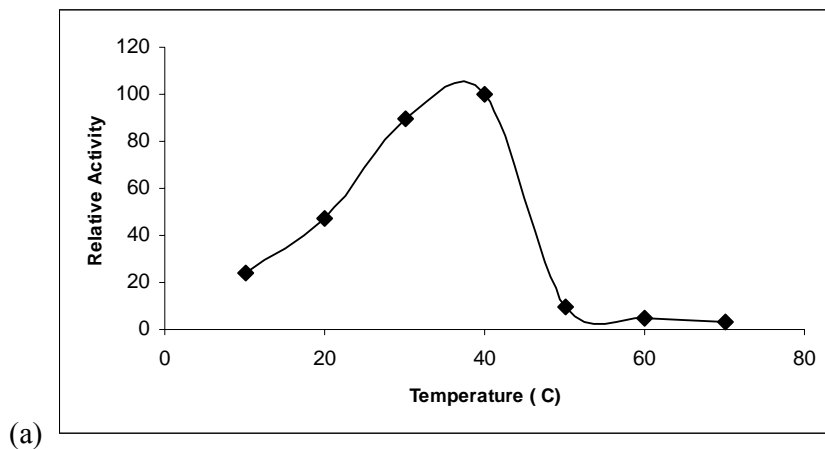


Figure 3.23 Temperature stability of (a) Free PPO (b) Ppy/PPO (c) PM-2/PPO (d) CNPS/PPO (e) MBTA/PPO

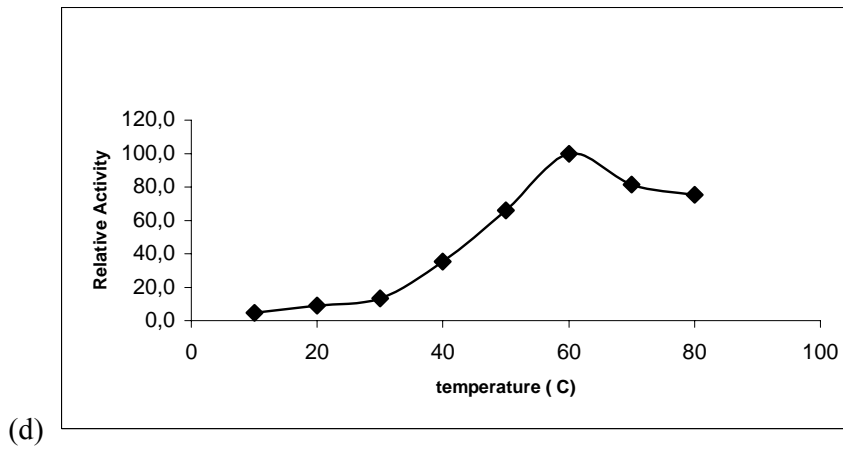
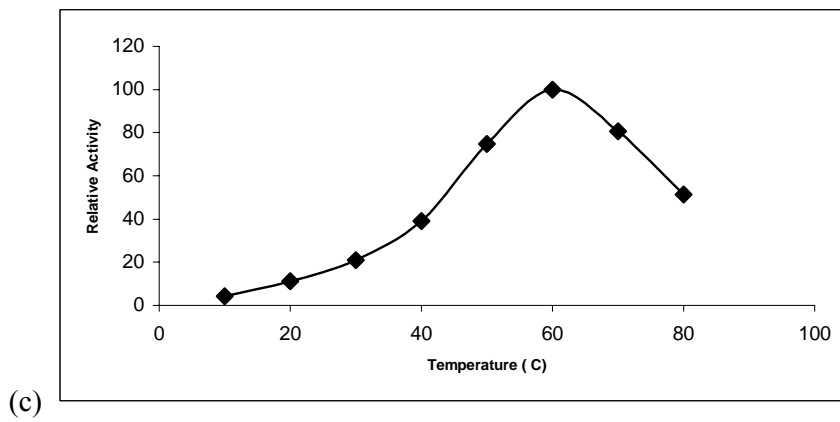
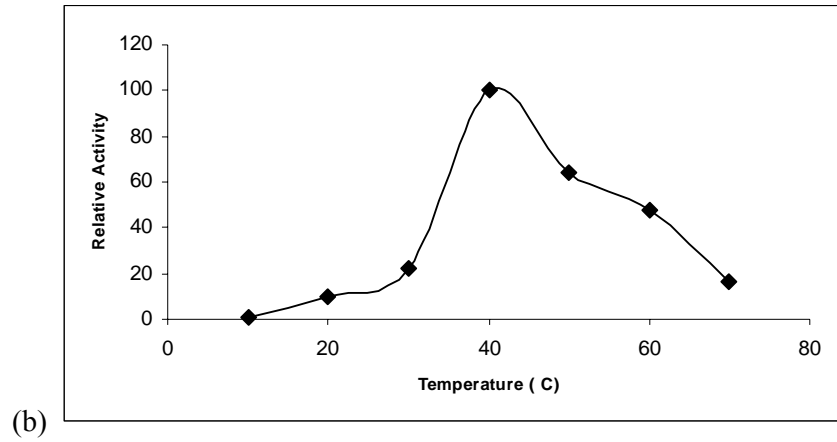


Figure 3.23 (Cont.)

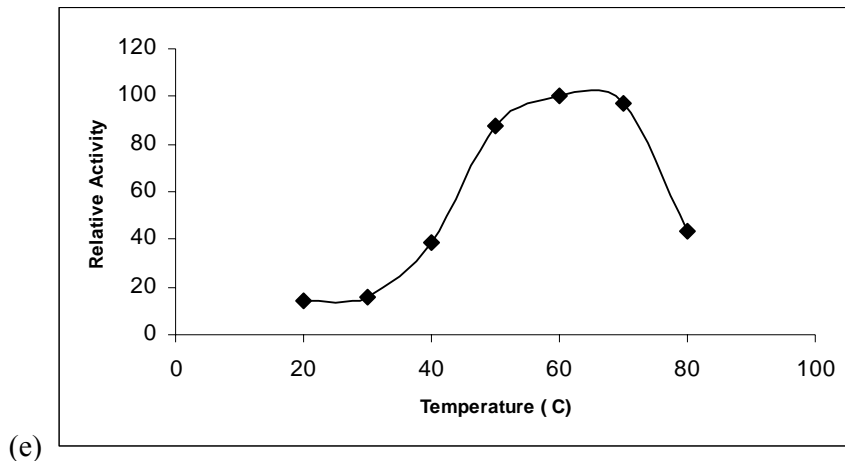


Figure 3.23 (Cont.)

### 3.5.2.6 Effect of pH on Enzyme activity

Free PPO had an optimum pH of 5 (Fig.3.24). Immobilized PPO revealed an optimal pH for Ppy/PPO and PM-2/PPO electrodes as 7 and 9 respectively, thus, pH stability is increased for both electrodes. At levels of pH lower than 6 the activity of immobilized PPO was less sensitive to the pH change, indicating a better resistance of the immobilized protein molecules to the ionization, since the ionic state of the functional groups in or close to the active center has a great effect on its activity.

The optimum pH value of both enzyme electrodes was shifted towards the alkaline side compared to that of the free enzyme. This might be explained by the partitioning of protons. The negative groups of the matrix protons are concentrated around the enzymes and protect them against the high concentration of  $\text{OH}^-$ . This tendency makes the pH around enzyme lower than that of the bulk. Higher the tendency of matrix to concentrate protons in it, higher the pH stability of enzyme in this matrix.



In case of Ppy and PM-2 electrodes, at pH levels greater than the maximum points, the activity of entrapped PPO was much affected by the pH change than that of the free enzyme. The positive charges on the matrix should decrease with increasing pH and so does the net charge of PPO where isoelectric point is 6.1. Therefore, the repulsive forces might have caused a split in the enzyme electrodes resulting in a less favorable conformation of the enzyme molecules.

The same behavior in pH dependence was observed for CNPS and MBTA electrodes, but these electrodes exhibit greater stability towards high pH (Figure 3.24). From pH 7 to 11 there is no change in the enzyme activity. This shows that these electrodes can protect enzymes against high OH concentration.

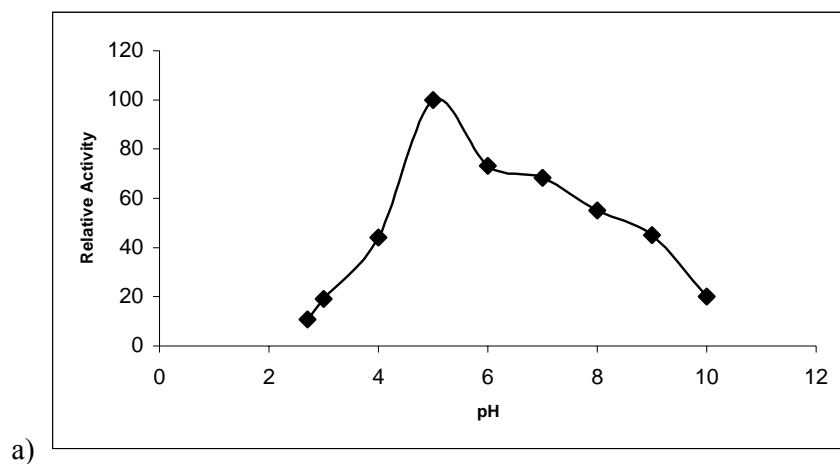


Figure 3.24 pH stability of (a) Free PPO (b) Ppy/PPO (c) PM-2/PPO (d) CNPS/PPO (e) MBTA/PPO

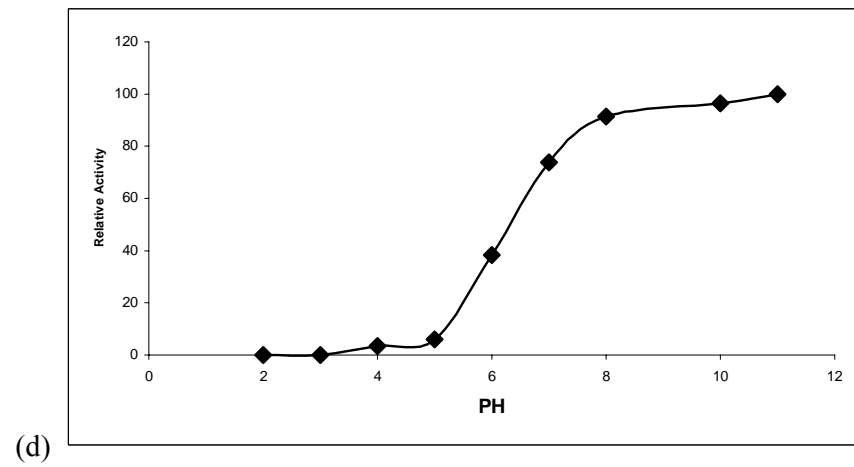
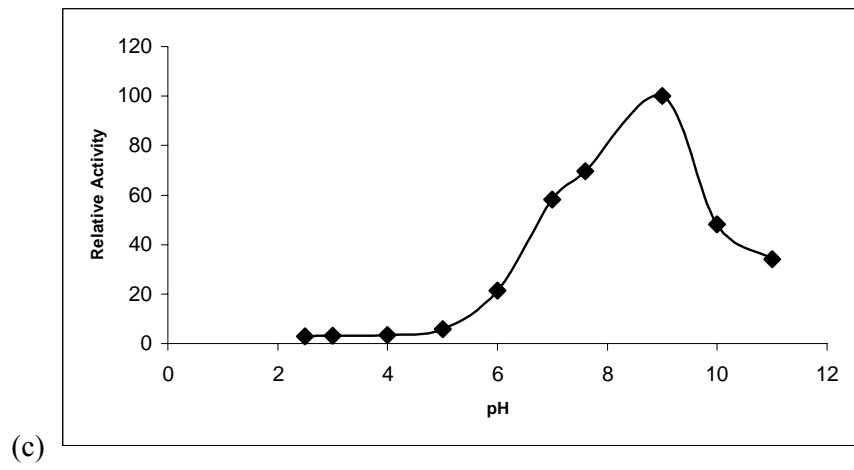
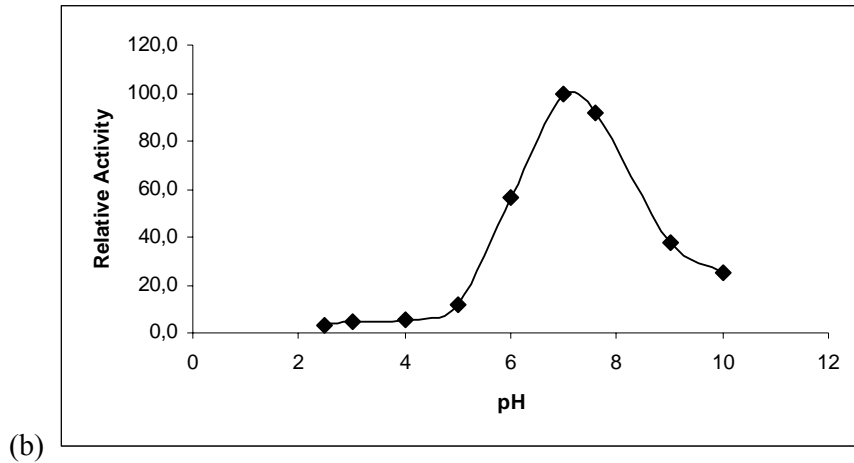


Figure 3.24 (Cont.)

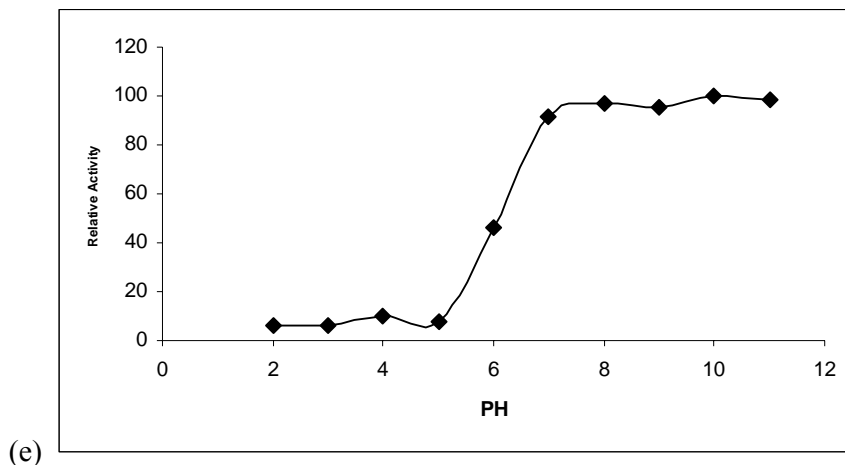


Figure 3.24 (Cont.)

### 3.5.2.7 Operational Stability of Enzyme Electrodes

Enzymes can easily lose their catalytic activity and denatured, thus, careful storage and handling are essential. Stability of electrodes in terms of repetitive uses was performed in 40 successive measurements. Ppy/PPO electrode showed activity that gradually decreased up to 10<sup>th</sup> use and then stayed constant at 60% activity (Figure 3.25). As to the temperature and pH stability, PM-2/PPO electrode exhibits very high operational stability and retained 85% of its activity up to 40<sup>th</sup> use.

CNPS and MBTA enzyme electrodes reveal similar amount of activity loss. CNPS electrode exhibit a fluctuation up to the 20<sup>th</sup> use but its activity stay constant in the further measurements.

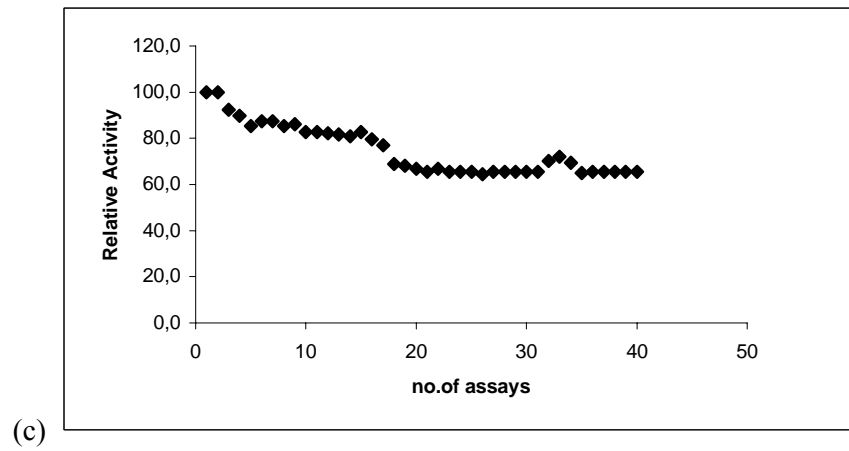
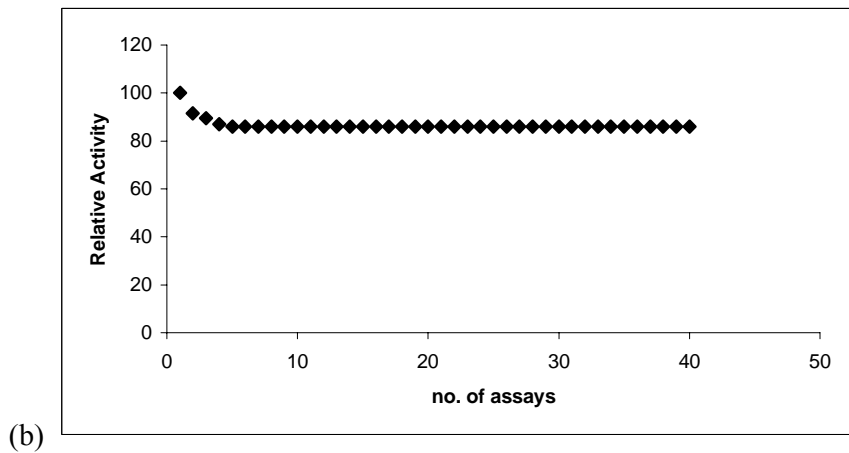
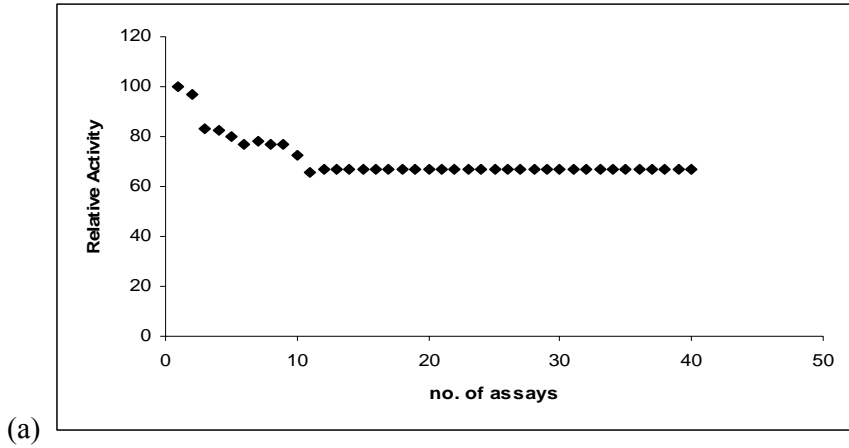


Figure 3.25 Operational stability for (a) Ppy/PPO (b) PM-2/PPO (c) CNPS/PPO (d) MBTA/PPO

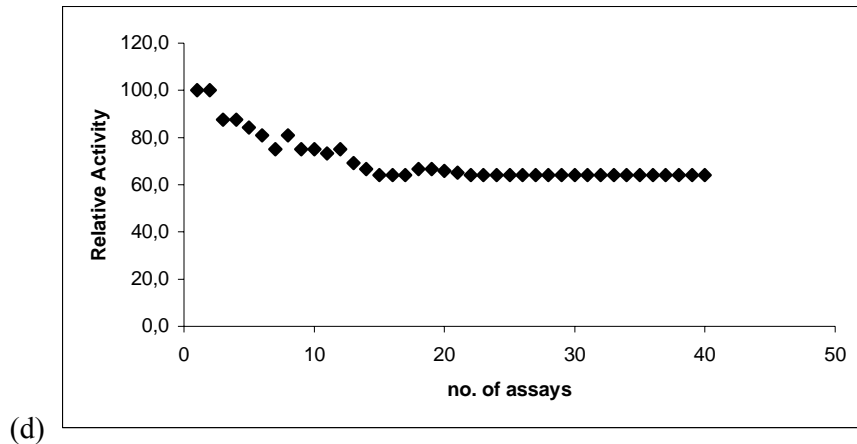


Figure 3.25 (Cont.)

### 3.5.2.8 Shelf-Life of Enzyme Electrodes

The activity of immobilized PPO was determined as a function of time over a period of 40 days. Before performing the enzyme assays, the electrodes were washed by the buffer solution, to remove any loosely bound enzyme that might have diffuse to the surface of the film with time.

There is a continuous gradual decrease for Ppy and CNPS electrodes which have maximum activity loss up to 40 %, whereas PM-2 electrode exhibit the least activity loss among four enzyme electrodes. After the 10<sup>th</sup> day enzyme activity almost stay constant up to 40<sup>th</sup> day.

Upon examining the activity change with time we see that there is a rapid decrease in the activity of MBTA electrode which slows down after the 20<sup>th</sup> day.

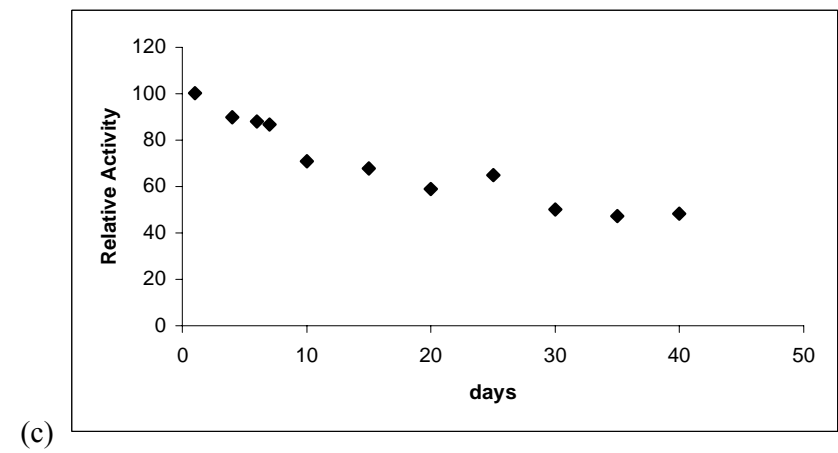
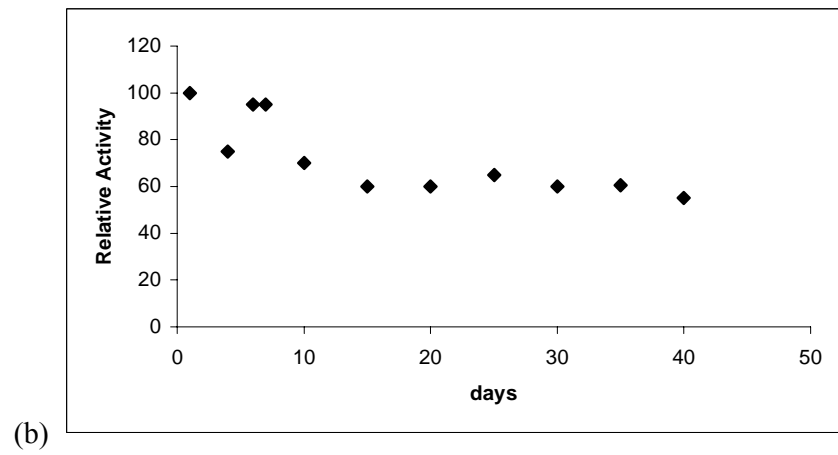
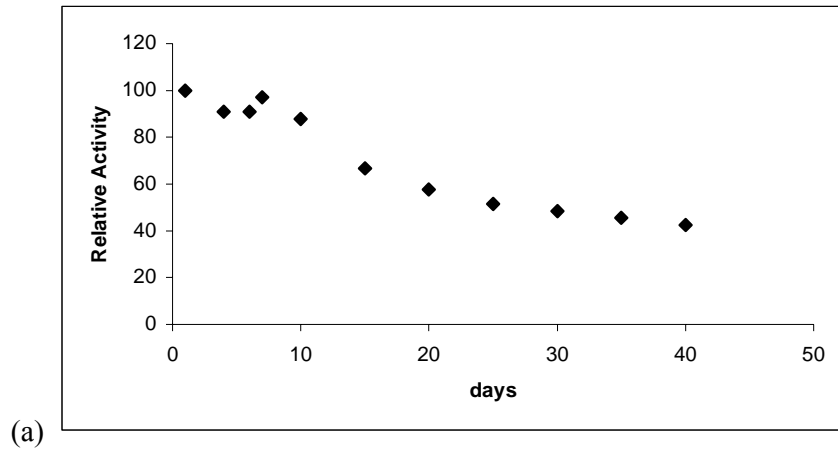


Figure 3.26 Shelf life for (a) Ppy/PPO (b) PM-2/PPO (c) CNPS/PPO  
(d) MBTA/PPO

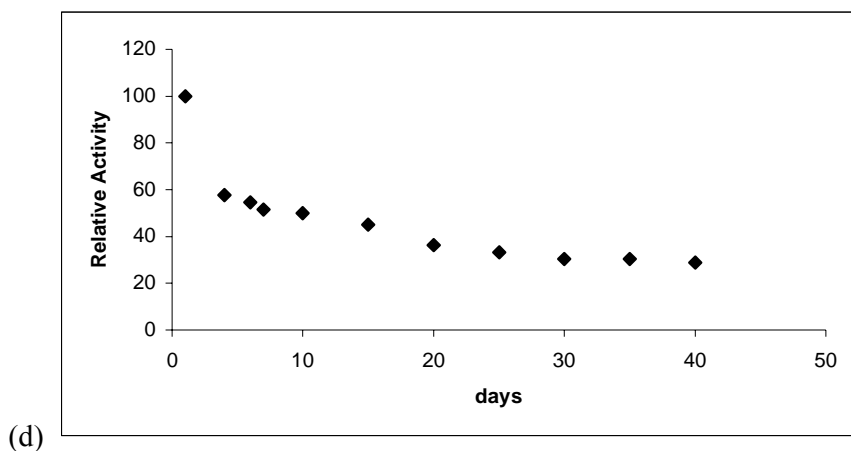


Figure 3.26 (Cont.)

### 3.5.2.9 Determination of Phenolic Compounds in Red Wines

This study was designed to determine total phenolic compounds in wines by using the fabricated enzyme electrodes. Total phenolic compounds in Turkish wines were reported as 2000-3000 mg/L [117-119].

Polyphenol oxidase enzyme act on  $-OH$  groups on phenolic compounds. Via activity determination of enzyme electrodes in red wines we obtain the total  $-OH$  groups (Table 3.5).

Two Turkish red wines (Brand K and Brand D) were analyzed for their concentration of phenolic compounds by using Ppy/PPO, PM-2/PPO, CNPS/PPO and MBTH/ PPO electrodes.

Results for phenolic determination by using free PPO enzyme give very small values when compared with both enzyme electrodes. As it is known from the literature, benzoates act as inhibitors for free PPO. So PPO is inhibited

by benzoates, found naturally in wines, before it complete its enzymatic reactions. Immobilized PPO was protected by the matrix that it entrapped and was not affected by the inhibitors found in the wine.

Brand K contains twice the amount of phenolics compared to that of Brand D. This result was confirmed by all enzyme electrodes. High amount of phenolics in Brand K is responsible for the bitter taste of the wine [121,122].

Results are reported in Gallic Acid Equivalent (GAE) [116].

Table 3.5 Total phenolics in two different red wines, determined by enzyme electrodes.

	<b>Brand K</b>	<b>Brand D</b>
<b>Free Enzyme</b>	0.004M -OH 220mg/L	0.005M -OH 270mg/L
<b>Ppy/PPO</b>	0.072M -OH 4000mg/L	0.04M -OH 2200mg/L
<b>PM-2/PPO</b>	0.112M -OH 6000mg/L	0.06M -OH 3300mg/L
<b>CNPS/PPO</b>	0.075M-OH 4160mg/L	0.038M-OH 2140mg/L
<b>MBTA/PPO</b>	0.075M -OH 4160mg/L	0.035M -OH 1950mg/L



## **CHAPTER 4**

### **CONCLUSION**

A new thiophene derivative containing menthyl group (MM) was synthesized and polymerized via chemical and electrochemical (constant current) methods. Polymers and MM itself were used to synthesize copolymers with pyrrole under conditions of constant potential electrolyses. These copolymers were used as enzyme immobilization matrices.

In terms of surface morphology, water/PTSA solvent/electrolyte couple is the most interesting medium for copolymerization. In terms of conductivity best films were obtained in water/SDS medium. Hence, copolymers of MM were prepared with an appreciable conductivity.

This study shows that invertase and polyphenol oxidase can be successfully immobilized in all used matrices synthesized for that purpose. For both enzymes, as regards to operational stability and shelf-life PM-2 matrix exhibits significant improvement among the enzyme electrodes. In case of temperature and pH stability, enzyme electrodes constructed in the presence of homopolymers reveal better results.

Immobilization of polyphenol oxidase enzyme in a conducting polymer electrode was studied as an alternative method for determination of phenolic compounds in wines and obtained results reveal that this significant development can successfully replace the classical methods.

## REFERENCES

1. C.K. Chiang, CR. Finche Y.W. Park, A.J. Heeger. H. Shirakawa, E.J.Louis, S.C. Gua, and A.G. MacDiarmid. *Phy. Rev. Lett*, 39:1098, 1977.
2. N.P. Cheremisinoff (Ed), *Encyclopedia of Engineering Materials, Part A, Polymer science and Tchnology*, Marcel Dekker Inc., New york, 1998, vol.1, chapter8.
3. Shirakawa, E.J. Louis, AG. MacDiarmid, and AJ. Heeger *J. Chem. Soc.Chem. Comm.*, page 578, 1977.
4. W.R. Salaneck and J.L. Bredas. *Solid State Comm.*, 92:31, 1994.
5. T. Skotheim, J.R. Reynolds, and RL. Elsenbaumer(Eds.). *Handbook of Conjugated PoIymers II* Marcel Dekker INC., NY, 1997.
6. S.Roth, W. Graupner, and P. McNeillia. *Acta Phys. Polon.*, 85:1, 1995.
7. M. Aldissi(Ed.). *Intrinsically Conducting Polymers: An Emerging Technology*. Kluwer, Dordrecht, 1993.
8. S.A. Jenekhe and K.J. Wynne (Eds). *Photonic and Optoelectronic Polymers*. ACS Symposium Series, Whashington DC, 1995.
9. A.J. Heeger, S. Kivelson, J.R. Schrieffer, and WP. Su. *Rev. Mod. Phys.*, 60:781, 1988.

10. JL Brédas, RR. Chance, R. Silbey, G. Nicolas, and P. Durand. *J. Chem. Phys.*, 75:255, 1981.
11. K. Lee and A.J. Heeger. *Synth. Met.*, 84:715, 1997.
12. RS. Kohlman, T. Ishiguro, H. Kaneko, and A.J. Epstein. *Synth. Met.*, 69:325, 1995.
13. R.S. Kohlman, A. Zibold, D.B. Tanner, G.G. Ihas, T. Ishiguro, Y.G. Min, AG. MacDiarmid, and AJ. Epstein. *Phys. Rev. Lett.*, 78:3915, 1997.
14. W.R. Salaneck, D.T. Clark, and E.J. Samuelsen (Eds.). *Science and Technology of Conducting Polymers*. Adam Hilger. Bristol, England, 1991.
15. K. Mullen and G. Wegner (Ed.). *Electronic Materials: The Oligomer Approach*. Wiley-VCH, NY, 1998.
16. F. Garnier, R. Hajlaoui, A. Yassar, and P. Srivastava. *Science*, 265:684, 1992.
17. H. Sirringhaus, N. Tessler, and R.H. Friend. *Science* 280:1741,1998.
18. J.J.M. Halls, C.A. Walsh, N.C. Greenham,, E.A. Marseglia, R.H Friend, S.C. Moratti, and AB. Holmes. *Nature*, 376:498, 1995.
19. R.H. Friend, R.W. Gymer, A.B. Holmes, E.G.J. Staring, c. Taliani, D.DC.Bradley, DA. dos Santos, J.L. Bredas, M. Lögdlund, and W.R. Salaneck.*Nature* 397:121,1998.
20. F. Hide, MA. Diaz-Garcia, B. Schwartz, MR Anderson, Q. Pei, and A.J. Heeger *Science*, 273:1833, 1996.
21. Y.Z. Wang and AJ. Epstein. *Acc. Che. Res.*, 32:217, 1999.

22. D.D Gebler, Y.Z. Wang, D.-K. Fu, T.M. Swager, and A.J. Epstein. *J.Chem. Phys.*, 108:7842, 1998.
23. A.O. Patil, A.J. Heeger, F. Wudl, American Chem. Soc. (Chem. Review) Vol.88, 183 (1988).
24. P. Kovacic, A. Kyriakis, J. Am. Chem. Soc., Vol.85, 454 (1963).
25. D.M. Ivory, G.G. Miller, J.M. Sowa, L.W. Shacklette, R.R. Chance, R.H. Baughmann, J. Chem. Phys., Vol.71, 1506 (1979).
26. G.E. Wnek, J.C. Chine, F.E. Karasz, C.P. Lillya, Polymer, Vol.20, 1441 (1979).
27. E.M. Genies, G. Bidan, A.F.Diaz, J. Electroanalyt. Chem., Vol.149, 101 (1983).
28. A.F. Diaz, A. Martinez, K.K. Kanazawa, M. Salmon, J. Electroanalyt. Chem., Vol.130, 181 (1980).
29. K. Kaneto, K. Yoshino, Y. Inushi, Solid State Comm., Vol.46, 389 (1983)
30. Jan Bartus, J. Macromol. Sci.-Chem.A(28), Vol.9, 917 (1991).
31. A.J. Heeger, P. Smith, A. Fizazi, J. Moulton, K. Pakbaz, S. Rughooputh, Synthetic Metals, 41-43, 1027 (1991).
32. Semih Yiğit, Ph.D.Thesis, METU, 1996.
33. N.Balci, U. Akbulut, L. Toppare, d. Stanke and M.L. Hallensleben, Mat. Res. Bull.,32, 1997, 1449.

34. Tanaka, M.; Watanabe, A.; Fujimoto, H; Tanaka, J. *Mol Cryst. Liq. Cryst.* 1982,83,277.
35. Plochaski, J. In *Material Science Forum*; Murch G.E. Ed.; Trans Tech Pub. Ltd.: Switzerland, 1987; Vol.21, p 173-178
36. Miller, D.L. PhD. Dissertation, Texas A&M University, 1990.
37. Salmon, M.; Diaz, A. F.; Logan, A. J.; Krounbi, M. Bargon, J. *Mol Cryst. Liq Cryst.* 1982,83,265.
38. Bredas, J.L.; Scott, J. C.; Yakushi, K; Street~ G. B. *Phys. Rev. B* 1984,30, 1023
39. Wegner, G. Angus, Clue., hit. Ed. Engi. 1931,20,361.
40. Kaufman, J. H Colaneri. N.; Scott, J. C; Kanazawa, K. K.; Street, G. B. *Mol. Cryst. Liq. Cryst.* 1985, 118, 171.
41. Y. Ito, H. Shirakawa and S. Ikeda, *J Polym. Sci*, 13 (1975) 1943.
42. R B. Kaner, *Electrochemical Science and Technology of Polymers*, R. G. Linford (Ed), 97, Elsevier Applied Science, Essex, England, 1990.
43. J. Roncali, *Chem. Rev.*, 92(4) (1992) 711.
44. D.J.Walton, *Mater.Des.*, 11(3) (1990)142
45. S. Hotta, T. Hosaka and W. Shimotsuma, *Synth. Met*, 6(1983) 319.
46. F. Diaz and J. Bargon, *Handbook of Conducting Polymers*, T. J. Skotheim (Ed.), Marcel Dekker, New York, 1986, p. 81.

47. H. Koezuka, S. Etoh, *J. Appl. Phys.* 54, 2511 (1983)
48. K. K. Kanazawa, A. F. Diaz, W. Will, P. Grant, G. B. Street, G. P. Gardini, G. Kwak, *Synth. Met.* 1, 320 (1980)
49. S. Kuwabata, S. Ito, H. Yoneyama, *J. Electrochem. Soc.* 135, 1691 (1988)
50. Inganas, B. Liedberg, W. Hang-Ru, H. Wynberg, *Synth. Met.* 11, 239 (1985)
51. J. P. Ferraris, G. D. Skiles, *Polymer* 28, 179 (1987)
52. Niva, T. Tamamura, M. Kakuchi, *Macromolecules* 20, 749 (1987)
53. M. A. DePaoli, R. J. Waltman, A. F. Diaz and I. Bargon, *J. Polym. Sci. Polym. Chem. Ed.* 23, 1687 (1985).
54. G. Nagausubramanian, S. DiStefano, *J. Electrochem. Soc. Extended Abstr.* 85, 659 (1985)
55. H. L. Wang, L. Toppare and J. F. Fernandez, *Macromolecules* 23, 1053 (1990)
56. D. Stanke, M. L. Hallensleben, L. Toppare, *Synth. Met.* 55, 1108 (1988).
57. D. Stanke, M. L. Hallensleben, L. Toppare, *Macromol. Chem. Phys.* 196, 1697 (1988).
58. D. Stanke, M. L. Hallensleben, L. Toppare, *Synth. Met.* 73, 261 (1995).

59. F. Selampinar, U. Akbulut, T. Yilmaz, A. Gürgör, L. Toppare, I. *Polym. Sci. Polym. Chem.* 5, 3009 (1997)
60. F. Selampinar, U. Akbulut, T. Yalcin, S. Suzer, L. Toppare, *Synth. Met.* 62, 201 (1999)
61. F. Kalaycioglu, L. Toppare, Y. Yagci, V. Harabagiu, M. Pintela, R. Ardelean, B. Simunescu, *Synth. Met.* 97, 7 (1998)
62. N. Kizilyar, L. Toppare, A. Onen, Y. Yagci, *Polym. Bull.* 40, 639 (1997)
63. S. Oztemiz, L. Toppare, A. Onen, Y. Yagci, *JMS-Pure Appl. Chem.* A37, 277 (2000)
64. Dodabalapur, L. Torsi, H. E. Katz, *Science* 268, 270 (1995)
65. J. C. Gustafson, O. Inganas, A. M. Andersson, *Synth. Met.* 62, 17 (1994)
66. Kraft, A. C. Grimsdale, A. B. Holmes, *Angew. Chem. Int. Ed.* 37, 402 (1998)
67. F. Jonas, G. Heywang, W. Schmidtberg, J. Heinze, M. Dietrich, *M. Europ. Pat. Appl.* 339, 340 (1988)
68. J. C. DuBois, O. Sagnes, F. Henry, *Synth. Met.* 28, C871 (1989)
69. J. P. Ferraris, M. M. Eissa, I. D. Brotherson, D. C. Loveday, *Chem. Mater.* 10, 3528 (1998)
70. G. Heywang, F. Jonas, *Adv. Mater.* 4, 116 (1992)
71. P. N. Bartlett, R.G. Whitaker, *J. Electroanal. Chem.* 224, 37 (1987)



72. N. C. Foulds, C. R. Lowe, *J. Chem. Soc. Faraday Trans.* 82, 1259 (1986)
73. W. Schuhmann, *Microchim. Acta.* 121, 1 (1995)
74. P. Novak, K. Muller, K. S. V. Santhanam, O. Hass, *Chem.Rev.* 97, 207 (1997)
75. T. F. Otero, H. Grande, in *Handbook of Conducting Polymers*, (1998) 2nd ed.; I. A. Skotheim, R. L. Elsenbaumer, J. R. Reynolds, (Eds).; Marcel Dekker: New York
76. D. T. McQuade, A. E. Pullen, T. M. Swager, *Chem. Rev.* 100, 2537 (2000)
77. J. Pernaut, J. R. Reynolds, *J. Phys. Chem.* B.104, 4080 (2000)
78. B. Sankaran, J. R. Reynolds, *Macromolecules* 30, 2582 (1997)
79. S. A. Sapp, G. A. Sotzing, J. R. Reynolds, *Chem. Mater.* 10, 2101 (1998).
80. P. M. S. Monk, R. J. Mortimer, D. R. Rosseirisky, *Electrochromism: Fundamentals and Applications* (1995) VCH mc: Weinheim.
81. T. Palmer, *Understanding Enzymes* (1995) Prentice Hall London.
82. a. Rosevear. J. F. Kennedy, M.S. Cabral, *Immobilized Enzymes and Cells* (1997). IOD Publishing Ltd. Bristol
83. K. Mosbach (Ed), *Methods in Enzymology, Immobilized Enzymes.* (1976)Academic Press, New York.
84. R.A. Alberty (1956) *Advances in Enzymology* 17, 1.

85. J. B. S. Haldane (1930) *Enzymes*, Longmans, Green & Co., New York.
86. L. Massart, *The Enzymes*, (1950) Academic Press, New York.
87. L. Michaelis, m. L. Menten, *Biochem, Z.* 4(1913).
88. T. Godfrey, S. West, *Industrial Enzymology*, (1996), Macmillan Press Ltd, U.K
89. G. S. Mittal, *Food Biotechnology* (1992), Technomic Publishing Company USA
90. W. Hartmeimer, *Immobilized Biocatalysts* (1998) Springer-Verlag, Berlin
91. P. W. Carr, L. D. Bowers, *Immobilized Enzymes in Analytical and Clinical Chemistry* (1980) John Wiley & Sons, Inc. New York
92. O. R. Zaborsky, *Immobilized Enzymes* (1973), CRC Press, Cleveland
93. . Marconi, S. Gulinelli, F. Morisi, *Biotechnol. Bioeng.* **16**, 501 (1974)
94. H. Maeda, H. Suzuki, A. Yamauchi, A. Sakimal, *Biotechnol. Bioeng.* 17, 119 (1975)
95. S. S. Wang, W. R. Vieth, *Biotechnol. Bioeng.* 15, 93 (1973).
96. C. Olson, W. L. Stanley, *I. Agric. Food. Chem.*, 21, 440 (1973).
97. H. Filippusson, W. E. Hornby, *Biochem. J.* 120, 215 (1970).
98. F. Selampinar, U. Akbulut, M. Y. ~zden, L. Toppare, *Biomaterials* 92, 1163 (1997)

99. N. Kizilyar, M. Y. Ozden, L. Toppare, Y. Yagci., *Synth. Met.* 104, 50 (1998)
100. R. Erginer, L. Toppare, S. Alkan, U. Bakır, *React and Funct Polymers* 45 (2000) 227.
101. J. M Nelson, C.R. Dowson, , *Advances in Enzymology*, 4:99 (1944)
102. J.F. Maddaluno, K.F. Faull, *Applied Radiation and Isotopes*, 41 (9):873 (1990)
103. F. Stocchi, N.P. Quinn, L. Barbato, P.N. Patsalos, M.T. O'Connell, S. Ruggieri, C.D. Marsden, *Clinical Neuropharmacology*, 17 (1): 38 (1994)
104. K.H. Lanouette, *Chemical Engineering*, 84(22): 99 (1977)
105. S.C. Atlow, L. Banadonna-Aparo, A.M. Klivanov, *Biotechnology and Bioengineering*, 26: 599 (1984)
106. J.G. Schiller, A.K. Chen, C.C. Liu, *Analytical Biochemistry*, 85:25(1978)
107. K. Zachariah, H.A. Mottola, *Analytical Letters*, 22(5): 1145 (1989)
108. C.R. Tiliyer, P.T. Gobin, *Biosensors and Bioelectronics*, 6(7): 569 (1991)
109. A.J. Winder, H. Harris, *European Journal of Biochemistry*, 198: 317 (1991)
110. Vinas P, Lopez-Erroz C, Marin-Hernandez JJ, Hernandez-Cordoba M.. *J.Chrom A* 2000; 871: 85-93.

- 111.Zhang S, Zhao H, John R.. *Anal Chim Acta* 2001; 441: 95-105.
- 112.Kiralp S, Alkan S, Toppare L, Cianga I, Yagci Y *J. Macrom. Sci. Pure and Appl. Chem., A40, 251(2003)*.
- 113.A. Levent, L.Toppare, I. Cianga, Y. Yağci, *Macr.Chem.Phys*, 204, 1118(2003).
- 114.Mazzocco F, Pifferi PG.. *Anal Biochem* 1976; 72: 643-647.
- 115.Russell IM, Burton SG. *Anal Chim Acta* 1999; 389: 161-170.
- 116.Rodriguez-Lopez JN, Escribano J, Garcia-Canovas FA. *Anal Biochem* 1994; 216: 205-212.
- 117.Lopez M, Martinez F, Del Valle C, Orte C, Miro M. *J Chrom A* 2001; 922: 359-363.
- 118.Sakkiadi AV, Stavrakakis MN, Haroutounian SA. *Lebensm Wiss Technol* 2001; 34: 410-413.
- 119.Karakaya S, El SN, Taş AA. *Inter J Food Sci Nutr* 2001; 52: 501-508.
- 120.Kıralp S, Toppare L, Yağcı *Synth. Met., 135, 79(2003)*
- 121.Kıralp S, Toppare L, Yağcı Y *Int. J. Biol. Macrom., 33, 37(2003)*
- 122.Kıralp S, Toppare L, YağcıY *Des Monomers Polym., 7,3 (2004)*

## VITA

Senem Kıralp was born on September 15 1976 in Cyprus. She graduated from Middle East Technical University, Faculty of Arts and Science in 1997. She began her MS studies at chemistry department of METU where she became a research assistant. During this time she worked on electrochemistry under the supervision of Prof. Dr. Zuhâl Küçükyavuz. She began doctoral studies in 2000 with Prof. Dr. Levent Toppare in the area of electrochemical polymerization, conducting polymers and enzyme immobilization. Within this time she has published 8 papers in international journals.

1. S. Kıralp, S. Alkan, L. Toppare, I. Cianga, Y. Yagci “Synthesis and Characterization of Conducting Copolymers of Menthyl Ester of 3-Thiophene Acetic Acid with Pyrrole”. *J. Macrom. Sci. Pure and Appl. Chem., A40, 251(2003)*.
2. S.Kıralp, L.Toppare, Y.Yağcı “Immobilization of İnetase in Copolymers of thiophene Functionalized Menthyl Ester with pyrrole” *Synth. Met., 135, 79(2003)*
3. S. Kıralp, L. Toppare, Y. Yağcı “Immobilization of Polyphenol Oxidase in Conducting Copolymers and Determination of Phenolic Compounds in Wines with Enzyme Electrodes” *Int. J. Biol. Macrom., 33, 37(2003)*

4. S.Kiralp, Z.Küçükyavuz, A.F.Qasrawi “Preparation and characterization of Conducting polybutadiene/Polythiophene Composites” *Turkish J. Chem.* 27, 417(2003)
5. S. Kiralp, L. Toppare, Y. Yağcı “Determination of Phenolic Compounds in Wines with Enzyme Electrodes Fabricated by Immobilization of Polyphenol Oxidase in Conducting Copolymers” *Des Monomers Polym.*, 7,3 (2004)
6. S. Kiralp, A. Cirpan, L. Toppare “Enzyme Electrodes for Determination of Total Phenolic Capacity of Red Wines” *Biosens and Bioelect* (submitted)
7. H.B.Yildiz, S.Kiralp, L.Toppare, Y. Yağcı “Immobilization of invertase in conducting polypyrrole/PMMA-co-PMTM graft copolymers” *J.Appl. Polm. Sci.* (submitted)
8. H.B.Yildiz, S.Kiralp, L.Toppare, F.Yilmaz, Y.Yağcı, K.Ito, T.Senyo “Conducting copolymers of 3-methyl methacrylate and *p*-vinylbenzyloxy poly(ethyleneoxide) and their electrochromic properties1” *Polymer Journal* (submitted)
9. H. B.Yildiz, S.Kiralp, L.Toppare, F.Yilmaz, Y.Yağcı, K.Ito, T.Senyo “Polyethylene oxide enzyme electrodes for determination of total phenolic capacity of red wines” *J. Appl. Polm. Sci.* (submitted)